



UNIVERSIDAD DE CHILE
FACULTAD DE CIENCIAS FÍSICAS Y MATEMÁTICAS
DEPARTAMENTO DE GEOLOGIA

**SIMULACIÓN NUMÉRICA DE FLUIDOS CON APLICACIÓN A
SISTEMAS GEOTERMALES ACTIVOS Y FÓSILES**

**TESIS PARA OPTAR AL GRADO DE MAGÍSTER EN CIENCIAS,
MENCION GEOLOGÍA**

DAVID ANDRES CALISTO LEIVA

**PROFESOR GUÍA:
DANIEL MONCADA DE LA ROSA**

**MIEMBROS DE LA COMISIÓN:
LINDA DANIELE
BRIAN TOWNLEY CALLEJAS
ERIC SONNENTHAL**

Este trabajo ha sido financiado por el Centro de Excelencia en Geotermia de los Andes (CEGA),
proyecto FONDAP-CONICYT 15090013 y Conicyt (Fondecyt) Iniciacion 11170210

**SANTIAGO DE CHILE
2022**

**RESUMEN DE LA TESIS PARA OBTAR AL
GRADO DE:** Magíster en Ciencias, Mención
Geología
POR: David Calisto Leiva
PROFESOR GUÍA Daniel Moncada

SIMULACIÓN NUMÉRICA DE FLUIDOS CON APLICACIÓN A SISTEMAS GEOTERMALES ACTIVOS Y FÓSILES

Los depósitos epitermales son considerados el análogo fósil de los sistemas geotermales activos, sin embargo, no todos los sistemas geotermales forman depósitos epitermales, una combinación particular de factores en el tiempo es necesaria para que un sistema geotermal forme una acumulación económica de recursos minerales. En este trabajo, las condiciones de formación del depósito epitermal de Zn-Pb-Ag Patricia ubicado en el norte de Chile, son estudiadas por medio de un modelo de transporte reactivo implementado con el código TOUGHREACT.

El depósito Patricia es un depósito epitermal de sulfuración baja a intermedia, su mineralización presenta un marcado control estructural, y se encuentra en vetas de cuarzo, esfalerita y galena. Estudios previos, de mineralogía e inclusiones fluidas, han establecido que el depósito tiene tres estadios paragénéticos distintivos que evidencian cambios en la composición de los fluidos hidrotermales de este depósito, la ausencia de evidencias de ebullición de fluidos durante estos tres estadios es una característica particular de este depósito.

Estudios de solubilidad de metales base indican que para las temperaturas estimadas de formación de Patricia los fluidos mineralizadores transportaron los metales en complejos clorurados y tuvieron bajas concentraciones de azufre reducido. Siendo necesaria para la formación de la mineralización de sulfuros, un aporte de azufre, se propone la mezcla de fluidos de distinta composición como el mecanismo más probable de formación de mineralización en este depósito. Eventos sucesivos de circulación de fluidos pobres en metales y de fluidos ricos en metales formaron la alteración y mineralización del depósito.

Para un período de 10,000 años de actividad geotermal y considerando valores conservadores de permeabilidad, tasas de flujo de fluidos y carga metálica en solución, se ha evaluado un modelo de transporte reactivo, que replica la paragénesis, la mineralización de sulfuros y la cantidad estimada de recursos minerales de Patricia, estimándose la duración total del evento mineralizador en 5,000 años. Aproximadamente 1,000 simulaciones distintas fueron realizadas para calibrar y refinar este modelo. Sin embargo, esta estimación para el evento de mineralización no es única, se ha determinado que existe más bien una amplia combinación de variables con el potencial de replicar la formación del depósito epitermal de Patricia, la más crítica y necesaria es la circulación de fluidos que aportaran metales al sistema. La distribución de la permeabilidad de la roca de caja, y la presencia de contrastes de permeabilidad entre rocas intactas y fracturadas ejercieron un control de primer orden en la distribución y concentración de esta mineralización en fracturas.

Finalmente, los factores que permitieron la formación del depósito de Zn-Pb-Ag Patricia, fueron primero una distribución de permeabilidad favorable para la formación de un sistema geotermal, luego la presencia de estructuras, capaces de canalizar los fluidos hidrotermales ascendentes y formar una zona de mezcla eficiente de fluidos, estas condiciones no hubieran sido suficientes para formar el depósito sin el ingreso de un fluido enriquecido en metales al sistema, este fluido fue en definitiva el factor crítico para la formación del depósito de Patricia.

“Palabra fiel y digna de ser recibida por todos:
que Cristo Jesús vino al mundo para salvar a los pecadores,
de los cuales yo soy el primero.”

“Porque de tal manera amó Dios al mundo, que ha dado a su Hijo unigénito,
para que todo aquel que en él cree, no se pierda, mas tenga vida eterna.”

Diciendo él estas cosas en su defensa,
Festo a gran voz dijo: Estás loco, Pablo; las muchas letras te vuelven loco.
Mas él dijo: No estoy loco, excelentísimo Festo,
sino que yo hablo palabras de verdad y de cordura.

AGRADECIMIENTOS

Habiendo recibido ayuda de Dios, persevero hasta el día de hoy y agradezco a las personas que Él puso en esta etapa de mi camino, la cual concluye en esta tesis.

Primeramente, agradezco al Dr. Daniel Moncada, mi Profesor Guía en este proyecto, por plantearme la aplicación de modelos de transporte reactivo a la formación de depósitos epidermales, por su guía, su infatigable perseverancia y su paciencia para esperar resultados concretos.

Agradezco a la Dra. Linda Daniele, al Dr. Brian Townley, y al Dr. Eric Sonnenthal por mejorar este trabajo con sus contribuciones e ideas incorporadas en el manuscrito de esta tesis.

Agradezco de manera muy especial al Dr. Diego Morata, por su apoyo, confianza y paciencia.

Agradezco de todo corazón a Maritza Acuña, secretaria del programa de postgrado de Geología, sus incansables gestiones, y por resolver todo el procedimiento administrativo necesario para titularme, y reconozco que sin su iniciativa y preocupación esta tesis nunca habría visto la luz.

Agradezco a Pablo Molina mi amigo y compañero de puesto en la sala de postgrado, testigo de mis esfuerzos y de mis frustraciones, gracias Pablo por escucharme mil y un veces, y animarme en mil y una ocasiones.

Agradezco a Nelson Román Moraga, por su inspirador trabajo de tesis, del cual obtuve no pocas ideas.

Agradezco el aporte de recursos computacionales proporcionados por el Laboratorio Nacional de Computación de Alto Rendimiento (NLHPC)

Finalmente, agradezco el apoyo financiero del Centro de Excelencia en Geotermia de los Andes, CEGA, proyecto FONDAP-CONICYT #15090013 por financiar mis estudios mediante una beca de Magíster.

Tabla de Contenido

AGRADECIMIENTOS	iv
Tabla de Contenido.....	v
Índice de Figuras	ix
Índice de Tablas.....	xiv
1 INTRODUCCIÓN	1
1.1 Estructura de la Tesis	1
1.2 Introducción y Antecedentes del estudio.....	1
1.2.1 Sistemas Geotermales y Depósitos Epitermales	1
1.2.2 Modelos de Transporte Reactivo y Sistemas Magmáticos e Hidrotermales	2
1.2.3 El depósito epitermal de Zn-Pb-Ag Patricia	3
1.3 Motivación.....	4
1.4 Hipótesis de estudio	4
1.5 Objetivos.....	4
1.5.1 Objetivo General	4
1.5.2 Objetivos Específicos.....	4
1.6 Metodología.....	5
1.6.1 Etapa Conceptual y Consideraciones Generales.....	5
1.6.2 Parámetros para modelar condiciones de transporte.....	8
1.6.3 Parámetros para describir el sistema geoquímico y las interacciones fluido-minerales	9
2 NUMERICAL SIMULATION OF A FOSSIL GEOTHERMAL SYSTEM IN CHILE	11
2.1 ABSTRACT.....	11
2.2 INTRODUCTION	12
2.2.1 Relationship between continental geothermal systems and epithermal precious metal deposits.....	13
2.2.2 Characteristics of the Epithermal Base Metal Deposits.....	14

2.2.3	Duration of mineralization events on hydrothermal deposits in the epithermal environment.....	15
2.2.4	Previous studies to estimate the duration of Ore-Forming processes from active geothermal systems.....	15
2.2.5	Previous studies to estimate the duration of Ore-Forming processes from fossil epithermal systems.....	16
2.2.6	Previous studies to estimate the duration of Ore-Forming processes from permeability and numerical simulations.....	17
2.3	GEOLOGICAL BACKGROUND OF THE PATRICIA DEPOSIT	20
2.3.1	Mineralogy.....	21
2.3.2	Textures and Paragenesis	22
2.3.3	Fluid Inclusions and Fluid Evolution path for the Patricia deposit.....	23
2.3.4	Fluid Metal Content in Fluid Inclusions from the Patricia deposit	25
2.4	CONCEPTUAL MODEL FOR THE FORMATION OF THE PATRICIA DEPOSIT	26
2.5	NUMERICAL MODEL.....	30
2.5.1	Reaction Rates	30
2.5.2	Kinetics of mineral dissolution and precipitation	31
2.5.3	Changes of Porosity and Permeability.....	31
2.6	GEOCHEMICAL SYSTEM.....	33
2.6.1	Rock Mineralogy.....	33
2.6.2	Rock Properties for the model.....	34
2.6.3	Spatial Scale and geometry of the model.....	34
2.6.4	Fluid Geochemical Conditions and Model Stages.....	36
2.7	RESULTS.....	40
2.7.1	Base Metal Solubility and Batch Models Results.....	40
2.7.2	Formation of Base Metal Sulfides, mixing as ore forming mechanism	44
2.7.3	Estimation of the Ore Stage duration.....	45
2.7.4	Results of Reactive Transport Models of the Patricia deposit	45

2.8	DISCUSSION.....	63
2.8.1	Conceptual Model.....	63
2.8.2	Modelling approach: Single porous media and double porosity media models	63
2.8.3	Fluid-rock interaction along the vertical up flow pathway.	65
2.8.4	Sulfide distribution and fluid chemistry	67
2.8.5	Pyrite Formation	67
2.8.6	Limitations	67
2.9	CONCLUSIONS.....	69
2.10	Acknowledgments.....	70
3	DISCUSIÓN.....	71
3.1	Revisión del Modelo de Formación del depósito de Zn-Pb-Ag Patricia.....	71
3.2	Mezcla de Fluidos en la formación de Depósitos Epitermales	72
3.3	El modelo de Mezcla de Fluidos implementado para el depósito Patricia.....	73
3.4	El rol de la Permeabilidad.....	74
3.4.1	Distribución de la Permeabilidad del Sistema	74
3.4.2	Permeabilidad y Duración de la Actividad del Sistema.....	74
3.4.3	Permeabilidad y Duración de la Etapa de Mineralización	75
3.5	Consideraciones de Balance de Masas y Duración de la Etapa de Mineralización.....	75
3.5.1	Tasas de Flujo	77
3.5.2	Concentraciones de Metales en Solución	78
3.6	¿Si la mezcla de fluidos es un proceso tan extendido, porque no hay más recursos minerales en sistemas geotermales activos?.....	78
4	CONCLUSIONES.....	80
5	BIBLIOGRAFIA	82

Índice de Figuras

Figure 1. Modelo Conceptual del depósito epitermal de Zn-Pb-Ag Patricia, modificado de Chinchilla (2017) y Albinson et al. (2001) y concepto principal del modelo de transporte reactivo a implementar con TOUGHREACT: si la mineralización se formó en un volumen limitado del sistema geotermal, es razonable modelar los procesos e interacciones que tuvieron lugar en este volumen, evitando así tener que modelar la circulación de fluidos de todo el sistema geotermal. . 6

Figure 2. Esquema conceptual del primer modelo de transporte reactivo usado para estudiar la formación del depósito Patricia. En este modelo se consideró el enfriamiento gradual de un solo fluido, sin considerar procesos de mezcla de fluidos. Distintas configuraciones de transporte y diferentes composiciones químicas fueron evaluadas, sin lograr reproducir la distribución vertical de la mineralización de Patricia. 7

Figure 3. Esquema conceptual del segundo modelo de transporte reactivo usado para evaluar la formación del depósito Patricia. En este modelo, se plantea que la mineralización es causada por un proceso de mezcla de fluidos, entre un fluido rico en metales de origen profundo, que asciende hacia la superficie y que se mezcla en su ascenso con fluidos aportados por corrientes laterales los cuales contienen el azufre necesario para formar sulfuros de metales base..... 7

Figure 4. Range of permeabilities observed in geological media. Showing characteristic process-limiting values. Geothermal systems are hosted in rocks with high permeability than unfractured rocks but lower than typical aquifers values. Sustained fluid and heat circulation through advection requires permeability higher than 10^{-16} m² for an active geothermal system. For commercially viable geothermal reservoirs the minimum permeability is $\sim 10^{-15}$ m². After Ingebritsen and Appold (2012) 18

Figure 5. Ubication of the Patricia Zn-Pb-Ag ore deposit. Patricia is an unusual deposit in the Eocene-Oligocene metallogenic belt of northern Chile known for hosting porphyry copper deposits such as Chuquicamata and La Escondida. Modified from Chinchilla et al. (2016b). 20

Figure 6. Geological map of the Patricia deposit showing main lithological units, and the main mineralized veins Campamento and Caterdral. Patricia is divided in two blocks, the western and eastern block, the latter being more exposed. The deposit is exposed within an area of 2 km² of extension, but most of the mineralization is related to the fault structures confined to a smaller area (in red) of $\sim 90,000$ m². Modified from Chinchilla et al. (2016b). 21

Figure 7. Simplified paragenesis of the Patricia deposit. Three paragenetic stages are defined: The pre-ore stage (1) with precipitation of early quartz and pyrite. The main ore stage (2) which has two substages: 2A with precipitation of sphalerite only; and 2B with precipitation of both sphalerite and galena. The post-ore stage (3) has precipitation of mainly late quartz. After Chinchilla et al. (2016a)..... 22

Figure 8. Sulfides mineralization in a symmetric vein of the Patricia deposit. In (1), (2) and (3) is possible to appreciate the paragenetic sequence from the pre-ore stage up to the end of the ore stage. (1) Pre-ore stage mineralization with quartz and pyrite in the rim of the vein. (2) Substage 2A, with just sphalerite filling reopened veinlets of the pre-ore stage. (3) Substage 2B, mineralization of sphalerite and galena. (4) Brecciated sulfides of the second substage filled with

late quartz in the post-ore stage. Modified from Chinchilla et al. (2016a), (Chinchilla et al. 2016b).
..... 23

Figure 9. A possible fluid evolution path for the Patricia deposit showing mean homogenization temperatures and salinities for each stage from fluid inclusion data by Chinchilla et al. (2016b): (1) Pre-ore stage, with a mean temperature of ~220 °C and ~10 wt.% NaCl. The second stage is the Main ore stage, divided in two substages The first substage 2A has mean values of ~200 °C and ~5 wt. % NaCl and the second substage of ~180 °C and ~7 wt. % NaCl. Finally, the last stage is the post-ore stage with mean temperatures and salinities of ~200 °C and ~2.5 wt. % NaCl. For each stage, the temperatures are minimum estimates from fluid inclusión data. 24

Figure 10. Conceptual model of the Patricia ore deposit, this model is built upon the model for the Patricia deposit proposed by Chinchilla (2017): In the vicinity of the volcanic rock formation hosting Patricia, of high enough permeability to allow sustained fluid convection, a magmatic intrusion at a unknown location formed and sustained a convective cell of hydrothermal fluids forming the geothermal system that gave origin to the Patricia deposit. The fluid-rock interaction formed the extended propylitic alteration in the rocks with lower permeability, and in the zones of higher permeability fractured by the activity of the tectonic structures, focused flow of episodic pulses of metal bearing fluids from a deep magmatic brine and mixing with meteoric fluids incorporated by lateral flow forms the Zn-Pb-Ag mineralization. The only difference between this model and the one previously proposed for Patricia is that fluid mixing is an active process for all the system’s lifetime, including the main ore stage. The rectangle shows the system’s section considered for the model (Modified after Albinson et al. 2001, Chinchilla 2017). 27

Figure 11. Classification of epithermal deposits based on physical conditions and depth of formation: Epithermal deposits have been classified in shallow boiling systems formed at < 500 m. depth; deep boiling systems formed between 500-1,500 m. depth; and deep non-boiling systems, formed at >1,000 m. depth. The Patricia Zn-Pb-Ag deposit features suggests conditions similar to those of deep no-boiling systems, with temperatures between 150°C- 250°C and depths below 1,000 m. The lithostatic curve and the curve of shallow to deep boiling system with 0 to 5 wt. % NaCl are depicted for reference. Modified from Albinson et al. (2001). 28

Figure 12. Model grid constructed to simulate fluid-rock interaction. [1] Model grid of 14 blocks of 50x 300 x 300 m. Pressure gradient is under hydrostatic conditions, temperature at surface is 100 °C. [2] Single porous media model, with homogeneous rock properties. [3] Dual porosity model, with 2 different porous media, matrix and fractures. 35

Figure 13. Methodology used to estimate the model’s ore solution: The data available from previous work from (Chinchilla et al. 2016a and 2016b) provide the mineral and fluid inclusion data to allow estimates for the fluids of both the pre-ore and post-ore stages. But for the main ore stage, batch modelling was performed with TOUGHREACT, assuming fluid-mineral equilibrium, to estimate a range of potential ore fluid compositions for the conditions of the ore stage. From the resulting array of possible ore solutions, further constrains were imposed on account of flow rate and time considerations. The results of the reactive transport models were used to retroactively calibrate these estimates, through comparison with the resource estimates available for the Patricia deposit. More than 1,000 models were made to constrain the conditions of the models presented. 37

Figure 14. Zinc solubility calculated through TOUGHREACT, for all calculations pH set to 4.0 and aqueous sulfur concentration as HS⁻ set to 1•10⁻³ mol/kg. (A) Zinc solubility at constant 10 wt. % NaCl for temperatures between 300°C to 140 °C, solubility decreases with lower temperatures. (B) Base metal concentration as a function of fluid salinity at constant temperature, for a range of 20 to 2.5 wt% NaCl. (C) Activity of chloride and sulfide complexes of Zinc between 300°C to 140°C at constant 10 wt.% NaCl, Zn-chloride complexes are more active than Zn-bysulfide complexes, and more sensible to cooling. 42

Figure 15. Zn and Pb solubility response to changes in pH and reduced sulfur (HS⁻) in fluid. Solubility calculated for 200 °C and 5 % wt. NaCl. (A) and (B) base metal concentration (ppm) as a function of aqueous sulfur at constant pH= 4.0. Zn and Pb solubility decreases as aqueous sulfur concentration increases. (C) and (D) base metal concentration as a function of fluid acidity, at constant aqueous sulfur concentration (1•10⁻⁴ mol/kg of HS⁻; ~3 ppm). Acid pH favors a higher solubility of both Zn and Pb..... 43

Figure 16. Model configurations implemented with TOUGHREACT: (1) Batch models were made to estimate fluid composition through fluid-mineral equilibrium (2) Reactive transport models with a single porous media model, with homogeneous rock properties to estimate the duration of the ore stage. (3) Reactive transport models with a dual porosity model, were made to study the differences of fluid-rock interaction between matrix and fractures, the fractured volume was assumed a 10% of the total modelled volume. All reactive transport models have dimensions of 700 m of vertical depth, and a square base of 300 m. 46

Figure 17. Changes of porosity and vertical permeability for Model 1. Each curve is traced at the end of a paragenetic stage. (A) Porosity increases by dissolution of the primary mineralogy below 300 m depth, but from 300 m upwards porosity decreases down to < 5%. (B) Permeability follow a similar trend, decreasing from ~300 m depth upwards from ~10⁻¹³ to <10⁻¹⁴ m². (C) Vertical permeability initial/final ratio along the vertical profile highlights the increase in permeability at depth followed by a significant decrease upwards. 48

Figure 18. Temperature and pressure conditions of Model 1. (A) The temperature profile for pre-ore stage, ore stage A and, B, and post-ore stage looks isothermal up to ~250 m depth. (B) The pressure profile follows the hydrostatic pressure profile, over time pressure increases gradually all along the system. 49

Figure 19. Changes over time in the alteration mineral assemblage for Model 1. The relative abundance of each alteration mineral is displayed along the vertical profile of the model at the end of each paragenetic stage. From the initial stage with andesite mineralogy, the silicate mineralogy develops into an assemblage of plagioclase + epidote + chlorite + daphnite + quartz, typical of the propylitic alteration..... 50

Figure 20. Changes in pH, reduced sulfur concentration [HS⁻], Zn⁺² and Pb⁺² for all the modeled lifetime of Model 1. (A) Vertical pH profile for all stages, (B) Reduced sulfur concentration, (C) Total Zn⁺², (D) Total Pb⁺². Fluid acidity is buffered by the rock mineral assemblage up to pH~5.5. Initial Zn⁺² concentration during the ore stage is 10 ppm, and initial Pb⁺² concentration during substage 2B is 6ppm. 51

Figure 21. Vertical profile of base metals resources precipitated after each paragenetic stage for Model 1. Most of the base metals precipitated below 200 m depth, base metals are more abundant

at depth and gradually decrease in abundance up to the surface. (A) Lead precipitated as galena (B) Zinc precipitated as sphalerite..... 52

Figure 22. Changes of porosity and vertical permeability at different times for fractures and matrix media in Model 2. For fractures, porosity and permeability increased from 600 to 200 m depth, but decreased at the system's boundaries, especially at the system's bottom boundary: (A) Changes of porosity in the fractures. (B) Vertical permeability in m^2 in the fractures. (C) Vertical permeability initial/final ratio in the fractures. For the rock matrix, porosity and permeability showed significant increase below 600 m depth: (D) Changes of porosity in the rock matrix. (E) Vertical permeability in m^2 in the rock matrix. (F) Vertical permeability initial/final ratio in the rock matrix..... 53

Figure 23. Temperature and pressure profile at different times for Model 2. (A) The temperature profile followed an isothermal trend up to 200 m depth, and then the boiling point curve upwards 200 m depth (B) The pressure profile followed the hydrostatic curve for most of the simulation, but by the end of the simulation increased below 600 m depth..... 54

Figure 24. Changes in the alteration mineral assemblage of Model 2. Changes in relative abundance of each mineral, at different times for fractured and matrix media. (A) Alteration mineral assemblage of the fractures, in the fractures epidote is replaced by chlorite, Fe-chlorite (daphnite) is most abundant at the system's bottom boundary. (B) In the matrix, the alteration minerals had only slight changes in relative abundance, remaining almost constant through time. 55

Figure 25. Changes of pH, reduced sulfur concentration $[HS^-]$, Zn^{+2} and Pb^{+2} for Model 2. Model 2 simulated Patricia's ore stage, the first 2,000 years simulated sub-stage 2A, the following 3,000 years simulated sub-stage 2B. (A) pH profile at different times, for the first 2,000 years the fluid's acidity is buffered \sim pH 6.0 of 2,000 years, after 3,000 acidity increased below 300 m depth to \sim pH 5.0 (B) Reduced sulfur concentration (C) Total Zn^{+2} (D) Total Pb^{+2} . Base metals concentrations are maximum at bottom and decrease up to 300 m. depth. Initial Zn^{+2} is 10 ppm at all times, from 3,000 years initial Pb^{+2} is 6 ppm. 56

Figure 26. Vertical profile of base metals abundance at different times during ore substages 2A and 2B for Model 2. Most of the base-metal ore resources precipitated at fractures below 300 m depth, sulfide minerals did not precipitate in the matrix. (A) Lead precipitated as galena in fractures. (B) Zinc precipitated as sphalerite in fractures..... 57

Figure 27. Changes in the porosity and vertical permeability distribution at different times for fractures and matrix media in Model 3. In Model 3, permeability and porosity changes at both fractures and matrix media were similar, with a decrease above 200 m. depth. (A) Changes of porosity in the fractures. (B) Vertical permeability in m^2 in the fractures. (C) Vertical permeability initial/final ratio of the fractures. (D) Changes of porosity in the rock matrix. (E) Vertical permeability in m^2 in the rock. (F) Vertical permeability initial/final in the rock matrix. 58

Figure 28. Temperature and pressure profile at different times for Model 3. (A) The temperature profile was isothermal below 200 m. depth, and followed the boiling point curve upwards. (B) Pressure profile, the pressure profile followed the hydrostatic curve during this simulation..... 59

Figure 29. Changes at different times of the alteration mineral assemblage of the fractured media of Model 3. In this model, both fractures and matrix's responses to the fluid-rock interaction were similar, the alteration assemblage remained constant over time..... 60

Figure 30. Changes of pH, reduced sulfur concentration $[HS^-]$, Zn^{+2} and Pb^{+2} for Model 3. Model 3 simulated Patricia's ore stage, the first 2,000 years simulated sub-stage 2A, the following 3,000 years simulated sub-stage 2B. (A) pH profile at different times, fluid acidity changes from substage 2A to substage 2B, pH decreases over time. (B) Reduced sulfur concentration (C) Total Zn^{+2} (D) Total Pb^{+2} . Base metals concentrations were maximum at bottom and decreased up to 300 m. depth. Initial Zn^{+2} is 10 ppm at all times, from 3,000 years initial Pb^{+2} is 6 ppm. 61

Figure 31. Vertical profile of base metals abundance at different times during ore stages 2A and 2B for Model 3. Most of the base-metal ore resources precipitated at fractures below 300 m depth, sulfide minerals did not precipitate in the matrix. (A) Lead precipitated as galena in the fractures. (B) Zinc precipitated as sphalerite in the fractures. 62

Figure 32. Tiempo necesario para depositar los recursos estimados de Zinc para Patricia, con diferentes tasas de fluidos, para distintas concentraciones de Zinc (~10, 30 y 60 ppm). El eje vertical representa el tiempo transcurrido y se encuentra en escala logarítmica. Para una tasa constante de 100 kg/segundo y 10 ppm de Zn en solución, son necesarios ~5,300 años para depositar el total de las reservas estimadas de Zinc. Sin embargo, para una tasa de 60 kg/segundo, con 30 ppm este período disminuye a ~3,000 años, y a la mitad de esto (~1,500 años) para una concentración de 60 ppm de Zn en solución. 76

Figure 33. Tiempo necesario para depositar los recursos estimados de Plomo para Patricia, con diferentes tasas de fluidos, para distintas concentraciones de Pb en solución (~6, 30 y 60 ppm). El eje vertical se encuentra en escala logarítmica. Para una tasa constante de 100 kg/segundo y ~6 ppm de Pb en solución, son necesarios ~3,100 años para depositar el total de las reservas estimadas de Plomo. Sin embargo, para una tasa de 60 kg/segundo, con 30 ppm este período disminuye a ~1,000 años, y a la mitad de esto (~500 años) para una concentración de 60 ppm de Pb en solución. 77

Índice de Tablas

Table 1. Parameters for calculating kinetic rate constants for minerals using the rate law described in Equations (2), (3) and (4), k_{25} is the kinetic constant at 25° C, E_a is the activation energy, additional mechanisms for some minerals are detailed with the species involved and the exponents of each specie according to equation (3) . All rate constants are listed for dissolution (Palandri and Kharaka 2004, Xu et al. 2006, Acero et al. 2007a, Acero et al. 2007b, Zhang et al. 2011).	32
Table 2. Simplified mineralogy considered for the geochemical system based on the mineralogy observed at the Patricia deposit, primary mineral phases and abundances are from an unaltered andesite (Chinchilla 2016a and Chinchilla 2017, Valenzuela et al. 2014). Reactive mineral surfaces for each mineral are from BET estimations (Zhong et al. 2011).	33
Table 3. Rock properties and fluid flow parameters used in the single porous and double porous media models.....	34
Table 4. Aqueous chemical compositions for each fluid considered in the simulations, concentration units are in [mol/kg].	39
Table 5. List of models, characteristic features of each one indicated according to minerals considered, porous media representation and simulated period.	46

1 INTRODUCCIÓN

1.1 Estructura de la Tesis

El presente trabajo estudia la formación y evolución del depósito de Zn-Pb-Ag Patricia ubicado en el norte de Chile, por medio de un modelo numérico de transporte reactivo.

En el Capítulo 1 se presenta una breve introducción al tema, los antecedentes y la motivación del estudio. Una síntesis de la metodología empleada cierra este capítulo.

En el Capítulo 2, se presentan los resultados del estudio propiamente tal. Este capítulo, en inglés, consiste en el manuscrito "Numerical Simulation of a Fossil Geothermal System in Chile". Este capítulo es auto-contenido, con la salvedad no tener incorporadas sus propias referencias (contenidas como un ítem independiente de esta tesis).

En el Capítulo 3 se discute de manera más específica los alcances de los resultados presentados en el Capítulo 2 para el estudio de Patricia y algunas implicancias de interés para el estudio de la formación de depósitos en condiciones epitermales. Finalmente, en el Capítulo 4 se presentan las principales conclusiones de este trabajo.

1.2 Introducción y Antecedentes del estudio

1.2.1 Sistemas Geotermales y Depósitos Epitermales

Los sistemas geotermales son un ambiente geológico asociado a la actividad magmática caracterizados por la circulación de fluidos producto de los gradientes termale causados por el enfriamiento de cuerpos magmáticos (Henley y Ellis 1983, Hedenquist y Lowenstern 1994). Estos sistemas están distribuidos en áreas cercanas y escalas de tiempo similares a las de los sistemas y procesos magmáticos.

Dada la extensa escala y la variabilidad inherente de los procesos magmáticos en la corteza terrestre, los depósitos hidrotermales exhiben también una amplia gama de diversidad en sus expresiones y características (White y Hedenquist 1990). Esta diversidad ha sido agrupada en un continuo de depósitos minerales denominada el ambiente Porfirico-Epitermal los cuales tienen una común asociación a procesos magmáticos y a actividad hidrotermal (Einaudi et al 2003). En este ambiente, la categoría de los depósitos epitermales constituye el análogo fósil de los sistemas geotermales activos en el tiempo presente.

Los depósitos epitermales constituyen importantes reservas de metales preciosos y de metales base, siendo explotados mayoritariamente por su contenido en metales preciosos, por esta razón el estudio de la mineralización de metales preciosos en depósitos epitermales presenta un mayor grado de desarrollo comparado al estudio de los procesos y causas de formación de mineralización de metales base en el mismo ambiente.

En este trabajo, se estudia la formación de mineralización de metales base en condiciones epitermales tomando como caso de estudio el depósito de Zn-Pb-Ag Patricia, ubicado en el norte de Chile (Chinchilla et al. 2016a, Chinchilla et al. 2016b y Chinchilla 2017).

1.2.2 Modelos de Transporte Reactivo y Sistemas Magmáticos e Hidrotermales

No solo los sistemas geotermales y los depósitos epitermales exhiben una gran diversidad de características y manifestaciones, sino que además en estos sistemas se produce una compleja interacción de procesos físicos de transporte de masa y calor, y reacciones de interacción fluido-roca en distintas escalas espaciales y temporales (Ingebritsen et al. 2010, Ingebritsen and Appold 2012). Esta inherente complejidad incrementa la dificultad para entender estos sistemas, y plantea la necesidad de una metodología integral que cuantifique la evolución e interacción de estos procesos, ahora esta problemática no es exclusiva de los sistemas magmáticos e hidrotermales, sino que es característica de múltiples problemas en Ciencias de la Tierra (Steefel et al. 2005), los modelos de transporte reactivo surgen como respuesta a esta demanda por una metodología integral para abordar problemas en los cuales varios procesos interactúan dinámicamente en diferentes escalas espaciales y temporales (Steefel et al. 2005).

Inicialmente los modelos numéricos aplicados a problemas relacionados con los sistemas magmáticos-hidrotermales, abordaron los procesos de transporte y de interacción entre minerales y fluidos por separado. A continuación, se mencionarán algunos de los trabajos más relevantes por sus aportes para el desarrollo de modelos de transporte reactivo aplicados a sistemas magmáticos e hidrotermales y en particular por su relevancia para este trabajo.

En lo concerniente a procesos de transporte de masa y calor, los primeros estudios en modelación numérica de circulación de fluidos en la vecindad de cuerpos magmáticos fueron realizados por (Cathles 1977, Norton y Knight 1977), a pesar de contar con escasos recursos computacionales, y por necesidad emplear múltiples simplificaciones, estos trabajos establecieron rigurosamente el rol de la permeabilidad como control de primer orden en la ocurrencia de procesos de advección de fluidos y calor en ambientes magmáticos-hidrotermales (Norton y Knight 1977) y en la tasa de enfriamiento de un cuerpo magmático producto de la circulación de fluidos (Cathles 1977), además estos trabajos plantearon que un sistema hidrotermal podía tener un período de actividad significativamente menor al de un sistema magmático. Posteriormente, la duración de un sistema geotermal sostenido por un solo evento intrusivo, fue modelada y acotada en función de la distribución de permeabilidad de la roca en la vecindad de una intrusión a un período inferior a 1 Ma, los sistemas hidrotermales con períodos de actividad más extensos requerirían de múltiples intrusiones para mantenerse activos (Cathles et al. 1997). La formulación teórica necesaria para modelar el transporte de calor y masa y la importancia del rol de la permeabilidad en la formación de depósitos minerales de origen hidrotermal ha sido confirmada cuantitativamente por Ingebritsen y Appold (2012) y de manera aún más detallada para depósitos en el ambiente porfírico-epitermal por Weis (2015), quien considerando una distribución dinámica de permeabilidad y fluidos salinos logro modelar cuantitativamente el sistema hidrológico planteado de manera conceptual por Hedenquist y Lowenstern (1994) para depósitos en el ambiente porfírico-epitermal.

Pionero en la integración de modelos de transporte con la descripción de las reacciones que describen la interacción entre fluidos y roca, es el trabajo de Steefel y Lasaga (1994), quienes presentaron un modelo teórico y numérico que simultáneamente integraba el transporte de masa y calor con la descripción de las reacciones químicas entre agua, roca y fracturas de un sistema hidrotermal. Este trabajo planteo la base teórica para la formulación de la primera versión del modelo de transporte reactivo conocido como TOUGREACT (Xu y Pruess 2001, Xu et al. 2011b), este modelo ha sido aplicado a varios estudios en condiciones hidrotermales (Dobson et al. 2004, Todaka et al. 2004, Xu et al. 2006, Wanner et al. 2014). Especialmente relevante para esta tesis son los resultados de Wanner et al. (2014), al integrar permeabilidad, tasas de flujo de fluidos y

reacciones minerales en un modelo numérico y calibrar este modelo con datos del campo geotermal Dixie Valley, Nevada, USA.

Todos estos avances aportan el marco teórico y conceptual y los métodos para aplicar un modelo de transporte reactivo al estudio de un depósito mineral con condiciones similares a las de los sistemas hidrotermales activos previamente estudiados.

1.2.3 El depósito epitermal de Zn-Pb-Ag Patricia

Patricia forma parte un antiguo distrito minero explotado alrededor de 1880, actualmente pertenece al proyecto minero Paguanta, propiedad de la compañía minera “Golden Rim Resources”. Campañas de exploración, con ~40,000 m. de sondajes han caracterizado el yacimiento y estimado recursos de 2.4Mt con leyes de 5.0% Zn, 1.4% Pb, 88g/t Ag y 0.3g/t Au (Golden Rim Resources 2017).

Patricia ha sido clasificado como un depósito epitermal de metales base y sulfuración baja a intermedia, y considerado un hallazgo peculiar (Chinchilla et al. 2016b) al encontrarse ubicado en el extremo norte de la franja metalogénica de edad Eoceno superior – Oligoceno, conocida por depósitos de pórfidos de cobre de clase mundial como Chuquicamata, La Escondida o Quebrada Blanca.

El depósito se encuentra emplazado en una sucesión de rocas volcánicas de composición andesítica afectadas por intensa alteración propilítica, la mineralización presenta un claro control estructural y se encuentra en vetas y stockworks (Chinchilla 2017). La asociación mineral se formó en tres estadios principales, el estadio 1 previo a la mineralización, el estadio 2 al cual se asocia la precipitación de la mineralización consistente en sulfuros de metales base y sulfosales de Ag y el estadio 3 posterior a la mineralización (Chinchilla et al. 2016b).

Estudios de inclusiones fluidas han determinado las temperaturas y salinidad características de los fluidos de cada uno de estos tres estadios, y han establecido que estos fluidos no experimentaron ebullición (Chinchilla et al 201b, Chinchilla 2017)

A partir de todos los antecedentes disponibles, se ha propuesto que la formación de la mineralización de sulfuros fue a consecuencia del enfriamiento progresivo de un fluido de salinidad moderada-baja (10 -1 % eq. NaCl), que transportaba los metales mayoritariamente como complejos sulfurados (Chinchilla et al. 2016b, Chinchilla 2017).

La detallada caracterización de la mineralogía e inclusiones fluidas de Patricia, la ausencia de evidencias de ebullición de fluidos en los tres estadios de mineralización, y un modelo relativamente simple de formación de esta mineralización de metales base, hacen factible la posibilidad de realizar un modelo de transporte reactivo que replique la formación de este depósito epitermal.

1.3 Motivación

Las siguientes preguntas resumen la motivación del este trabajo:

¿Cuáles son las condiciones y procesos favorables para la formación de mineralización de metales base en los depósitos epitermales similares al depósito Patricia?

¿Cuánto tiempo sería necesario para la formación de un depósito epitermal de estas características?

Para responder a estas preguntas se ha propuesto un modelo numérico de transporte reactivo implementado con TOUGHREACT (Xu and Pruess 2001, Xu et al. 2011b), con el fin de tener otra perspectiva de la formación de mineralización de metales base en el caso del depósito Patricia.

1.4 Hipótesis de estudio

En los sistemas geotermales fósiles la mineralogía y estructura del sistema es producto de la interacción fluido-roca durante el período de actividad geotermal del sistema. La evolución y los procesos que concluyeron en el estado final del sistema activo pueden ser replicados mediante un modelo de transporte reactivo que acople el transporte de masa y calor con las interacciones entre el fluido hidrotermal y los minerales de roca del sistema geotermal durante su período de actividad.

1.5 Objetivos

1.5.1 Objetivo General

Estudiar el proceso de formación del depósito epitermal Patricia utilizando un modelo de transporte reactivo.

1.5.2 Objetivos Específicos

1. Proponer un modelo conceptual para la formación de la mineralización de metales base en el caso del depósito Patricia que defina las condiciones geoquímicas de los fluidos y de transporte del sistema geotermal.
2. Elaborar un modelo de transporte reactivo con TOUGHREACT, calibrado con la información disponible del caso de estudio.
3. Determinar los factores más relevantes para la formación de mineralización de metales base a partir de dicho modelo.
4. Estimar la duración del evento de mineralización.

1.6 Metodología

1.6.1 Etapa Conceptual y Consideraciones Generales

A continuación, se presenta el diseño y desarrollo de la metodología usada para elaborar el modelo de transporte reactivo cuyos resultados son presentados en el Capítulo 2.

Los modelos de transporte reactivo son una metodología en la cual se acopla el aspecto concerniente al transporte de masa y energía de un sistema, con el aspecto enfocado en describir las interacciones químicas que ocurren en este sistema (Steeffel et al. 2005, Ingebritsen et al. 2010).

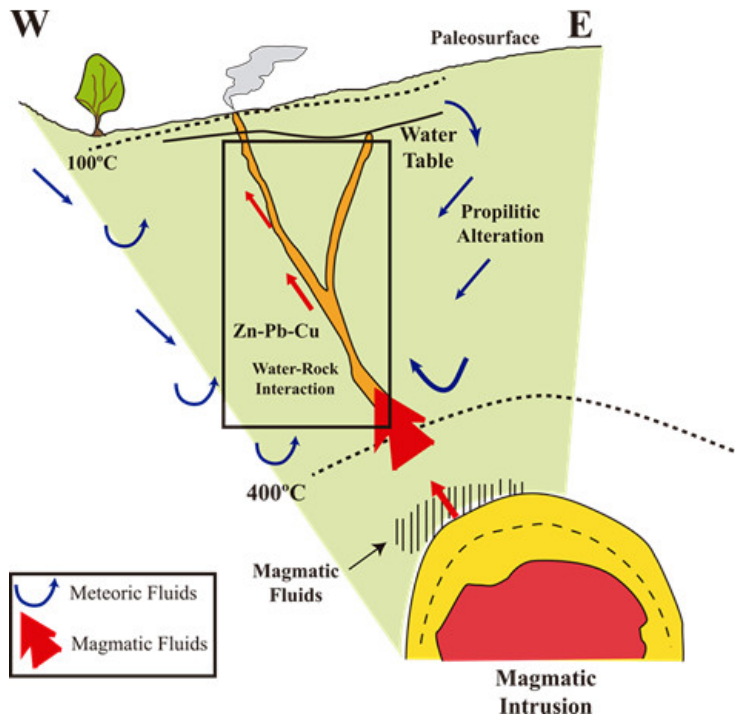
En este estudio el problema a estudiar es la formación de mineralización de sulfuros de metales base en un sistema geotermal. Es de interés establecer los procesos y parámetros más relevantes para la formación del depósito Patricia, y eventualmente la escala temporal de estos procesos. Para esto es necesario simular las condiciones de transporte durante la actividad del sistema geotermal fósil que formó esta mineralización. Y simultáneamente establecer y acoplar a este modelo de transporte, el sistema químico que describe la interacción y las reacciones entre los fluidos hidrotermales y la roca de caja del sistema geotermal.

El modelo conceptual del depósito Patricia considerado en primera instancia fue el mismo propuesto por Chinchilla et al. (2015) y Chinchilla (2017), presentado en la Figura 1, el cual corresponde a una modificación al modelo para depósitos epitermales de sulfuración intermedia de Hedenquist y Lowenstern (1994). En este modelo se plantea que la mineralización se formó producto del enfriamiento gradual de un único fluido el cual transportó los metales base como complejos bisulfurados durante el estadio principal de mineralización del depósito. Aunque existen evidencias de mezcla de fluidos en las etapas previa y posterior a la mineralización (Chinchilla 2017), se estimó que la mezcla de fluidos no fue relevante para la formación de la mineralización de Patricia. Este modelo conceptual fue usado para construir un modelo de transporte reactivo (Figura 2) usando el código TOUGHREACT. Con este modelo no se obtuvieron los resultados esperados. Este modelo, asumiendo un solo fluido, y el enfriamiento gradual del fluido mineralizador durante su ascenso como mecanismo de formación de la mineralización no replica el horizonte vertical de mineralización de metales base, reportado en el mapeo geológico del depósito (Golden Rim Resources 2017) y descrito por el modelo clásico de depósitos epitermales de metales base (Buchanan 1981).

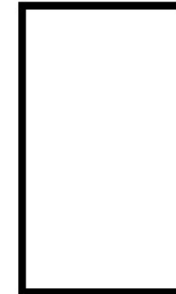
Para plantear un modelo conceptual alternativo, primero se analizó la solubilidad de los complejos acuosos de metales base (Zn y Pb) en condiciones epitermales (<350°C) por medio de “batch models” para distintas soluciones en un amplio rango de temperatura y salinidad. Se concluyó que a diferencia de lo planteado en estudios anteriores (Chinchilla et al. 2015, Chinchilla 2017) los metales fueron transportados en complejos clorurados, en fluidos con bajas concentraciones de azufre. Estas soluciones son incapaces de transportar simultáneamente metales base y azufre en solución para las condiciones de Patricia.

En este trabajo se propone entonces un modelo de formación alternativo, en el cual se plantea que la mineralización fue el resultado de un proceso de mezcla de fluidos, entre un fluido mineralizador que transporta metales base en solución como complejos clorurados y otro fluido que aporta el azufre necesario para formar la mineralización de sulfuros.

Conceptual Model of the Patricia Deposit



Reactive Transport Model



Representative Volume Transport & Reactive Processes

Figure 1. Modelo Conceptual del depósito epitermal de Zn-Pb-Ag Patricia, modificado de Chinchilla (2017) y Albinson et al. (2001) y concepto principal del modelo de transporte reactivo a implementar con TOUGHREACT: si la mineralización se formó en un volumen limitado del sistema geotermal, es razonable modelar los procesos e interacciones que tuvieron lugar en este volumen, evitando así tener que modelar la circulación de fluidos de todo el sistema geotermal.

El modelo numérico formulado con el código TOUGHREACT, es muy demandante en recursos computacionales, por lo cual fue necesario simplificar lo más posible la geometría del modelo y también la malla de celdas empleada para representar esa geometría. Considerando que la mineralización se encuentra controlada por estructuras, y ubicada preferentemente en la vecindad de un sistema de fallas (Figure 6) se decidió modelar un volumen representativo de esas fallas y de sus vecindades. Este volumen corresponde a una columna vertical de roca, en la cual tienen lugar simultáneamente, los procesos de transporte y las interacciones entre fluidos y roca. A continuación, se indican los criterios considerados para elegir los parámetros requeridos por el código TOUGHREACT para modelar los procesos de transporte y las reacciones químicas.

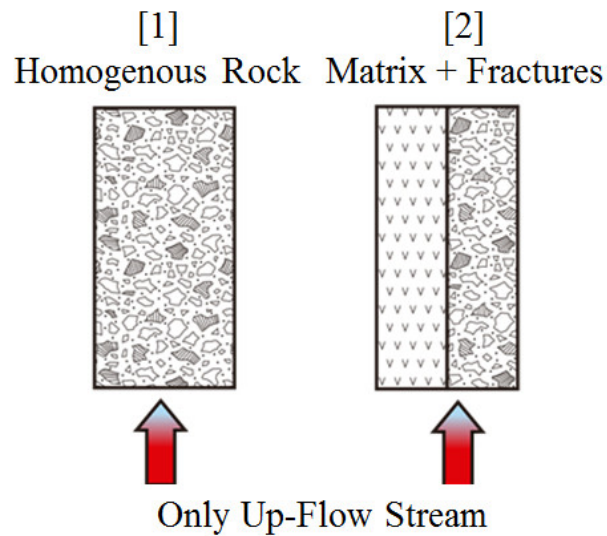


Figure 2. Esquema conceptual del primer modelo de transporte reactivo usado para estudiar la formación del depósito Patricia. En este modelo se consideró el enfriamiento gradual de un solo fluido, sin considerar procesos de mezcla de fluidos. Distintas configuraciones de transporte y diferentes composiciones químicas fueron evaluadas, sin lograr reproducir la distribución vertical de la mineralización de Patricia.

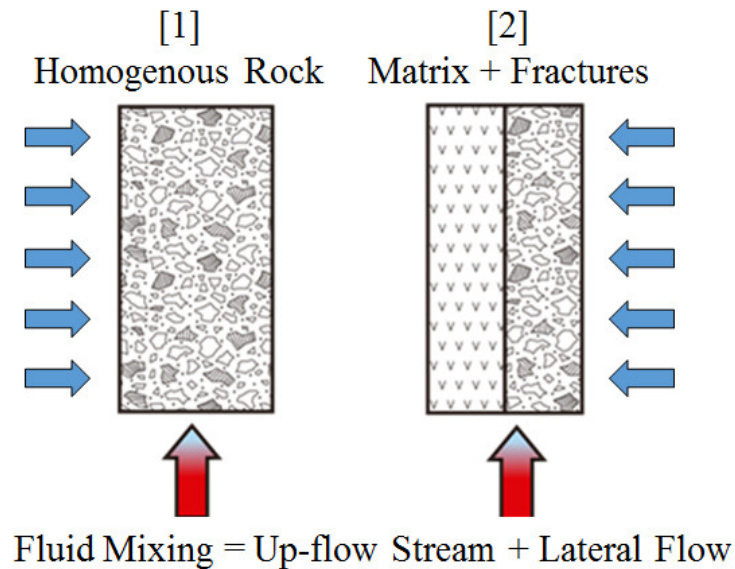


Figure 3. Esquema conceptual del segundo modelo de transporte reactivo usado para evaluar la formación del depósito Patricia. En este modelo, se plantea que la mineralización es causada por un proceso de mezcla de fluidos, entre un fluido rico en metales de origen profundo, que asciende

hacia la superficie y que se mezcla en su ascenso con fluidos aportados por corrientes laterales los cuales contienen el azufre necesario para formar sulfuros de metales base.

1.6.2 Parámetros para modelar condiciones de transporte

I. Propiedades de Roca y Permeabilidad

Para modelar el transporte de masa y de calor en un medio poroso, TOUGHREACT, requiere varias propiedades del medio, en este caso, de la roca de caja en la cual se emplazó el sistema geotermal, como densidad, conductividad térmica, porosidad, permeabilidad y grado de fracturamiento de la roca de caja del sistema. Para la elección de estos parámetros se consideraron los valores usados por Todaka et al (2004) y Wanner et al. (2014) para modelar sistemas geotermiales con rocas intactas y fracturadas de composición andesítica.

Para la elección de la permeabilidad de la roca de caja no fracturada, se consideraron especialmente los resultados de los análisis de parámetros hidrogeológicos en sistemas geotermiales y en depósitos magmático-hidrotermales realizados por Ingebritsen et al. (2010) y Ingebritsen y Appold (2012). Para la elección de la permeabilidad de roca fracturada se consideraron las compilaciones de datos de permeabilidad de corteza continental tectónicamente perturbada, recopilados por Ingebritsen y Manning (2010). Los valores de permeabilidad escogidos han sido usados en otros estudios de modelación numérica de formación de sistemas geotermiales y depósitos magmáticos hidrotermales (Cathles et al. 1997, Hayba y Ingebritsen 1997, Weis 2015).

II. Ecuaciones de Estado

TOUGHREACT requiere escoger las ecuaciones de estado de los fluidos a modelar, en la simulaciones, se consideró el módulo de ecuaciones de estado EOS1 de TOUGHREACT, el cual describe el flujo de un fluido en una sola fase, en condiciones saturadas y para temperaturas no constantes. Al considerar un fluido en una sola fase, el modelo no puede describir ebullición de fluidos. Sin embargo, para simular la formación de Patricia, esto no es un problema, considerando la ausencia de evidencias de ebullición en este depósito (Chinchilla et al. 2015).

III. Escala Espacial del Modelo

Para estimar el volumen representativo del sistema, se consideró el área ligada a la mineralización de acuerdo con el mapeo geológico de Patricia y la profundidad estimada de la mineralización a partir de los datos de sondajes del depósito. Del mapa geológico (Figure 6) se estimó que esa área corresponde aproximadamente a 90,000 m². La extensión vertical de la mineralización ha sido estimada en 600 m. (Golden Rim Resources 2017), para efectos del modelo numérico se asumió una extensión vertical de 700 m para la columna de roca a modelar. La representación espacial del sistema fue simplificada a la representación más simple y eficiente posible en uso de recursos computacionales.

IV. Tasas de flujo y duración de la actividad geotermal

Las tasas de flujo y la duración de la actividad geotermal son dos de los factores en torno a los cuales hay mayor incertidumbre para depósitos de origen hidrotermal. Considerando la literatura existente en el tema se escogió una tasa de flujo de 100 kg/segundo, el principal argumento para

esta elección es que esta magnitud es considerada moderada para sistemas geotermales activos con el potencial de formar un depósito epitermal (Wilkinson et al. 2013, Simmons et al. 2016a).

Para la duración de la actividad geotermal se consideraron los resultados de los estudios numéricos de Hayba y Ingebritsen (1997) para sistemas geotermales y de Weis (2015) para sistemas geotermales en el ambiente epitermal. Estos estudios estiman la duración de la actividad geotermal en función de la permeabilidad del sistema, en un rango de 10,000-100,000 años. Por razones de recursos computacionales, específicamente la memoria necesaria para una larga simulación y el tiempo de cálculo necesario para ejecutar dicha simulación, se escogió el límite inferior de estas estimaciones.

1.6.3 Parámetros para describir el sistema geoquímico y las interacciones fluido-minerales

I. Mineralogía

Las rocas primarias asociadas al depósito Patricia en las cuales se encuentra la mineralización, son rocas volcánicas de composición andesítica sometidas a intensa alteración hidrotermal propilítica (Chinchilla 2017). Para las fases minerales primarias, previas al inicio de la alteración hidrotermal, se ha considerado la mineralogía de una andesita con bajo grado de alteración descrita para la Formación Cerro Empexa (Valenzuela et al. 2014) la cual ha sido correlacionada tentativamente con las rocas volcánicas andesíticas del depósito de Patricia (Chinchilla 2017).

La mineralogía de alteración, los sulfuros de metales base y los minerales de plata del depósito Patricia, han sido descritos detalladamente, para el sistema químico a simular se consideraron los minerales de mayor relevancia para la paragénesis del depósito con la excepción de los minerales de plata.

II. Descripción de la interacción entre fluidos y minerales

TOUGHREACT usa la formulación planteada por Lasaga (1984) para describir reacciones de precipitación y disolución producto de la interacción de fluidos y minerales en condiciones cinéticas. Los parámetros cinéticos requeridos por dicha formulación se hayan detallados en el Capítulo 2.

Para la descripción de las interacciones geoquímicas se siguieron las prácticas y métodos utilizados en estudios previos realizados con TOUGHREACT, aplicados a sistemas geotermales activos, se consideró especialmente la metodología usada por Xu y Pruess (2001) para modelar alteración mineral y flujo de fluidos en sistemas hidrotermales. Para la estimación de superficies de reacción mineral, se consideraron los resultados de las simulaciones calibradas y validadas en un sistema geotermal activo realizadas por Wanner et al. (2014) usando TOUGHREACT.

III. Estimación de la composición de las soluciones hidrotermales

En principio, al contar con datos de LA-ICP-MS para las inclusiones fluidas de los 3 estadios paragéneticos de Patricia, y asumiendo que las inclusiones son representativas de los fluidos de dichos estadios, se consideraron esos valores para las composiciones de los fluidos. Sin embargo, los análisis de LA-ICP-MS disponibles no proporcionan información válida para las concentraciones de metales en solución del estadio de mineralización. Para estimar la composición de dichas soluciones, se consideraron los datos de temperatura y salinidad estimados por medio de las inclusiones fluidas y se realizaron “batch models” asumiendo condiciones de equilibrio entre el

fluido mineralizador y la asociación mineralógica descrita para el estadio de mineralización, de esta manera fue posible estimar la composición del fluido.

2 NUMERICAL SIMULATION OF A FOSSIL GEOTHERMAL SYSTEM IN CHILE

David Calisto¹, Daniel Moncada¹, Eric Sonnenthal², Lorena Ortega³, Darío Chinchilla³

¹ Departamento de Geología, Facultad de Ciencias Físicas y Matemáticas, Universidad de Chile, Plaza Ercilla 803, Santiago, Chile

² Energy Geosciences Division, Lawrence Berkeley National Laboratory, Berkeley, CA, 94720 USA

³ Departamento de Cristalografía y Mineralogía, Facultad de Ciencias Geológicas, Universidad Complutense de Madrid, and Instituto de Geociencias IGEO (UCM-CISC), C/José Antonio Novais, s/n, 28040, Madrid, Spain

2.1 ABSTRACT

Fossil and active geothermal systems are products of a series of complex processes that are related to the amount of ore fluid that flows through the system, depositional efficiency, concentration of metal in the ore fluid, and the duration of the ore-forming process. Of all these factors, the duration of the mineralizing event is one of the least understood aspects of ore genesis.

We used fluid inclusion data, chemical compositions of base metal sulfides, and fluid flow rates to constrain a numerical model of a fossil geothermal system, as the Patricia Zn-Pb-Ag deposit located in northern Chile. The Patricia deposit consists of quartz and base metal sulfide veins of hydrothermal origin with structural control, hosted in a volcanic succession with intense propylitic alteration. The fluid inclusion data indicates that the hydrothermal fluids were liquid-rich and had circulation temperatures that range from 215 to 140°C, and salinities between 22 to 1 wt.% NaCl, with no evidence of boiling in the system. Sulfide mineralogy indicates low to intermediate sulfidation conditions.

Hundreds of models were evaluated using the reactive-transport code TOUGHREACT to identify the most relevant geochemical and transport parameters controlling the formation of this fossil geothermal system. The paragenesis of the deposit is mimicked by a model of successive stages of fluid circulation consistent with the observed mineral assemblage distribution, the fluid inclusion data and the estimated resources in the deposit.

First, the entire geothermal activity of the system was modeled considering 10,000 years of fluid-rock interaction. In this model, periods of circulation of metal-barren fluids are followed by metal-rich fluids driving the ore formation. Base metal solubility with predominant chloride complexing suggests that the most efficient ore-forming mechanism for the Patricia deposit was the result of the interaction of two different fluids, one fluid transporting metals and another fluid transporting reduced sulfur mixing in a rock volume of high permeability. Mass balance estimations with this model give a period of 3,500 to 5,000 years for the ore stage duration in which all the ore resources of the Patricia deposit could have been precipitated by fluid mixing.

In a second model, the previous estimates for the duration of the main ore stage were used to simulate the fluid-rock interaction during the ore stage for a period of 3,500 years, the second

model's results highlights: First, the importance of the permeability of the host rock enhanced by fractures to concentrate the volume of the mineralization. And second, the role of the hydrothermal alteration assemblage in controlling the circulating fluid acidity. A higher efficiency in the formation of sulfide minerals appears to coincide with pH values in a range from 5.1 to 5.3.

The results of both models are validated by replicating the system evolution, reproducing the same mineral alteration assemblage, the expected base metal resource distribution and similar amounts of ore resources to those of the Patricia deposit.

Even with simplifications, reactive-transport modeling is able to reproduce the main features of the Patricia deposit, and provide insights into the formation process of this epithermal deposit, supporting the importance of the mixing of fluids as a relevant process in the formation of sulfide base metal mineralization in the epithermal environment.

2.2 INTRODUCTION

Geothermal systems are a geologic environment, related to magmatic activity (magmatic-geothermal), with characteristic fluid circulation driven by the cooling of magmatic bodies (Henley and Ellis 1983, Hedenquist and Lowenstern 1994). This fluid flow transports mass and heat across large extents of the Earth crust, allowing interaction between the fluid and crustal rocks, this interaction has the potential to transport and concentrate metals forming hydrothermal ore deposits classified as epithermal deposits (Hedenquist and Lowenstern 1994).

The magmatic systems have a variety of expressions across different tectonic settings and since geothermal systems are spatially close to magmatic systems, the hydrothermal ore deposits, the fossil counterpart of the active geothermal systems, also display a wide degree of variability (White and Hedenquist 1990). This variability has been grouped in a continuum of ore deposits related to magmatic and hydrothermal activity known as the Epithermal-Porphyry environment (Einaudi et al 2003).

The epithermal deposits are relatively more distal to the magmatic bodies than the porphyry deposits and are classified by their mineralization in precious metals (Au-Ag) deposits and base metals (Zn-Pb-Ag) deposits. The formation of base metals epithermal deposits is comparatively less studied and less understood than the formation of precious metal mineralization.

In this paper we studied the mechanisms and formation of the Zn-Pb-Ag Patricia deposit, from northern Chile (Chinchilla et al. 2016a, Chinchilla et al. 2016b). We used a reactive transport model implemented with TOUGHREACT (Xu and Pruess 2001, Xu et al. 2011b) to understand the ore-forming process for the base metal mineralization in this deposit.

Most of our observations, assumptions and boundary conditions for our model come from field and fluid inclusion data from the Patricia deposit. These observations are supplemented by data from the physical and geochemical processes observed in active geothermal systems assuming that present processes were the same involved in the formation of fossil geothermal environments (Henley 1985). Thus, from the knowledge of active systems, we get the geochemical framework to construct a reactive transport model consistent with the available data from the Patricia deposit that provides insight into the ore-forming process of this base metal deposit.

2.2.1 Relationship between continental geothermal systems and epithermal precious metal deposits

Terrestrial hydrothermal systems are analogues of fossil epithermal systems based on similar tectonic and spatial setting, alike physical conditions and processes, alteration mineral assemblages and related fluid chemistry (White 1955, Henley and Ellis 1983, Henley 1985, Simmons et al. 2005a). Hydrothermal systems in volcanic arcs and rifts form by deep convective circulation of fluids driven by shallow intrusions of magma at < 5 km depth (White and Hedenquist 1990). Thermal and pressure gradient is controlled by the boiling point curve (Haas 1971).

Active hydrothermal systems are classified in geothermal systems and magmatic-hydrothermal systems, each type reflecting the pH of the hydrothermal solutions (Giggenbach 1984, Giggenbach 1997a, Einaudi et al. 2003, Simmons et al 2005).

Geothermal systems have reduced and near neutral pH fluids that are close to equilibrium with the altered host rock (Giggenbach 1992b). The compositions of the fluids are dominated by meteoric waters with small magmatic contributions and isotopic data shows that Cl, Pb and S are of magmatic origin (Giggenbach 1995). The circulating fluids in the geothermal systems might contain 10s to 100s ppm of H₂S (Simmons et al. 2005b). This fluid interacts with the country rock to form a propylitic alteration assemblage (Giggenbach 1997a). Active geothermal systems have a sulfidation state ranging from low to intermediate (Einaudi et al. 2003).

Magmatic hydrothermal systems are proximal to volcanic centers, with fluids that are far from equilibrium with the host rock (Einaudi et al. 2003). The fluids are oxidized and highly acidic owing a direct contribution of condensed magmatic volatiles (Simmons et al. 2005b). The hydrothermal fluids have a direct magmatic source and show little degree of rock-fluid interaction. Isotope data confirms a magmatic signature (Giggenbach 1997a). Product of the fluid circulation the magmatic hydrothermal systems display a characteristic advanced argillic alteration containing alunite and kaolinite (Giggenbach 1992a, Sillitoe and Hedenquist 2003). Magmatic hydrothermal systems have an overall sulfidation state ranging from intermediate to high and might show wide variations (Einaudi et al. 2003).

For the fluids in active hydrothermal systems their temperatures of circulation, pressure and chemical compositions are known, much of the current understanding of the epithermal deposits come from direct observation of these systems and from the comparison between the mineralogy and fluids in the active hydrothermal environment with trapped fluids in the crystals of minerals (fluid inclusions) from the fossil epithermal deposits.

However, despite all the similarities between active hydrothermal systems and epithermal deposits, there is considerable uncertainty about the nature and amount of magmatic contributions in the ore forming process. The vast majority of the active hydrothermal systems do not show significant ore formation, and even with important amounts of fluid circulation, significant economic enrichment in base or precious metals is rare in active systems (Simmons et al. 2016a). This observations suggests that the formation of epithermal ore deposits might be either episodic, requiring small periods of time for the fluid mineralized or rather a continuous process taking a long time in forming and requiring long periods of sustained hydrothermal fluid flow (Moncada et al. 2019).

One important question related to our case of study is the mechanism by which base metals are transported and deposited in the epithermal/hydrothermal environment. Base metal mineralization in epithermal deposits is associated with 23-7 wt. % NaCl equiv salinities but volcanic hosted

hydrothermal systems have salinities limited to < 7 wt. % NaCl equiv (Albinson and Rubio 2001, Bodnar et al. 2014). Furthermore, there is no known active system that is a counterpart of epithermal systems with fluids salinities >5 % NaCl equiv and similar to those salinities ranges characteristic of base metal epithermal deposits (Simmons et al. 2005b), and also there are no reports of active geothermal systems in arc settings with fluids transporting base metal concentrations > 10 ppm. We address these questions that remains uncertain through the observation of active hydrothermal systems through a reactive transport model of the Patricia deposit.

2.2.2 Characteristics of the Epithermal Base Metal Deposits

The physical conditions of formation of the epithermal deposits are given by temperatures of formation between 150-300 °C, at depths from 50 to 2000 m below the water table (Buchanan 1981, Albinson et al. 2001, Bodnar et al. 2014). The epithermal environment is under hydrostatic pressure conditions, where the pressure-temperature gradient is controlled by the boiling point curve (Haas 1971). Epithermal deposits are source of precious and base metals and the mineralization reflect the orebodies within a vertical interval of a few then to hundreds of meters.

The epithermal deposits are very diverse and highly variable in characteristics, owing this variety to a combination of physical and chemical factors therefore epithermal deposits have multiple classifications, however the more general schemes are based on alteration and gangue mineralogy (Simmons et al. 2005a), and sulfidation and oxidation states of the sulfide assemblage mineralogy (Hedenquist et al. 2000).

Two distinct end members are distinguished: The first, the low sulfidation epithermal deposits associated with quartz ± calcite ± adularia ± illite contain Au-Ag, Ag-Au, or Ag-Pb-Zn ores zones (Hedenquist et al. 2000). The ore mineralization is mostly in veins and stockworks, with colloform quartz, bladed calcite or bladed calcite preplaced by quartz and evidence of Fluid Inclusions Assemblages (FIAs) consisting of coexisting liquid-rich and vapor-rich inclusions are indicative of boiling conditions and FIAs containing only vapor-rich inclusions indicate flashing of the system (Bodnar et al. 1985, Moncada et al. 2012). Fluid inclusion studies indicate ore deposition from dilute to moderately saline solutions a temperatures between 150 C to 300 °C (Bodnar et al. 2014). The hydrothermal alteration is zoned and comprises a regional propylitic alteration, with quartz, adularia, illite and pyrite forming proximal alteration zones enveloping the ore bodies indicating fluids of neutral pH. Fluid inclusion data indicate salinities < 5 wt. % NaCl for Au-Ag deposits and <10 to >20 wt. % NaCl for Ag-Pb-Zn deposits. Stable isotope data indicate that hydrothermal solutions were composed mostly of deeply circulating meteoric water, with a variable component of magmatic fluid (Albinson et al. 2001, Bodnar et al. 2014). In these deposits sulfide mineral fluid inclusions N₂/Ar ratios indicates a magmatic source for the mineralizing fluid (Albinson et al. 2001) Gangue minerals from barren zones, have N₂/Ar ratios near air-saturated water signature indicating meteoric fluid contribution (Albinson et al. 2001).

The second end member are the high sulfidation epithermal deposits associated with quartz + alunite ± pyrophyllite ± dickite ± kaolinite assemblages containing Au ± Ag ± Cu ores (Simmons et al 2005). The characteristics of this type shows a vuggy zone and massive quartz alteration, which host ore, indicating circulation of acidic fluids. The external part of the system shows zones of quartz and phyllosilicate minerals that are surrounded by regional propylitic alteration (Simmons et al 2005). The ore distribution is controlled by structures and lithology, the sulfide assemblage ranges from intermediate to high (Hedenquist et al 2000, Sillitoe and Hedenquist 2005).

Fluid inclusion data indicate salinities between <7 to 12 wt. % NaCl and high salinities ranging between 21 to > 23 wt.% NaCl (Bodnar et al. 2014).

Fluid inclusion and oxygen and hydrogen isotope data indicate that the altering fluids are composed of magmatic fluids (vapor rich) with a minor to moderate component of meteoric water (Casadevall and Ohmoto 1977, Heald-Wetlaufer et al. 1983, Albinson et al. 2001).

At the higher depth in the system, the difference is caused by contrasting fluids, oxidized and acid fluids versus reduced and near neutral pH solutions, controlled by differences in the proportion of magmatic and meteoric components and the amount of water-rock interaction during the ascent of the fluid from the magmatic to the epithermal environment (White and Hedenquist 1990, Giggenbach 1997a, Simmons et al 2005). Higher distances from the magmatic source allows a higher degree of fluid rock interaction.

In the intermediate and main portion of the epithermal systems, it may be possible the development of boiling and/ or mixing conditions which creates abrupt physical and chemical gradients that could produce precious and base metal precipitation (Giggenbach and Steward 1982). Near the surface, on the shallow portion of the system, the position of the water table controls the hydrostatic pressure-temperature gradients at the depth where the epithermal mineralization forms (Henley 1985, Simmons et al. 2005).

Boiling is the main mechanism of precipitation for precious metals deposits, by changing the solubility of gold and silver (Kamilli and Ohmoto 1977, Buchanan 1981). Mixing of fluids of different composition, like hydrothermal brines and overlying groundwaters has been proposed as another mechanism able to produce base metal precipitation (Loucks et al. 1988, Hayba 1997).

2.2.3 Duration of mineralization events on hydrothermal deposits in the epithermal environment

During the last century many studies have improved our understanding on how much time is required to form an epithermal precious and base metal ore deposit. In this paper, we use observations of active and fossil geothermal systems, and numerical modeling to estimate the time required to form the Zn-Pb-Ag Patricia deposit.

Since the formative environments of epithermal deposits are related with those of active hydrothermal systems, it has been argued that the duration of the epithermal mineralization could be estimated from the lifetime of hydrothermal systems. We reviewed a continuation some of the studies on geothermal system's activity lifetime and on the duration and time scales of the ore formation stages in epithermal deposits, to the end of setting constrains to the time scale of our model of the Patricia deposit.

2.2.4 Previous studies to estimate the duration of Ore-Forming processes from active geothermal systems

Numerous studies have estimated the duration of the ore- forming event from active geothermal systems through mass flow balance, estimations of lifetime activity and estimates of metal budgets carried in solution by the hydrothermal fluids (Helgeson and Garrels 1968, Seward 1989, Simmons and Brown 2006, Moncada et al. 2019). Ore formation estimates through these methods have reported intervals between of 10,000 to 100,000 years.

Brown (1986) estimated that up to 4.7 kg/year of gold are transported through the Broadlands geothermal system, New Zealand, at minimum concentration of 1.5 ppb Au for an average up-flow rate of 100 kg/s, so, with this metal flux a deposit of 100 tonnes of gold could have been formed in a period < 25,000 years.

Hedenquist et al. (1993) estimated from measured metal fluxes, for the White Island volcanic hydrothermal system, New Zealand, the availability of 106 t of Cu, and 45 t Au over 10,000 years of hydrothermal activity.

Simmons and Brown (2006), considered a flux rate of 50 kg/s and measured concentrations of 0.05-0.2 ppb Au to calculate a total gold flow of 24 kg/year and estimated a total period of 55,000 years to account for all the gold (1,300 tons) in the Ladolam deposit, Papua New Guinea.

Heinrich (2007), considered the same flow conditions that Simmons et al. (2006) for the Ladolam deposit. However, the gold concentrations measured by Simmons and Brown (2006) are 100 to 1,000 times lower than measured gold concentrations in fluid inclusions in ore deposits with similar characteristics. A fluid with higher concentrations of sulfide and gold, similar to those of fluid inclusions, could form the Ladolam deposit under the same flow regime in an even shorter period of time < 1,000 years.

The Reykjanes geothermal system, Iceland, deep liquid fluids contain 14-17 ppm Cu, 5-27 ppm Zn and 9-140 ppm Fe. With a flux rate of 100 kg/s estimated from a heat flow of 130 MW and average metal concentrations, the metal flux for year is up to 47 t of Cu and Zn each, assuming a constant mass flux and metal concentrations, in 10,000 years of activity almost 0.5 Mt of Cu and Zn would have precipitated in the Reykjanes geothermal system (Hardardóttir et al. 2009).

The Rotokawa geothermal system, New Zealand, has an estimated flux rate of 150 kg/s with a flux of gold (37-109 kg/yr) and silver (5,200-11,400 kg/yr) higher than the estimated flux for the Ladolam geothermal system. Under constant metal and flow rates a world class precious metal deposit could be formed in < 20,000 years (Simmons and Brown 2007).

Simmons et al. (2016a) estimated fluid flux rates between 50-300 kg/s for individual systems, and 890-1,070 kg/s for the entire Taupo Volcanic Zone, with a total metal flux of 34-120 kg/y Au, and 37,900-107,600 kg/y Cu.

Therefore, active geothermal systems that could sustain similar fluid flow rates and metal fluxes for 10,000 to 100,000 years have significant ore forming potential.

2.2.5 Previous studies to estimate the duration of Ore-Forming processes from fossil epithermal systems

Various estimations for the duration of the ore stage in epithermal deposits have been made using measured metal concentrations from fluid inclusions and flow rates. The estimates of metal budgets and measured metal contents from an ore solution extracted from fluid inclusions from the ore of the Cerro Proaño Ag-Pb-Zn epithermal deposit, Fresnillo district in Mexico, suggests that ore formation could be even faster than the estimates obtained from active hydrothermal systems. LA-ICP-MS analysis of fluid inclusions of this epithermal deposit have reported Ag, Pb and Zn concentrations around 10's ppm, with an average of 14 ppm of silver and a maximum of 27 ppm, and maximum values around 40-60 ppm for Pb and Zn (Wilkinson et al. 2013). These concentrations are one order of magnitude higher than the measured in active hydrothermal

systems. Given an up-flow rate of 100 kg/s, a moderate up-flow rate relative to active hydrothermal systems, the required time to deposit all the silver produced in the Fresnillo district would be approximately 500 y (Wilkinson et al. 2013).

The temporal distribution of these fluids in the paragenetic sequence of this deposit suggest also an episodic occurrence of mineralization, through intermittent injection of Ag-rich brines of magmatic origin into an otherwise barren hydrothermal system (Wilkinson et al. 2013).

For the Ag-Pb-Zn Creed deposit, Colorado, the reconstruction of the formation of iron gradients in banded sphalerite by thermal diffusion, have given estimates between 1,000-10,000 years for the duration of mineralization event in this deposit (Campbell and Barton 2005).

A common conclusion from these studies on fossil epithermal systems, is that the ore stage period in a hydrothermal deposit represents only a fraction of the overall formation and lifespan of the hydrothermal system (Wilkinson et al. 2013, Moncada et al. 2019)

2.2.6 Previous studies to estimate the duration of Ore-Forming processes from permeability and numerical simulations

Numerous studies have been made to estimate the lifetime of hydrothermal systems and constraint the duration of the mineralization stage on hydrothermal deposits using numerical models. The range of lifetime estimates obtained through this approach range from 10^4 to $<10^6$ years (Cathles 1977, Norton and Knight 1977, Cathles et al. 1997, Hayba and Ingebritsen 1997, Moncada et al. 2019) and the range for the mineralization stage is from 10^3 to 10^5 years (Kostova et al. 2004, Weis 2015, Zou et al. 2017, Hu et al. 2020).

This studies have explored the physical processes related to a single hydrothermal system in the vicinity of a magmatic intrusion (Weis 2015). After evaluation of multiple variables controlling the life-time activity of a hydrothermal system related to a single magmatic intrusion, a major conclusion is that the permeability distribution of any system coupled with the heat supply from a magmatic source exerts the main control over the hydrothermal system evolution (Cathles 1977, Hayba and Ingebritsen 1997, Driesner and Geiger 2007).

The relevance of the intrinsic permeability distribution of a hydrothermal system cannot be overestimated: permeability determines how fast ground water can flow through a porous rock, therefore constraining the fluid circulation regimen of the hydrothermal system and controlling the fluid flow, the thermal balance and the transport of mass within the system (Ingebritsen et al. 2010, Ingebritsen and Appold 2012).

Permeability determines the system's cooling rate and the occurrence of processes such as fluid advection (Cathles 1977, Norton and Knight 1977) and boiling (Hayba and Ingebritsen 1997, Driesner and Geiger 2007, Weis 2015) and also provides a physical constraint in the duration of these processes and on the lifetime of an active geothermal system.

Permeability in the geologic media has an ample range over all the different rocks in the crust. However, three values have critical importance: 10^{-20} m², 10^{-16} m², and 10^{-15} m², (Ingebritsen and Appold 2012) in the behavior of any given system (Figure 4).

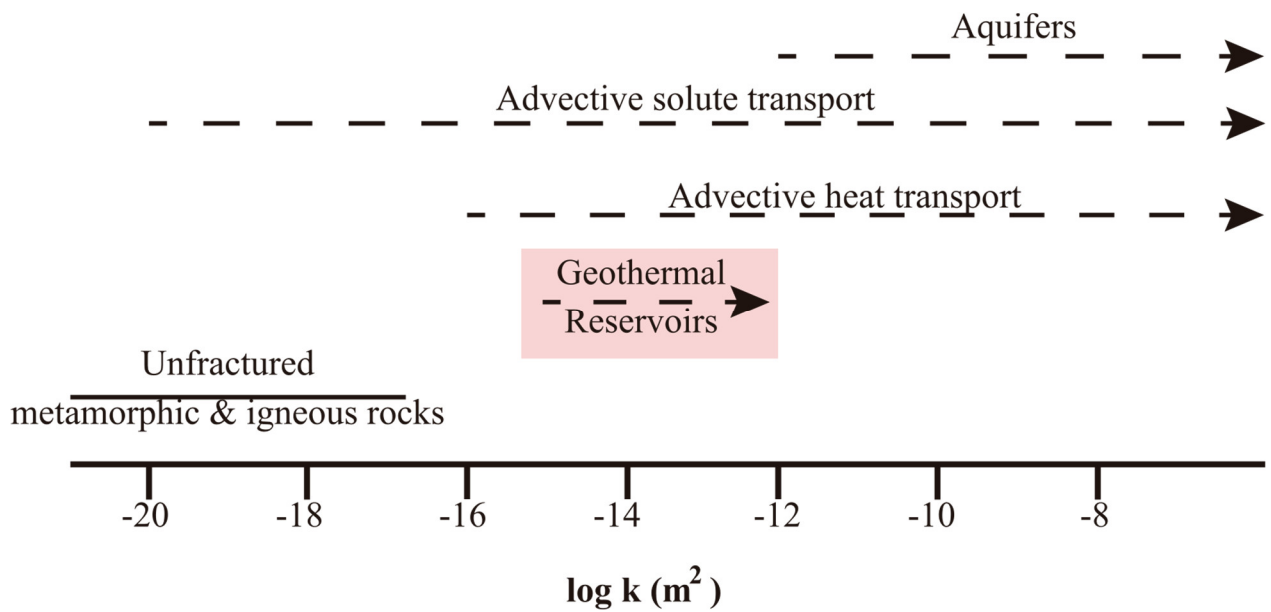


Figure 4. Range of permeabilities observed in geological media. Showing characteristic process-limiting values. Geothermal systems are hosted in rocks with high permeability than unfractured rocks but lower than typical aquifers values. Sustained fluid and heat circulation through advection requires permeability higher than 10^{-16} m^2 for an active geothermal system. For commercially viable geothermal reservoirs the minimum permeability is $\sim 10^{-15} \text{ m}^2$. After Ingebritsen and Appold (2012)

An intrinsic permeability of 10^{-20} m^2 allows advective mass transport, but heat transport occurs by conduction (Ingebritsen and Appold 2012). A permeability of 10^{-20} m^2 is considered very low for a hydrothermal system (Driesner and Geiger 2007).

The permeability value of 10^{-16} m^2 allows the occurrence of free heat and solute advection on a hydrothermal system (Norton and Knight 1977), for reference most viable geothermal reservoirs have permeabilities $\sim 10^{-15} \text{ m}^2$ (Ingebritsen and Appold 2012). Numerical models have also corroborated that the optimal value for generating a hot and potentially vapor-rich geothermal reservoir is 10^{-15} m^2 (Hayba and Ingebritsen 1997, Ingebritsen and Appold 2012).

Systems with permeabilities of 10^{-16} m^2 or less, are conduction dominated and they can sustain elevated temperatures near the magmatic intrusion for more than 50,000 years but with modest increases of the near surface temperature (Cathles 1977, Hayba and Ingebritsen 1997).

At permeabilities of $\sim 10^{-15} \text{ m}^2$, boiling conditions persist for thousands of years, boiling being possible for up to 20,000 years (Hayba and Ingebritsen 1997). The highest lifetime of a modeled hydrothermal system with a mean permeability of 10^{-15} m^2 has been estimated to be 800,000 years, so, in systems with longer periods of activity, the occurrence of multiple intrusions is suggested (Cathles et al. 1997).

Systems with permeabilities $> 10^{-15} \text{ m}^2$ have decreasing temperatures and life spans: a system with a permeability of 10^{-14} m^2 last for $\sim 5,000$ years with limited boiling and a more permeable system ($10^{-13.5} \text{ m}^2$) last for $< 3,500$ years without evidence of boiling (Hayba and Ingebritsen 1997). These results constrain the duration of the thermal event associated to the ore stage formation in epithermal environments as a function of the overall permeability of the system (Driesner and Geiger 2007).

Porphyry and epithermal ore deposits share a common relationship to magmatic intrusions (Hedenquist and Lowenstern 1994), but they also have clear differences: porphyry deposits are nearer to magmatic intrusions than epithermal deposits, this feature causes important differences in the conditions of each deposit type specially in their physical characteristics:

Porphyry systems fluid temperatures favorable to ore precipitation are in the 450-350 °C range (Landtwing et al. 2005, Bodnar et al. 2014) higher than for epithermal systems <300°C (Bodnar et al. 2014). Porphyry systems have also lower permeabilities ($< 10^{-16} \text{ m}^2$) than epithermal systems ($>10^{-16} \text{ m}^2$) and therefore longer periods of cooling and hydrothermal activity (Weis 2015).

Weis (2015) realized numerical simulations of the hydrology of porphyry copper and epithermal gold systems, considering multiphase fluid flow of H₂O-NaCl fluids and a dynamic permeability model describing the transition from brittle to ductile rock behavior and hydraulic fracturing. His simulations highlight the importance of the permeability, salinity and topography in the development of the porphyry-epithermal environment. According to his results, the entire ore-forming event in the porphyry-epithermal environment is predicted to last between 50,000 and 100,000 years for permeabilities in the range of 10^{-13} to 10^{-14} m^2 .

Hu et al. (2019), obtained similar results from numerical simulations of the Chatin Cu-Au porphyry deposit, China, combining predicted chemical reaction rates of chalcopyrite with known grades of Cu within the deposit, to estimate an ore-forming period of 9,600 – 75,000 yr for the Chatin deposit.

Epithermal systems have higher permeabilities distributions than porphyry systems, and near-hydrostatic pressure conditions. Under these conditions the life-time period of the associated hydrothermal system is between 10^3 to 10^4 yr (Cathles 1977, Hayba and Ingebritsen 1997).

Kostova et al. (2004), coupled the numerical simulations of Hayba and Ingebritsen (1997) with fluid inclusion spatial and thermal data of the Yuzhna Petrovitsa, Pb-Zn ore deposit of Madan, Bulgaria. They observed that the characteristic temperatures of each stage of the paragenetic sequence of the deposit were related to the thermal profile inferred by numerical modeling for a hydrothermal system with a permeability of 10^{-15} m^2 . In their numerical model the thermal event with similar temperatures ranges as the ore stage of the ore deposit lasted for up to 2,500 years (Driesner and Geiger 2007).

Zhou et al. (2017) for the Hutouya Pb-Zn skarn deposit, China, using numerical simulations to calculate reaction rates of sulfide minerals and considering known grades of Pb and Zn for the deposit, estimated the duration of the mineralizing process of galena and sphalerite to 10,000 to 60,000 years and 30,000 to 100,000 years respectively.

According to numerical models then, the formation and lifespan of a hydrothermal system depends mainly on the permeability structure of the host rock to the intrusion. Numerical models provides also further insight into the relationship between hydrothermal systems, geologic structures and ore mineralization, since the permeability structure of a system can be enhanced by the presence of geologic structures in a tectonic active crust (Ingebritsen et al. 2010, Weis 2015). Numerical models have shown how structures enhanced permeability and allow focused fluid circulation with increasing the potential of a hydrothermal system to produce mineralization rapidly (Cathles et al. 1997, Hayba and Ingebritsen 1997, Ingebritsen and Appold 2012).

2.3 GEOLOGICAL BACKGROUND OF THE PATRICIA DEPOSIT

The Patricia Zn-Pb-Ag deposit is an epithermal deposit of intermediate sulfidation. Patricia is located in the north of Chile, in the I Tarapacá Region ($19^{\circ} 51' S$, $69^{\circ} 6' W$) in the northern end of the Late Eocene-Oligocene metallogenic belt in Chile (Figure 5).

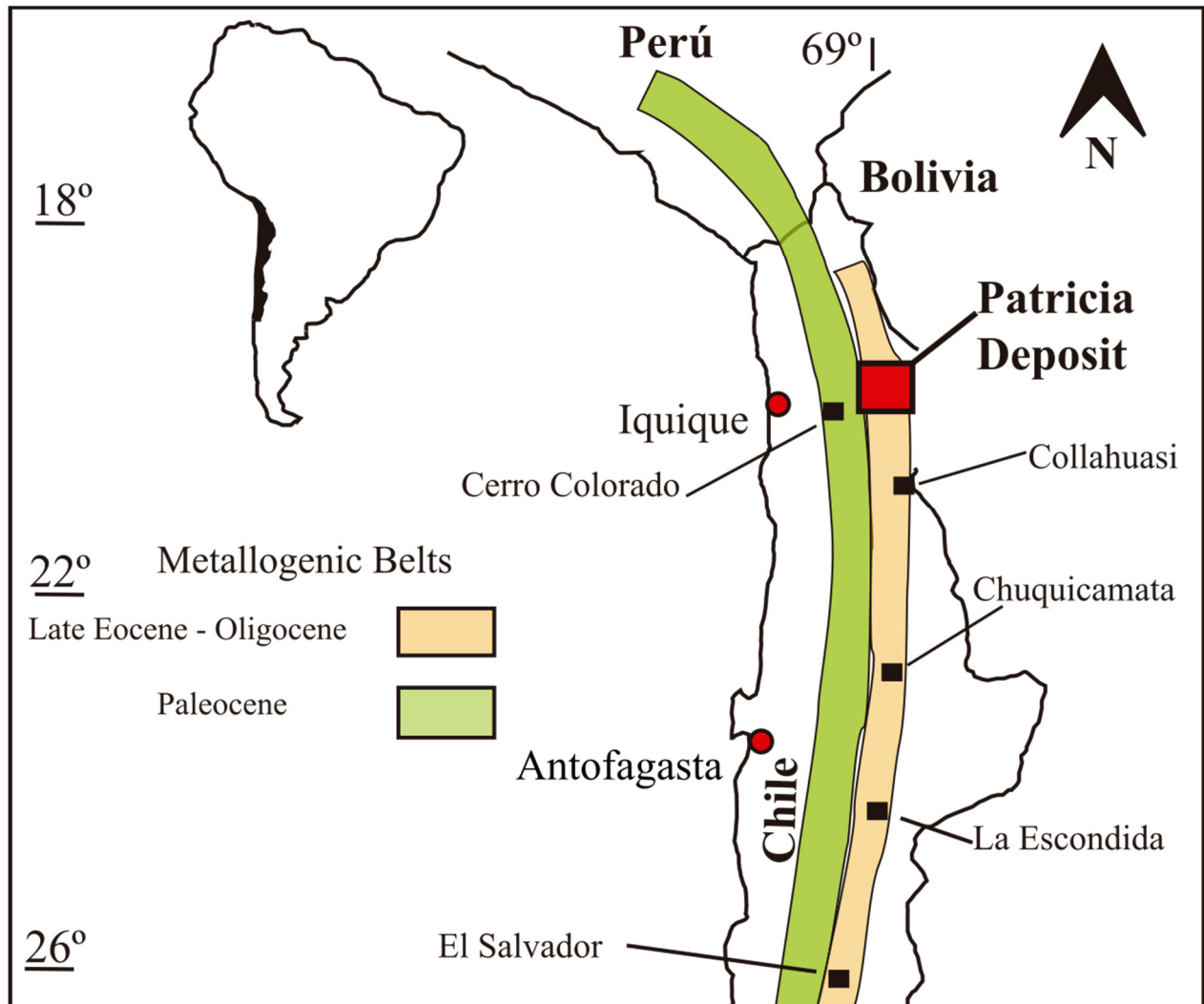


Figure 5. Ubication of the Patricia Zn-Pb-Ag ore deposit. Patricia is an unusual deposit in the Eocene-Oligocene metallogenic belt of northern Chile known for hosting porphyry copper deposits such as Chuquicamata and La Escondida. Modified from Chinchilla et al. (2016b).

The deposit is hosted in andesitic and sedimentary clastic rocks with an age of 75 ± 2 Ma (U/Pb) (Chinchilla et al. 2016b, Chinchilla 2017).

The deposit outcrops in an area of 2 km^2 and is divided in two blocks, by a set of NW-SE inverse faults (Figure 6). The western block represents a shallower part of the system with occurrence of cherts, amorphous silica and jasperoids, interpreted as thermal springs exposures (Chinchilla et al. 2016b). The eastern block represents a deeper portion of the system, with shallower levels not observed, this portion is the most studied of the Patricia deposit.

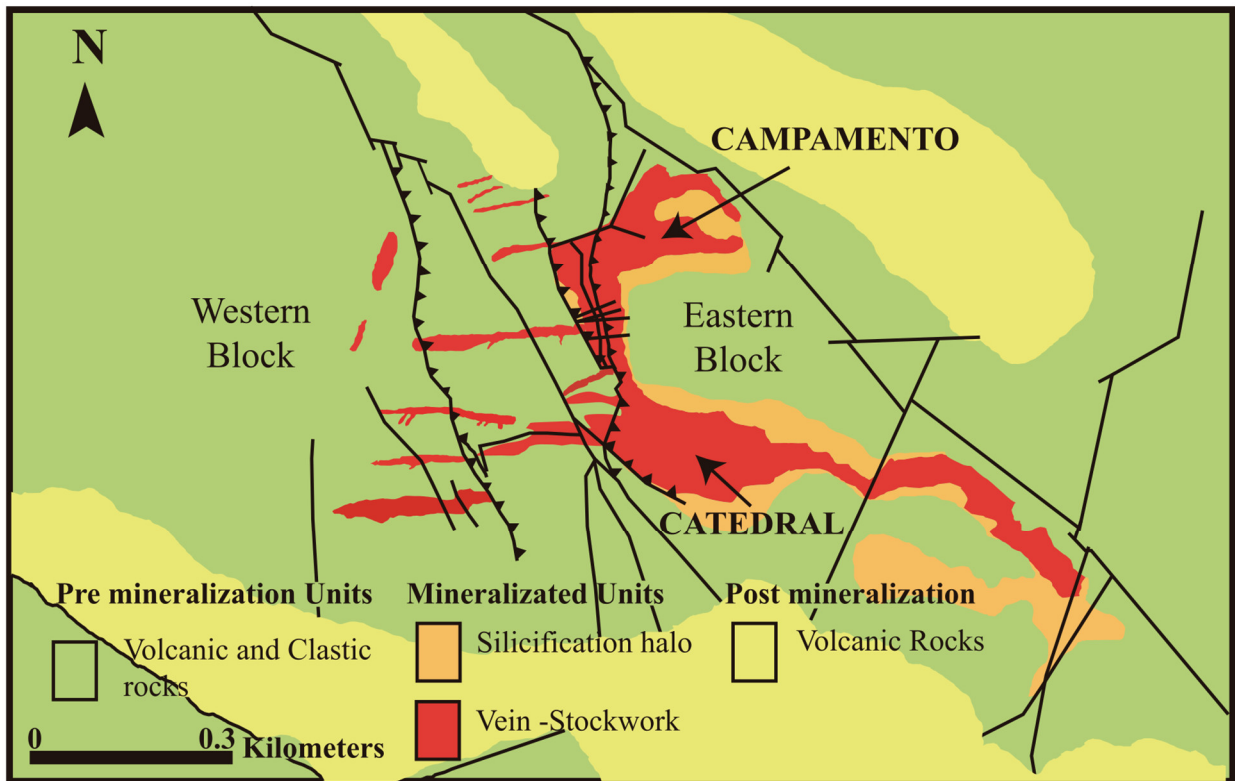


Figure 6. Geological map of the Patricia deposit showing main lithological units, and the main mineralized veins Campamento and Catedral. Patricia is divided in two blocks, the western and eastern block, the latter being more exposed. The deposit is exposed within an area of 2 km² of extension, but most of the mineralization is related to the fault structures confined to a smaller area (in red) of ~90,000 m². Modified from Chinchilla et al. (2016b).

The ore body consists of a system of subvertical veins of E-W orientation forming internally a stockwork of veinlets from 1 to 10 cm wide. The structural and textural features of the deposit indicate that the tectonic activity was an important factor in the formation of the deposit. The estimated mineral resources of the Patricia deposit are 2.4 Mt, grading 5.0% Zn, 1.4% Pb and 88g/t Ag, with an estimated model resource with a depth of 600 m, the deepest hole reported the higher grades intercepts leaving the resource open at depth (Golden Rim Resources 2017).

2.3.1 Mineralogy

The host rocks of Patricia are subaerial volcanic rocks: breccias and tuffs of andesitic composition. Host rocks are affected by intense propylitic hydrothermal alteration, with primary textures being poorly preserved. The propylitic alteration is overprinted by chloritization and sericitization. Chlorite and illite also occur associated with the mineralization in the veins (Chinchilla et al. 2016b).

The most abundant ore minerals in the Patricia deposit are pyrite, sphalerite, galena and arsenopyrite with minor amounts of chalcopyrite, pyrrotite and Ag-bearing minerals (Chinchilla et al. 2016b).

2.3.2 Textures and Paragenesis

Veinlets present open-space filling textures, symmetric and asymmetric banding and comb textures, and show evidence of opening of the earlier veinlets followed by the development of new ones. The ore mineralization is in symmetric, asymmetric and massive veins, and also disseminated in the host and in brecciated sulfides cemented with quartz (Figure 7). These textures indicate hydrostatic pressure conditions during the formation of the veins. According to the different veins and their textural relationships observed, three stages of mineralization have been defined (Figure 8). These are: the pre-ore stage, the base-metal and silver main stage and the post-ore stage (Chinchilla et al. 2016b)

Minerals	Stage 1	Base Metal Stage		Stage 3
		2A	2B	
Quartz	—	---	---	—
Pyrite	—	---	---	---
Sphalerite		—	—	
Galena			—	
Fluid Inclusion T_h (°C) Salinity (wt. %NaCl)	205-336 6-22	172-248 1-9	138-182 2-10	175-215 4-8

Figure 7. Simplified paragenesis of the Patricia deposit. Three paragenetic stages are defined: The pre-ore stage (1) with precipitation of early quartz and pyrite. The main ore stage (2) which has two substages: 2A with precipitation of sphalerite only; and 2B with precipitation of both sphalerite and galena. The post-ore stage (3) has precipitation of mainly late quartz. After Chinchilla et al. (2016a).

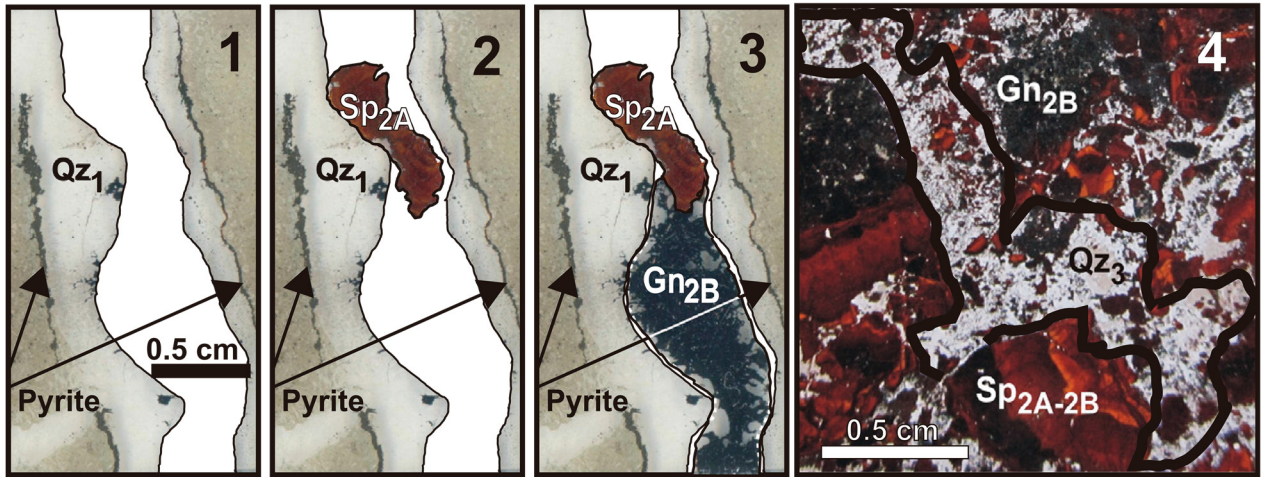


Figure 8. Sulfides mineralization in a symmetric vein of the Patricia deposit. In (1), (2) and (3) is possible to appreciate the paragenetic sequence from the pre-ore stage up to the end of the ore stage. (1) Pre-ore stage mineralization with quartz and pyrite in the rim of the vein. (2) Substage 2A, with just sphalerite filling reopened veinlets of the pre-ore stage. (3) Substage 2B, mineralization of sphalerite and galena. (4) Brecciated sulfides of the second substage filled with late quartz in the post-ore stage. Modified from Chinchilla et al. (2016a), (Chinchilla et al. 2016b).

The pre-ore stage is represented by quartz, pyrite and arsenopyrite in veins, some of them later filled with sphalerite and galena during the main stage of mineralization.

The base-metal and silver stage are divided in two substages (2A and 2B). The substage 2A has sphalerite and minor amounts of chalcopyrite and pyrrhotite. During substage 2A chlorite in the mineralized veinlets outlines sphalerite bands, forming rhythmic banding with sphalerite and is intergrowth with sphalerite and quartz. Chlorite formed during substage 2A is coeval to sphalerite and has been classified as chamosite (Fe-chlorite) (Chinchilla et al. 2016a).

The substage 2B is characterized by precipitation of sphalerite and galena, with minor chalcopyrite, pyrrhotite and Ag-bearing minerals in close textural relationship with galena, the most abundant of these Ag mineral phases is freibergite. During substage 2B, chlorite is not observed in paragenesis with the sulfide minerals in the veins (Chinchilla et al. 2016a).

The post-ore stage is characterized by brecciation of the sulfides of the second stage, the precipitation of late quartz, and minor sulfides cementing the brecciated sulfides of the second stage, and filling small veinlets.

2.3.3 Fluid Inclusions and Fluid Evolution path for the Patricia deposit

An evolution path for the fluids in the Patricia deposit has been proposed from the fluid inclusion data (Figure 9). Fluid inclusions from the pre-ore stage, have homogenization temperatures ranging from 236 to 205 °C, and salinities from 22 to 6 wt.% NaCl, some primary fluid inclusions have trapped illite crystals. In the base-metal and silver stage, for the substage 2A homogenization temperatures range between 248 to 172 °C, and salinities from 9 to 1 wt.% NaCl. The presence of chlorite within mineralized veins of substage 2A, allowed the use of chlorite as geothermometer to provide another temperature estimate for this mineralization, different methods were applied to

samples of chlorites from substage 2A, a maximum estimated temperature of 308° was obtained, with most of the estimated temperatures values being below 300°C, with a mean value of 260°C (Chinchilla et al, 2016a).

The late substage 2B, homogenization temperatures range 182 to 138 °C, with salinities between 10 to 2 wt.% NaCl. The temperatures estimated from fluid inclusions are in agreement with estimates using freibergite as a geothermometer. According to the freibergite geothermometer, most of the Ag mineralization from substage 2B took place in the interval between 230°C to <170°C, with most of the temperature estimates being <170°C (Chinchilla et al, 2016b).

Finally, fluid inclusions in the post-ore stage have homogenization temperatures between 232 to 150 °C and salinities between 8 to 2 wt. % NaCl, quartz inclusions from this stage also have trapped illite crystals.

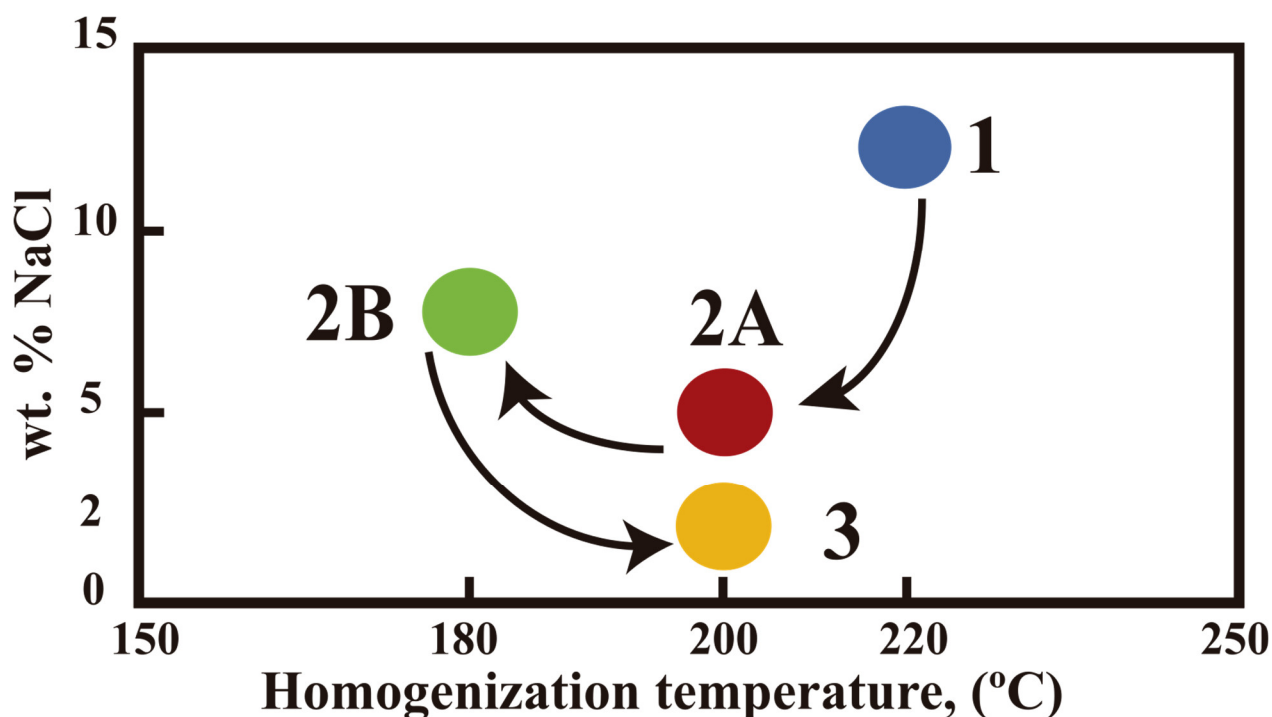


Figure 9. A possible fluid evolution path for the Patricia deposit showing mean homogenization temperatures and salinities for each stage from fluid inclusion data by Chinchilla et al. (2016b): (1) Pre-ore stage, with a mean temperature of ~220 °C and ~10 wt.% NaCl. The second stage is the Main ore stage, divided in two substages The first substage 2A has mean values of ~200 °C and ~5 wt. % NaCl and the second substage of ~180 °C and ~7 wt. % NaCl. Finally, the last stage is the post-ore stage with mean temperatures and salinities of ~200 °C and ~2.5 wt. % NaCl. For each stage, the temperatures are minimum estimates from fluid inclusion data.

No evidence of boiling was observed for the Patricia deposit (Chinchilla et al. 2016b). The evolution across each stage of temperature, salinity and absence of boiling, indicate that the mineralizing conditions changed over time and suggests that progressive cooling was the most likely process of mineral precipitation (Chinchilla et al. 2016b, Chinchilla 2017) (Figure 6).

The proposed model for the formation of the Patricia deposit states the following:

For the pre-ore stage, the observed salinity variation suggests a process of mixing between a brine and a more diluted fluid, the presence of illite within fluid inclusions of quartz grains of this stage, indicates that mineralization at this stage was under slightly acidic conditions, since illite is formed at pH from 5.8 to 6.3 (Romberger 1991).

For the main ore stage, the decrease of temperature from 250°C to 140°C with cooling at constant salinity (10-2 wt.% NaCl) suggests that cooling was the most important process for the main stage of ore precipitation (Chinchilla et al. 2016b).

A magmatic source of sulfur, evidenced by isotopic analysis (Chinchilla 2017) with a single fluid going under cooling are the main features of this stage. Under these conditions the ore metals were mainly transported as bisulfide complexes that became destabilized by cooling of the fluid resulting the precipitation of the base metal sulfides (Chinchilla 2017).

It has been discussed as a possibility the occurrence of dilution from stage 1 to stage 2, after isotopic analysis of oxygen sampled from the chlorites formed in substage 2A suggests the occurrence of mixing between fluids of meteoric and magmatic composition.

However, the progressive cooling of an ore fluid transporting base metals as sulfide complexes has been proposed to be the main ore forming mechanism for the Patricia deposit (Chinchilla 2017).

Finally, for the post-ore stage, the increased temperature of the fluids of this stage, suggests the introduction of a new pulse of hot fluids into the system.

2.3.4 Fluid Metal Content in Fluid Inclusions from the Patricia deposit

Elemental concentrations of inclusion fluids were measured using an Agilent 7500ce quadrupole ICP-MS coupled to a GeolasPro Excimer 193-nm ArF laser ablation system housed in the Department of Geosciences Fluids Research Laboratory at the Virginia Polytechnic Institute and State University. The instrument was calibrated to the NIST 610 glass standard. Samples were ablated in a 1.5 cm³ ablation cell using a laser output energy of 150 mJ and adjusting beam diameter to ensure ablation of the entire fluid inclusion. The ablated material was transported from the ablation cell by He gas flowing at a rate of 0.7 mL/min. The analyte was then mixed with 1.03 L/min Ar gas before introduction into the plasma. The ICPMS was operated at an RF power value of 1,500 W with a dwell time per isotope of 10 ms only for silver 3 ms. Reduction of the LA-ICP-MS fluid inclusion data was carried out using the AMS 6.1.1 software (Mutchler et al., 2008). Calculation of absolute elemental concentrations in fluid inclusions was accomplished using Na as an internal standard. An independent determination of Na concentration in the fluid inclusions was obtained from the last ice-melting temperature, which was converted to wt %NaCl using the equation of state of Bodnar (1993).

For the pre-ore stage, fluid inclusions in quartz have <1 ppm Zn, <2 ppm Pb, and 7 ppm Fe. For the main ore stage, fluid inclusions in sphalerite from Substage 2A, average 8 ppm Cu, and 0.1 ppm Pb. Fluid inclusion data from substage 2B, has average contents of 2 ppm Cu, and 10 to 35 ppm Pb in sphalerite crystals (Chinchilla 2017). For the post-ore stage, fluid inclusions in quartz have average contents of 1 ppm Zn and 0.4 ppm Pb (Chinchilla 2017).

2.4 CONCEPTUAL MODEL FOR THE FORMATION OF THE PATRICIA DEPOSIT

At first a conceptual model with a single fluid undergoing cooling carrying both base metals and sulfur together in solution was considered, as proposed by previous research on the Patricia deposit. A numerical model was made with the data of the Patricia deposit using TOUGHREACT. However, after numerous variations in the model configuration it was found not possible to form an extended vertical horizon of base metal mineralization, in our models the base metal mineralization was exclusively formed at the deepest level of our model, and base metals could not be carried by the fluid through the upper levels of the system.

Following this unexpected results, batch models with the fluid data were made with TOUGHREACT to understand the behavior of the potential ore fluids of the Patricia deposit. Our first important result was that for a fluid with temperatures of 300°C or less, with salinities between 15 to 1 wt.% NaCl, base metal transport is dominated by chloride complexes, sulfide complexing being of minor relevance for the temperature and salinity ranges of the Patricia deposit (Fig 11 (C)). Upon further review of the literature, it was found that for temperatures <400°C, Cu, Zn and Pb transport is dominated by chloride complexes over sulfide complexes (Zhong et al. 2015). Even if bisulfide base metal complexes were dominant for temperatures <300°C, simple cooling is not effective to form base metal sulfides given the stability of bisulfide complexes at temperatures <300°C as seen in Fig 11(C) (Bouvier and Barnes 1987).

Through batch modeling with ToughReact we could not find a fluid which could transport both reduced sulfur and metals for temperatures ranging 300 to 140°C, and salinities ranging 10 to 1 wt.% NaCl and which could also precipitate base metal sulfides by simple cooling along an extended vertical horizon.

After these results, an alternative conceptual model (Figure 10) that accounted for the features of the Patricia deposit, was proposed with the assumption that the ore forming solution transported base metals through chloride complexing, looking to further constrain the composition of the ore forming solutions and understand the formation of base-metal sulfide minerals in this ore environment.

This model for the Patricia deposit has the same general features than the classic model for the porphyry-epithermal environment (Hedenquist and Lowenstern 1994), with a deep magmatic source of heat and fluids and permeability conditions that allow fluid convection and is also based on the model for the formation of the Patricia deposit proposed by Chinchilla (2017).

The fluid flow and hydrothermal circulation is described by the combination of an up-flow stream, where the hydrothermal solution rises from the depth to shallower levels; coupled together with a lateral flow stream that may provide a different fluid of meteoric composition (Hedenquist and Lowenstern 1994, Weis 2015). Given the structural control over the mineralization, we assumed that the structures of the Patricia deposit controlled the fluid flow during the active period of the system, and that the hydrothermal fluid flow was focused through these structures. For this reason, we considered for the area of our model only the surface area of the deposit related to the structures, our analysis will also look to describe the evolution of the fractures that became the ore veins.

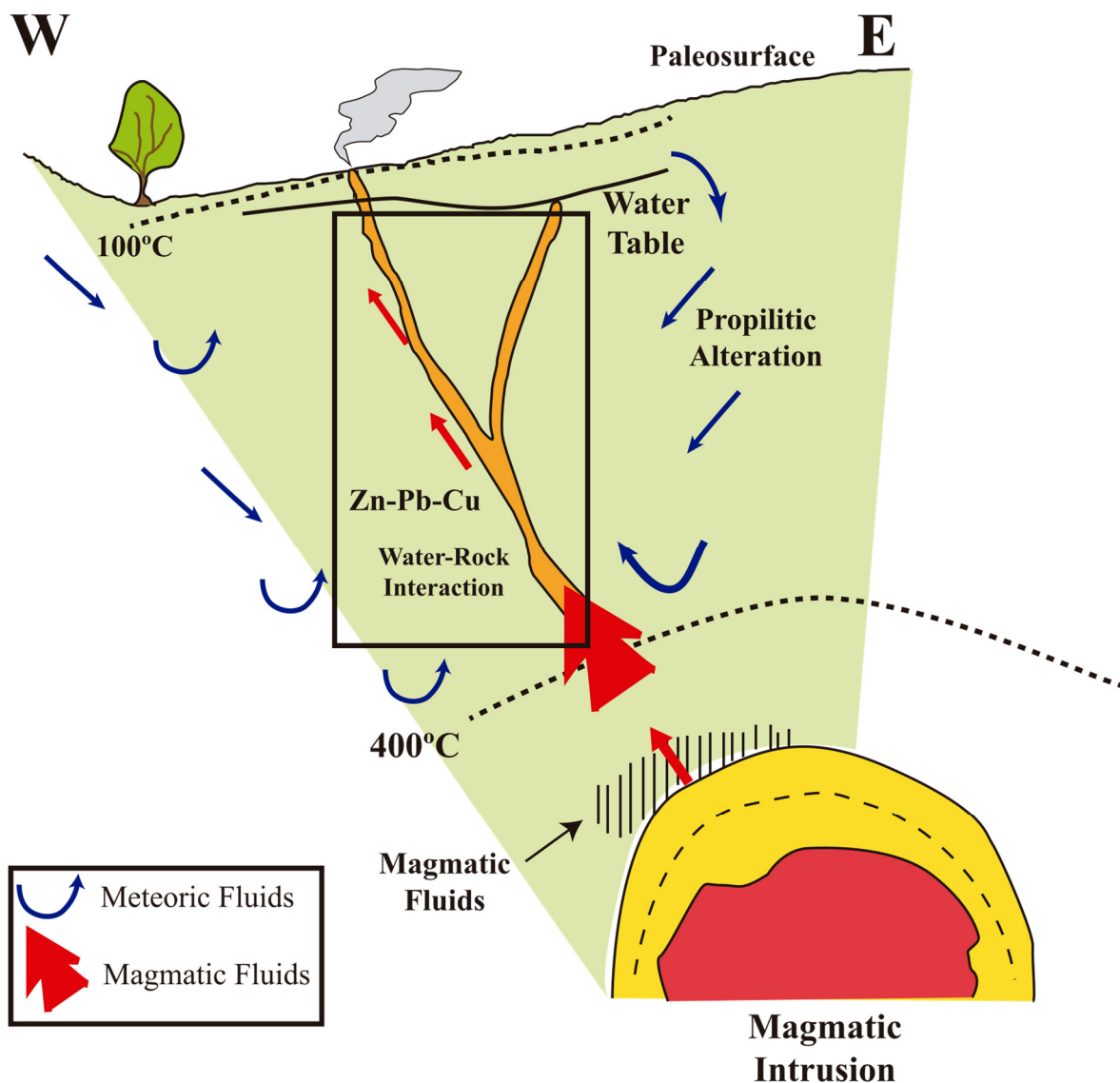


Figure 10. Conceptual model of the Patricia ore deposit, this model is built upon the model for the Patricia deposit proposed by Chinchilla (2017): In the vicinity of the volcanic rock formation hosting Patricia, of high enough permeability to allow sustained fluid convection, a magmatic intrusion at an unknown location formed and sustained a convective cell of hydrothermal fluids forming the geothermal system that gave origin to the Patricia deposit. The fluid-rock interaction formed the extended propylitic alteration in the rocks with lower permeability, and in the zones of higher permeability fractured by the activity of the tectonic structures, focused flow of episodic pulses of metal bearing fluids from a deep magmatic brine and mixing with meteoric fluids incorporated by lateral flow forms the Zn-Pb-Ag mineralization. The only difference between this model and the one previously proposed for Patricia is that fluid mixing is an active process for all the system's lifetime, including the main ore stage. The rectangle shows the system's section considered for the model (Modified after Albinson et al. 2001, Chinchilla 2017).

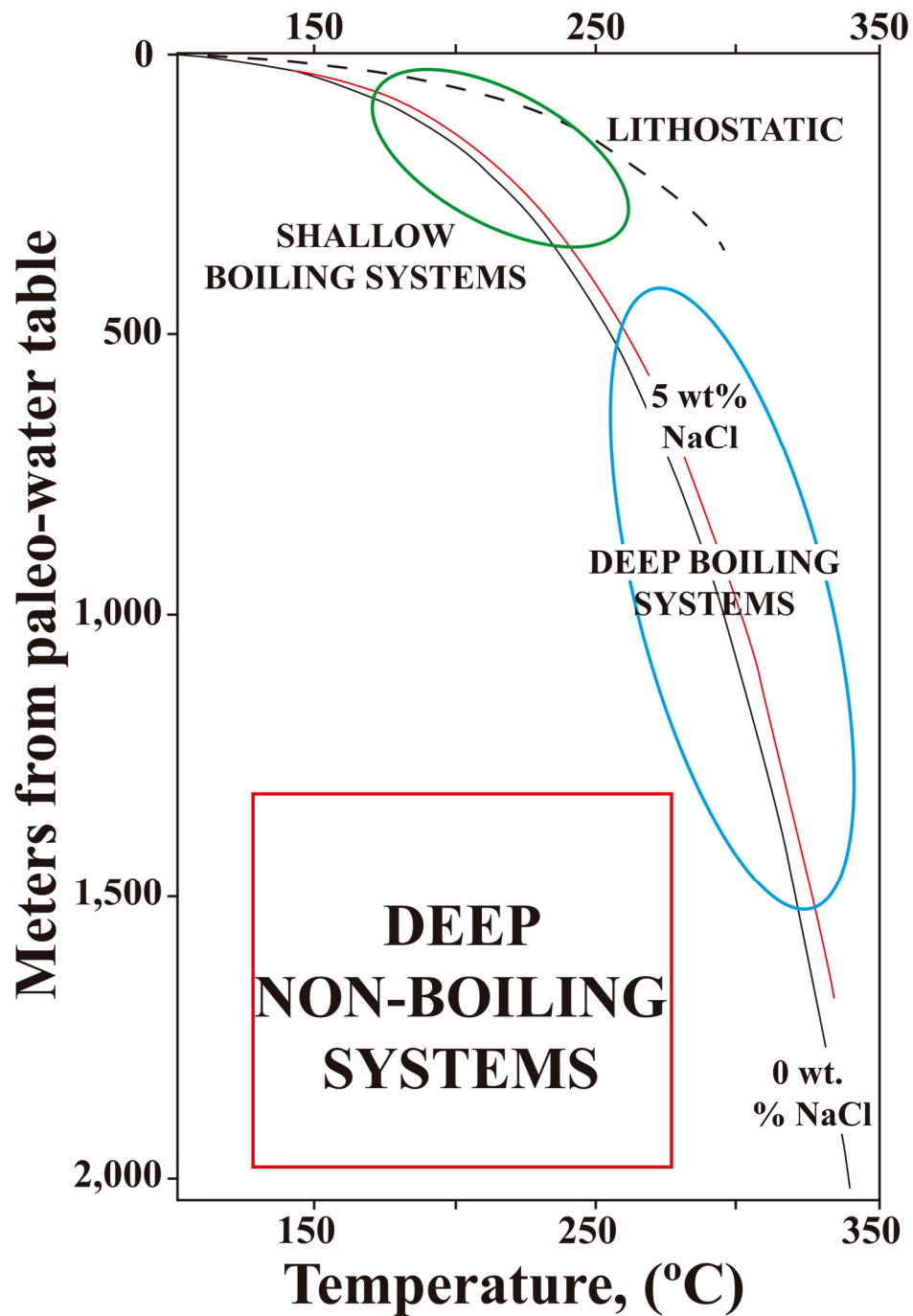


Figure 11. Classification of epithermal deposits based on physical conditions and depth of formation: Epithermal deposits have been classified in shallow boiling systems formed at < 500 m. depth; deep boiling systems formed between 500-1,500 m. depth; and deep non-boiling systems, formed at >1,000 m. depth. The Patricia Zn-Pb-Ag deposit features suggests conditions similar to those of deep no-boiling systems, with temperatures between 150°C- 250°C and depths below 1,000 m. The lithostatic curve and the curve of shallow to deep boiling system with 0 to 5 wt. % NaCl are depicted for reference. Modified from Albinson et al. (2001).

The most peculiar feature of the Patricia deposit is the absence of boiling evidence (Chinchilla et al 2016 b), for this reason we assume similar features as those characteristic of the deep base metals and non-boiling epithermal deposits (~2,000 m) under hydrostatic pressure conditions, as in Figure 11 (Albinson et al. 2001). Assuming therefore that during the hydrothermal system lifetime fluid was present in one phase liquid only. The temperature and salinity of this fluid through all the paragenetic stages of the deposit is constrained by fluid inclusion data from each stage.

In the absence of boiling, and after evidence supporting metal transport by chloride complexing, the proposed mechanism of ore formation is fluid mixing between the solution transported by the up-flow stream and the fluids from the lateral flow stream lowering the solubility of the base metal chloride complexes. One of the objectives of the model is to provide insight into the chemistry of these two solutions. To further estimate the ore solution composition, we assumed that the ore solution was in equilibrium with sphalerite and galena during the ore stage.

Figure 7 resumes the principal features considered in the numerical model of Patricia hydrothermal system. The heat from a magmatic source sustains convective cells and maintain the hydrothermal activity. A supply of metals, aqueous chloride and sulfur is necessary for the hydrothermal transport of metals and for precipitation of sulfide minerals; this supply is provided and controlled in most hydrothermal systems by a deeper source of magmatic fluid (Giggenbach 1995), further evidence of a magmatic origin of sulfur and lead was provided by isotopic analysis (Chinchilla 2017). A permeability distribution allowing fluid convection is also a critical factor for the existence of an active geothermal system, in particular, for the formation of an epithermal ore deposit, tectonic structures enhancing the rock permeability favor the occurrence of focused fluid flow in the system.

To account for the observed geologic features of the Patricia deposit, we consider an initial andesitic mineralogy for the host rock of the geothermal system. For the initial conditions of the system a near surface water table close to the surface is considered, with the host rock fully saturated. For the spatial scale of the model, given that the mineralization of the Patricia deposit is under structural control, and since we consider only the fluid flow around the area nearby to the fault structure, estimation from the geologic map (Figure 3), gave an area of 90,000 m² for the area affected by faulting.

Data from active geothermal systems in New Zealand provide a first order estimate for the magnitude of the hydrothermal mass flux. Estimate mass flow fluxes for the systems from the Taupo Volcanic Zone; provide a mean value of 100 kg/s (Simmons et al. 2016a). We consider 100 kg/s for the up-flow stream and a total lateral flow stream's contribution up to a ~15% of the mass flow from the up-flow stream.

For the system's permeability distribution, we followed the results of previous numerical model studies. Hydrothermal activity requires fluid and heat convection which is possible only if permeability is $>10^{-16} \text{ m}^{-2}$ (Ingebritsen et al. 2010). We considered a mean permeability of 10^{-15} m^{-2} for intact rock (non-fractured) allowing sustained hydrothermal fluid convection (Ingebritsen and Appold 2012) and a permeability of 10^{-13} m^{-2} for fractured rock in continental crust under tectonic perturbations (Ingebritsen and Manning 2010). A mean system's rock permeability of 10^{-14} m^{-2} is a conservative permeability range for geothermal systems with a dominant liquid phase and high permeability (Weis 2015). The lifetime of a geothermal system with this permeability is constrained to a period between 10,000-20,000 years (Weis 2015).

2.5 NUMERICAL MODEL

For the reactive transport model the ToughReact 2.0 code was used, a numerical code coupling reactive chemistry with the multiphase fluid and heat flow model from the Tough2 V2 code (Pruess 1999). Full details on governing equations and numerical methods used by TOUGHREACT are given in (Xu et al. 2011a). The TOUGHREACT code has been previously applied to model fluid-rock interaction in porous media at hydrothermal conditions (Dobson et al. 2004, Todaka et al. 2004, Xu et al. 2006, Wanner et al. 2014).

For all the simulations, the EOS1 equation of state module for pure water was used. The EOS1 module considers multiphase (water-steam) non-isothermal water flow. However, the pressure-temperature conditions in our model would not lead to boiling thus, boiling is not considered, which is consistent with the non-boiling conditions observed in the Patricia deposit.

2.5.1 Reaction Rates

TOUGHREACT can model mineral precipitation and dissolution under equilibrium and/or kinetic conditions. In the simulations, all mineral reactions were treated under kinetic conditions. For kinetic-controlled mineral dissolution and precipitation, we used the following rate law (Eq. 1) proposed by Steefel and Lasaga (1994):

$$r_m = \pm k_m A_m \left[\left(\frac{Q_m}{K_m} \right)^\mu - 1 \right]^n \quad [1]$$

Where m is the mineral index, r_m is the dissolution/precipitation rate (positive values indicating dissolution and negative values precipitation), A_m is the specific reactive surface area per kg of H₂O, k_m is the rate constant (in moles per unit mineral surface area and unit time) which is temperature dependent, K_m is the equilibrium constant for the mineral-water reaction written for the destruction of one mole of mineral m , Q_m is the ion activity product, exponents μ and n are two positive numbers determined experimentally they are taken as one (1).

The temperature dependence of the reaction rate constant is expressed by the following Arrhenius equation (Eq. 2) described by Steefel and Lasaga (1994):

$$k = k_{25} \exp \left[\frac{E_a}{R} \left(\frac{1}{T} - \frac{1}{298.15} \right) \right] \quad [2]$$

where E_a is the activation energy, k_{25} is the rate constant at 25 °C, R is the gas constant (8.314 J mol⁻¹ K⁻¹) and T is the absolute temperature.

For many minerals the kinetic rate law is the sum of multiple mechanisms (Lasaga et al. 1994, Palandri and Kharaka 2004) and the rate law could be expressed as follows in (Eq. 3):

$$k = k_{25}^{nu} \exp \left[\frac{E_a^{nu}}{R} \left(\frac{1}{T} - \frac{1}{298.15} \right) \right] + k_{25}^H \exp \left[\frac{E_a^H}{R} \left(\frac{1}{T} - \frac{1}{298.15} \right) \right] a_H^{nH} + k_{25}^{OH} \exp \left[\frac{E_a^{OH}}{R} \left(\frac{1}{T} - \frac{1}{298.15} \right) \right] a_{OH}^{nOH} + \sum_i k_{25}^i \exp \left[\frac{E_a^i}{R} \left(\frac{1}{T} - \frac{1}{298.15} \right) \right] \prod_j a_{ij}^{nij} \quad [3]$$

Where superscripts nu , H and OH indicate neutral, acid and base mechanisms respectively, superscript i is an additional mechanism and j is the additional aqueous species involved. Parameter a indicates the activity of the involved aqueous species.

2.5.2 Kinetics of mineral dissolution and precipitation

Equilibrium constants of aqueous species and minerals were obtained from the SOLTHERM database (Reed and Palandri 2006). Mineral dissolution and precipitation are considered to be kinetically controlled for all minerals, with the reaction kinetics described by equation [1]. Multiple mechanisms (neutral, acid or base) according to equation [3] could also be involved in a given mineral phase.

Kinetic data and mechanisms for most silicate minerals are taken from the compilation by Palandri and Kharaka (2004). For sphalerite and galena the kinetic data from (Acero et al. 2007a) is considered. The rate constant at 25°C (k_{25}), activation energy (E_a), and the involved aqueous species and power term for additional mechanisms for each mineral considered in the model are listed in Table 1. At any pH, the total reaction rate of a given mineral is the sum of each mechanism according to equation [3].

Table 1. Parameters for calculating kinetic rate constants for minerals using the rate law described in Equations (2), (3) and (4), k_{25} is the kinetic constant at 25° C, E_a is the activation energy, additional mechanisms for some minerals are detailed with the species involved and the exponents of each specie according to equation (3). All rate constants are listed for dissolution (Palandri and Kharaka 2004, Xu et al. 2006, Acero et al. 2007a, Acero et al. 2007b, Zhang et al. 2011).

Mineral reactive surface area values are taken from previous research with TOUGHREACT (Xu et al. 2006, Zerai et al. 2006, Zhang et al. 2011), the reactive surface areas considered here are 1 to 3 order of magnitude less than the minerals equivalent geometric area. The details of this estimate of the mineral reactive surface area could be reviewed in the work of Sonnenthal et al. (2005) and Zerai et al. (2006). These estimates of mineral reactive surfaces areas has been used successfully to calibrate geothermometry estimations using numerical modeling with ToughReact by Wanner et al. (2014). The reactive surface values for each of the minerals considered in the model are given in Table 2.

2.5.3 Changes of Porosity and Permeability

Temporal changes of porosity and permeability due to mineral dissolution and precipitation can modify fluid flow. This feedback between flow and chemistry is considered in our model. The changes in porosity are calculated from changes in mineral volume fractions. Porosity (ϕ) is calculated (Eq. 4)

$$\phi = 1 - \sum_{m=1}^{nm} fr_m - fr_u \quad [4]$$

Where nm is the number of minerals, fr_m is the volume fraction of mineral m in the rock ($V_{\text{mineral}}/V_{\text{medium}}$) and fr_u is the volume of non-reactive rock. Porosity is recalculated after each change of the mineral's volume fraction.

A cubic law model (Steeffel and Lasaga, 1994) is used to calculate changes in permeability (k), as a function of changes in porosity:

$$k = k_i \left(\frac{\phi}{\phi_i} \right)^3 \quad [5]$$

Where k_i and ϕ_i are the initial permeability and porosity respectively.

Table 1. Parameters for calculating kinetic rate constants for minerals using the rate law described in Equations (2), (3) and (4), k_{25} is the kinetic constant at 25° C, E_a is the activation energy, additional mechanisms for some minerals are detailed with the species involved and the exponents of each specie according to equation (3) . All rate constants are listed for dissolution (Palandri and Kharaka 2004, Xu et al. 2006, Acero et al. 2007a, Acero et al. 2007b, Zhang et al. 2011).

Mineral	k_{25} ($\text{mol m}^{-2} \text{s}^{-1}$)	E_a kJ mol^{-1}	Species 1	Exponent	Species 2	Exponent	Reference
Plagioclase	$6.91 * 10^{-11}$	65	H^+	0.457	-	-	Palandri and Kharaka (2004)
Albite	$2.75 * 10^{-13}$	69.8	-	-	-	-	
	$2.51 * 10^{-16}$	71	H^+	-0.572	-	-	
Diopside	$4.36 * 10^{-7}$	96.1	H^+	0.71	-	-	Palandri and Kharaka (2004)
	$7.76 * 10^{-12}$	40.6	-	-	-	-	
Quartz	$1.023 * 10^{-14}$	87.7	-	-	-	-	Palandri and Kharaka (2004)
Hematite	$4.07 * 10^{-10}$	66.2	H^+	1	-	-	Palandri and Kharaka (2004)
	$2.51 * 10^{-10}$	66.2	-	-	-	-	
Magnetite	$2.57 * 10^{-09}$	18.6	H^+	0.279	-	-	Palandri and Kharaka (2004)
	$1.66 * 10^{-11}$	18.6	-	-	-	-	
Illite	$4.36 * 10^{-12}$	62.8	H^+	0.17	-	-	Xu et al. (2006)
	$1.00 * 10^{-13}$	62.8	-	-	-	-	
Epidote	$2.51 * 10^{-11}$	71.1	H^+	0.338	-	-	Palandri and Kharaka (2004)
	$1.02 * 10^{-12}$	70.7	-	-	-	-	
Clinocllore	$3.02 * 10^{-13}$	88	0	-	-	-	Palandri and Kharaka (2004)
	$7.76 * 10^{-12}$	88	H^+	0.5	-	-	Zhang et al. (2011)
Calcite	$5.01 * 10^{-1}$	14.4	H^+	0.5	-	-	Palandri and Kharaka (2004)
	$1.54 * 10^{-6}$	23.5	-	-	-	-	
Pyrite	$3.02 * 10^{-8}$	56.9	H^+	-5	Fe^{3+}	0.5	Palandri and Kharaka (2004)
	$2.81 * 10^{-5}$	56.9	$\text{O}_{2(\text{aq})}$	0.5	-	-	
Galena	$1.99 * 10^{-6}$	23	H^+	0.43	-	-	Acero et al. (2007 b)
	$3.16 * 10^{-9}$	15	H^+	-0.78	$\text{O}_{2(\text{aq})}$	0.3	
Sphalerite	$3.23 * 10^{-7}$	14.3	H^+	0.54	-	-	Acero et al. (2007 a)

2.6 GEOCHEMICAL SYSTEM

2.6.1 Rock Mineralogy

The host rock is an intense altered volcanic rock with the primary mineralogy and textures poorly preserved, on some samples plagioclase, quartz and minor amounts of pyroxenes were reported as primary mineralogy. Primary minerals and possible secondary minerals were taken from field observations by (Chinchilla et al. 2016b, Chinchilla 2017). The initial primary mineral fraction of the host rock considered for the model is assumed similar to an andesitic assemblage typical of a volcanic formation of similar age (74-66 Ma) present in the same region (Valenzuela et al. 2014). Initial mineral volume fractions and secondary mineral phases are shown in Table 2. To describe chlorite, a mineral with a solid solution between an Mg- and Fe- extremes, two different mineral phases were considered clinochlore (Mg) and daphnite (Fe-chamosite).

Table 2. Simplified mineralogy considered for the geochemical system based on the mineralogy observed at the Patricia deposit, primary mineral phases and abundances are from an unaltered andesite (Chinchilla 2016a and Chinchilla 2017, Valenzuela et al. 2014). Reactive mineral surfaces for each mineral are from BET estimations (Zhong et al. 2011).

Mineral	Initial Volume Fraction	Reactive Surface Area A [cm ² /g]	References for Surface Area
Primary Mineral Phases			
Plagioclase	0.68	9.8	Zhang et al. (2011)
Diopside	0.15	9.8	Zhang et al. (2011)
Quartz	0.05	9.8	Zhang et al. (2011)
Hematite	0	12.9	Zhang et al. (2011)
Magnetite	0.06	9.8	Zhang et al. (2011)
Secondary Mineral Phases			
Illite	0	151.6	Zhang et al. (2011)
Epidote	0	9.8	Zhang et al. (2011)
Clinochlore	0	9.8	Zhang et al. (2011)
Daphnite	0	9.8	Zhang et al. (2011)
Calcite	0	9.8	Zhang et al. (2011)
Pyrite	0	12.9	Zhang et al. (2011)
Galena	0	12.9	Zhang et al. (2011)
Sphalerite	0	12.9	Zhang et al. (2011)

2.6.2 Rock Properties for the model

Rock properties for a typical andesite rock were considered for the system's host rock. Models for a single homogeneous porous media and for a dual continuum representation of both fractures and non-fractured matrix were made. For the hydrogeological parameters of each single media and dual media, conservative values for active geothermal system estimated from numerical modeling literature were considered (Ingebritsen et al. 2010). For the fractures-matrix representation, a permeability of 10^{-13} for fractures and 10^{-15} for the matrix host rock was considered. An initial porosity of 10% was considered for the unaltered andesite rock, and a porosity of 50% for the fractured rock. fractured rock was considered as 10% fraction of the system's volume, and the non-fractured matrix rock as 90% of the system's volume. All the rock's media thermal and hydrogeological parameters values are in Table 3.

Table 3. Rock properties and fluid flow parameters used in the single porous and double porous media models

Rock Properties and Fluid Flow Parameters			
Parameters	One Media	Dual Continuum	
	Andesite Rock	Rock Matrix	Fracture
Rock grain density [kg/m ³]	2700	2700	2700
Thermal conductivity [W m K]	2,5	2,5	2,5
Volume fraction	100%	90%	10%
Porosity	0,1	0,1	0,5
Permeability Horizontal [m ²]	10^{-15}	10^{-15}	10^{-13}
Permeability Vertical [m ²]	10^{-15}	10^{-15}	10^{-13}
Fracture spacing [m]	-	-	0,1

2.6.3 Spatial Scale and geometry of the model

The mineralization of the Patricia deposit is mainly in fractures which represent only a fraction of the total district area (Figure 3). The surface area in which is located the mineralization has an estimated area of 90,000 m². Since the current model of estimated resources of the Patricia deposit has 600 m depth (Golden Rim Resources 2017), the fluid-rock interaction was modelled considering a control volume with a square base of 300 m and a vertical depth of 700 m. This control volume has an area of 90,000 m² equivalent to the estimated exposed area of the fractures.

The water-rock interaction was modelled using a vertical column of fully saturated rock. A model with a 1-D vertical geometry was used. The model consists in 14 cubic grid blocks with constant vertical spacing of 50 m, with an injection block in the bottom.

From the bottom to the top a constant lateral injection of fluid is maintained during all the period of system activity, corresponding to the lateral geothermal flow into the system, for each block the

lateral injected mass is of 1 kg/sec with a total mass lateral flow of 13 kg/sec. The up-flow stream flow mass is set at 100 kg/sec and is injected at the bottom block.

Two different models were made (Figure 12), one considering only a single porous media, with a vertical permeability of $[10^{-13} \text{ m}^2]$ and horizontal permeability of $[10^{-15} \text{ m}^2]$, and another with two distinct porous media: intact rock and fractured rock implemented using the double porosity variant of the Multiple Interacting Continua approach employed by TOUGHREACT, this second model allows separate fluid-rock interaction for the matrix and fractured rock

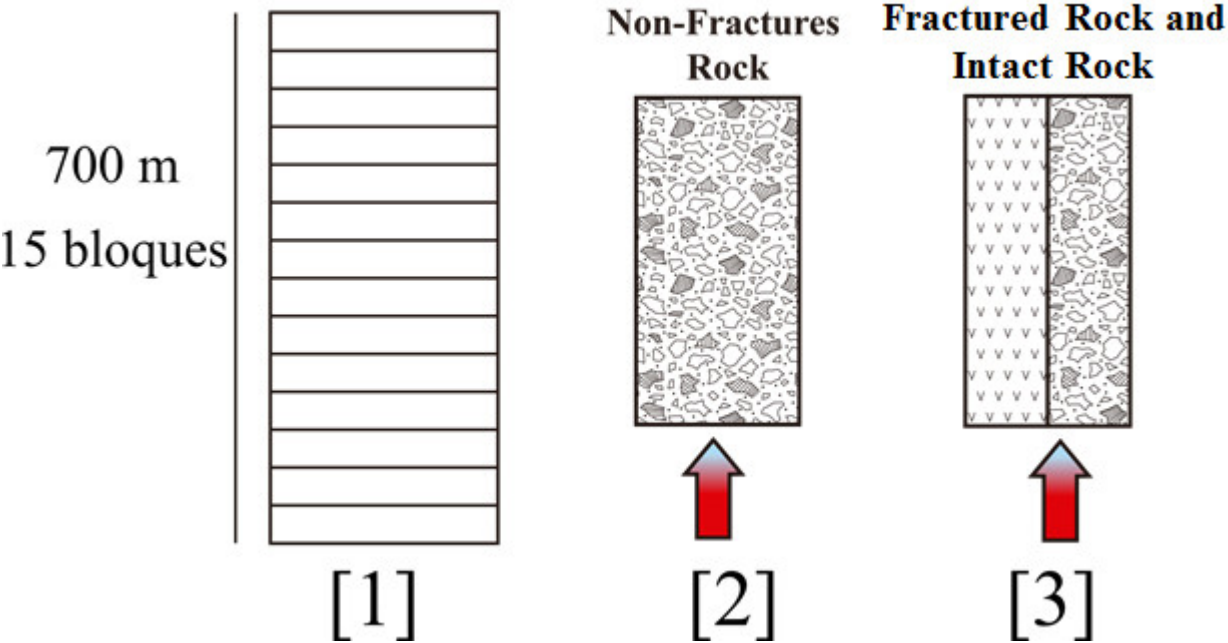


Figure 12. Model grid constructed to simulate fluid-rock interaction. [1] Model grid of 14 blocks of 50x 300 x 300 m. Pressure gradient is under hydrostatic conditions, temperature at surface is 100 °C. [2] Single porous media model, with homogeneous rock properties. [3] Dual porosity model, with 2 different porous media, matrix and fractures.

2.6.4 Fluid Geochemical Conditions and Model Stages.

Since the mineralogy of the Patricia deposit has four defined paragenetic stages the fluid–rock interaction model in Patricia is approached by a sequential model of four successive stages. For each stage a fluid, with its composition and temperature constrained by the mineral assemblages and the fluid inclusion data of each respective stage circulate through the host rock of the system. Table 4 contains the fluids compositions used for each stage in the models in the results section. Figure 9 shows the sequence used to estimate the fluid compositions for each stage of the system, the fluid composition of the ore stage was estimated by batch modelling.

Fluid composition estimates were made for each paragenetic stage, under the following conditions and assumptions: The temperature, salinity, and cations of each stage are constrained by fluid inclusion data measured of the respective stage. The initial system condition is fully saturated by a liquid fluid, this initial fluid has low salinity, neutral pH, and is a dilute solution typical of groundwaters in this zone of the North of Chile (Rissmann et al. 2015).

The following specific assumptions were made for each stage:

For the stage 1 (pre-ore stage), Iron concentration measured in fluid inclusions in quartz is assumed at equilibrium with pyrite this assumption constrains the acidity and the aqueous sulfur content $[HS^-]$ of the fluid.

For the Main-ore stage or stage 2, Zinc, Lead and Iron solubilities were estimated as a function of temperature and salinity (Figure 14) and pH and sulfur concentration (Figure 15) using batch models made with TOUGHREACT, assuming that Zn, Pb and Fe solubilities are constrained by equilibrium with sphalerite, galena and pyrite.

For the substage 2A (Sphalerite-only ore stage), the Zinc concentration range was assumed similar to Zinc concentrations for ore bearing solutions at 200°C (Yardley 2005), with a given concentration of aqueous zinc in solution the reduced sulfur $[HS^-]$ concentration in the ore fluid and the fluid's pH were determined by calculating the fluid mineral equilibrium with sphalerite. According to batch modeling a fluid with a pH of 4.5 could transport ~10 ppm of Zinc with $[HS^-] = 10^{-4}$ mol/kg at 200°C.

In the substage 2B (Sphalerite and Galena Ore stage), a fluid carrying ~12 ppm of Zinc and ~6 ppm of Lead was chosen as the potential ore solution.

Finally, for stage 3 (post-ore stage), base metals concentrations were obtained from fluid inclusion data from quartz from the post-ore stage. If the fluid is considered at equilibrium with the propylitic mineral assemblage, the fluid's pH is 6.0, a value consistent with the trapped illite crystals in quartz fluid inclusions of this stage, and the small concentrations of metals in solution.

Ore Solution Estimation Approach

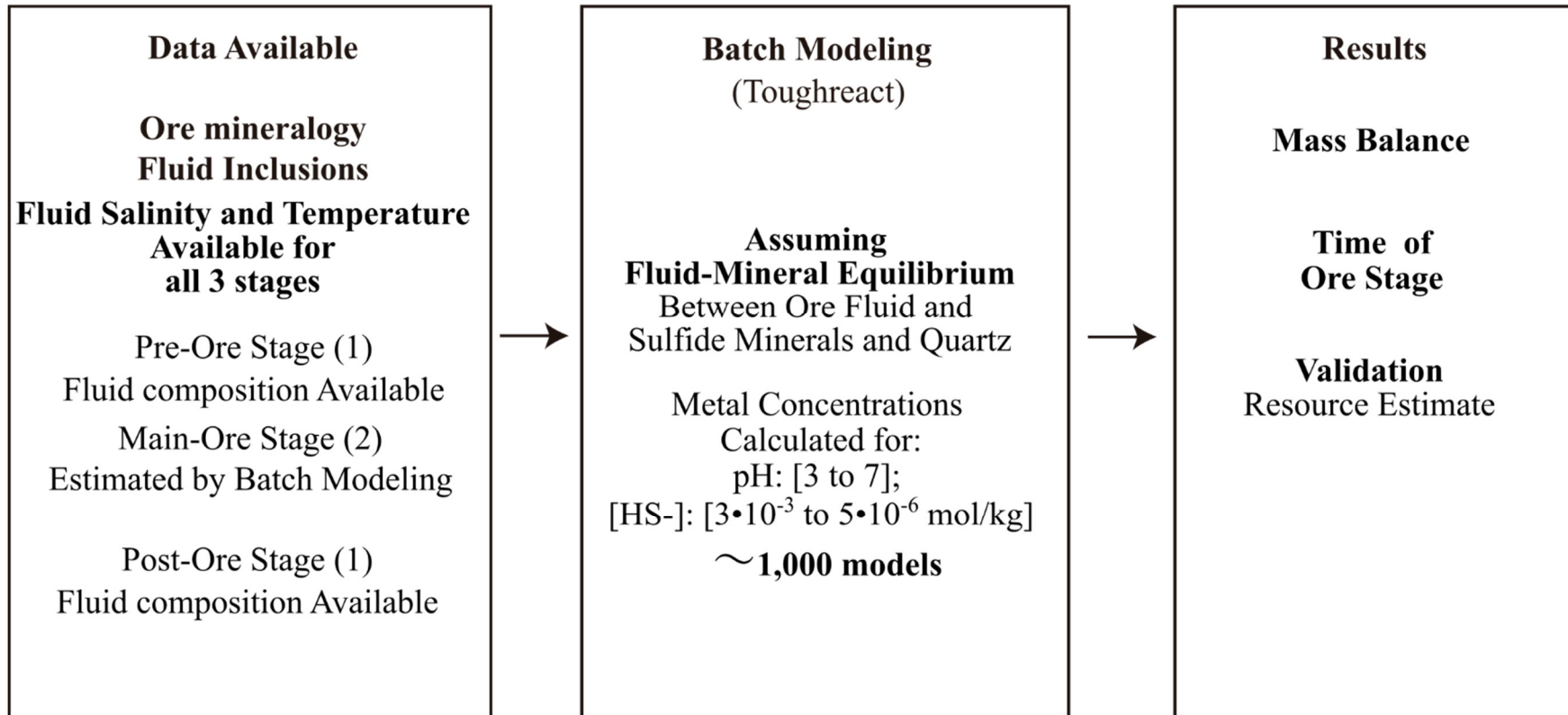


Figure 13. Methodology used to estimate the model's ore solution: The data available from previous work from (Chinchilla et al. 2016a and 2016b) provide the mineral and fluid inclusion data to allow estimates for the fluids of both the pre-ore and post-ore stages. But for the main ore stage, batch modelling was performed with TOUGHREACT, assuming fluid-mineral equilibrium, to estimate a range of potential ore fluid compositions for the conditions of the ore stage. From the resulting array of possible ore solutions, further constrains were imposed on account of flow rate and time considerations. The results of the reactive transport models were used to retroactively calibrate these estimates, through comparison with the resource estimates available for the Patricia deposit. More than 1,000 models were made to constrain the conditions of the models presented.

For all fluid compositions through the paragenetic stages of the system evolution, the silica concentration in each fluid was assumed to be at equilibrium with quartz.

The configuration used to replicate the Patricia paragenetic sequence is as follows:

The sequential model starts with an andesitic unaltered mineralogy, saturated in a neutral meteoric liquid fluid, as the system initial condition, for the pre-ore stage, the fluid characteristic of the pre-ore stage is injected at 220°C for 3,000 years at a constant 100 kg/s.

After a total of 3,000 years of hydrothermal fluid circulation, the fluid of substage 2A start flowing through the previously altered host rock of the pre-ore stage, for 2,000 years.

After a total of 5,000 years of hydrothermal fluid circulation, the fluid of substage 2B flows through the now mineralized rock after substage 2A, for 3,000 years.

After a total of 8,000 years of hydrothermal fluid circulation, the fluid of the post ore-stage flows through the mineralized rock after substage 2B, for 2,000 years for a total of 10,000 years of hydrothermal activity.

Along all the period of hydrothermal activity, a solution transporting reduced sulfur, flows into the system through lateral flow, this solution corresponds to a dilute fluid with similar composition to those reported for active geothermal systems from New Zealand (Simmons et al. 2016a) its compositions correspond to the "Lateral fluid" of Table 4.

Table 4. Aqueous chemical compositions for each fluid considered in the simulations, concentration units are in [mol/kg].

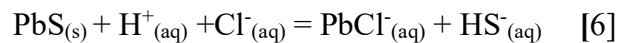
Fluid	Initial	Stage 1	Sub-stage 2A	Sub-stage 2B	Stage 3	Lateral Fluid
Temperature	100°C	220°C	220°C	180°C	200°C	100°C
pH	7.3	5.5	4.5	4.5	6.0	6.0
HCO3-	3.84E-06	1.91E-06	1.89E-06	1.89E-06	9.95E-10	1.89E-06
Ca+2	3.17E-03	1.63E-03	1.48E-04	7.65E-05	2.16E-04	1.64E-03
Mg+2	2.51E-03	1.23E-03	1.23E-08	1.23E-08	1.21E-04	1.23E-03
K+	5.24E-04	3.08E-04	9.30E-05	7.25E-05	9.02E-05	3.83E-04
Al+3	1.19E-07	6.13E-08	5.80E-08	5.80E-08	2.39E-03	5.80E-08
Na+	1.23E-02	2.29E+00	9.07E-01	1.20E+00	4.20E-01	1.23E-02
Cl-	8.04E-03	2.29E+00	9.07E-01	1.20E+00	4.20E-01	8.04E-03
SiO2(aq)	8.49E-04	4.36E-03	3.44E-03	2.67E-03	3.40E-03	7.65E-04
HS-	1.00E-10	4.74E-05	3.86E-05	1.30E-05	8.07E-06	3.00E-03
SO4-2	5.06E-4	8.92E-09	1.90E-10	2.61E-04	2.39E-05	1.00E-10
Pb+2	1.00E-10	9.41E-06	5.97E-07	2.90E-05	2.09E-06	4.05E-09
Zn+2	6.73E-08	1.18E-05	1.53E-04	1.92E-04	1.37E-05	5.64E-08
Fe+2	5.01E-07	1.25E-04	6.99E-04	3.41E-04	1.79E-05	4.90E-11
O2(aq)	1.00E-11	3.45E-11	8.45E-12	9.90E-12	2.57E-11	1.00E-11

2.7 RESULTS

2.7.1 Base Metal Solubility and Batch Models Results

The temperature range determined by the fluid inclusion data for the main ore stage of the Patricia deposit is 220-180 °C, this interval indicates minimum temperatures of fluid circulation for the ore stage. For substage 2A, different chlorite geothermometers estimated temperatures from 300° to 260°C (Chinchilla et al, 2016a), and the freibergite geothermometer estimated 230° to <170°C for substage 2B (Chinchilla et al, 2016b). Considering that for hydrothermal fluids at temperatures ≤400°C, recent research has established that base metal transport is dominated by chloride complexing over sulfide complexing (Zhong et al., 2015), it follows that the role of chloride complexing on the formation of the Patricia deposit must be considered.

For chloride complexing of base metals, the solubility of a sulfide mineral is described by the following reaction in equation (6) (Reed and Paladri 2006)



The equation [6] shows that a decrease in H⁺ activity (pH increase), drives sulfide mineral precipitation, similarly an increase in the activity of aqueous reduced sulfur (HS⁻) is favorable for the precipitation of sulfide minerals. For reduced hydrothermal fluids transporting both metal chloride complexes and sulfur together, the solubility of Cu, Zn and Pb increases with temperature, salinity and acidity (lower pH) (Huston, 1998, Yardley, 2005, Heinrich and Candela, 2014, Zhong et al., 2015).

For the Patricia deposit, both the temperature and salinity conditions of equation [6] are constrained by fluid inclusion data. But no data on the base metal concentrations on the ore fluid are available since the laser ablation analysis of fluid inclusions of the main ore stage were performed in sphalerite crystals. To address this issue batch models were made obtaining different metal solubilities as a function of both acidity and available sulfur complexes in solution (Figure 15), from these batch models, two solutions with moderate concentrations of zinc and lead were chosen as potential ore solutions for substages 2A and 2B.

These solutions have metal concentrations in the same order of magnitude as estimates for base metal concentrations in crustal ore fluids at the 200°-180°C range (~10 ppm Zn, 6 ppm Pb) (Yardley 2005).

The results of the batch modelling with TOUGHREACT used to estimate the fluid's compositions at the ore stage are displayed in Figure 14 and Figure 15.

For the conditions of the Patricia deposit, the activity of the chloride and bisulfide complexes of Zn and Pb, was compared for the interval from 300°C-140°C, chloride complexing of Zn and Pb is most stable and dominant in those conditions, Figure 14 [C].

Our results for the solubility of Zinc relative to salinity and temperature are described by Figure 14: Zinc solubility decreases with temperature at constant salinity, this indicates that cooling effectively decreases base metal solubility (Fig 14 [A]); Zinc solubility also decreases as salinity decreases at constant temperature indicating that dilution also decreases base metal solubility (Fig 14 B). For thermodynamical conditions similar to those of the Patricia deposit, 200°C, with a fluid in liquid phase and salinity ~10 wt.% NaCl, chloride complexing is dominant for Zinc, sulfide

complexes having lower activities and being more stable under cooling than Zn-chloride complexes for temperatures $<300^{\circ}\text{C}$ (Fig 14 [C])

Base metal solubility as a function of sulfur concentration and pH is described by Figure 15. At constant acid pH: 4.0, base metal solubility decreases as aqueous reduced sulfur concentrations increases in the fluid.

With low aqueous sulfur concentrations ($1 \cdot 10^{-4}$ mol/kg [HS⁻]), base metal solubility increases for lower pH values and decreases for higher pH values (Fig 15 [C] and [D]).

Base metal solubilities are highest at low pH values and low contents of reduced sulfur in solution: At 200°C , and pH 4.0, if the aqueous reduced sulfur concentrations are $> 10^{-3}$ mol/kg, the hydrothermal fluid is unable to transport even the base metals concentrations reported from the fluid inclusions on quartz from the barren pre-ore and post-ore stages (~ 1 ppm of Zn and Pb in solution). Furthermore, for a fluid with pH >5.0 , the fluid will transport lower base metals concentrations (~ 1 ppm), with this amount of base metals this fluid will be able to precipitate the total metal budget of the Patricia deposit after at least 100,000 years of constant fluid circulation, a period longer than the assumed potential lifetime of the now fossil geothermal system.

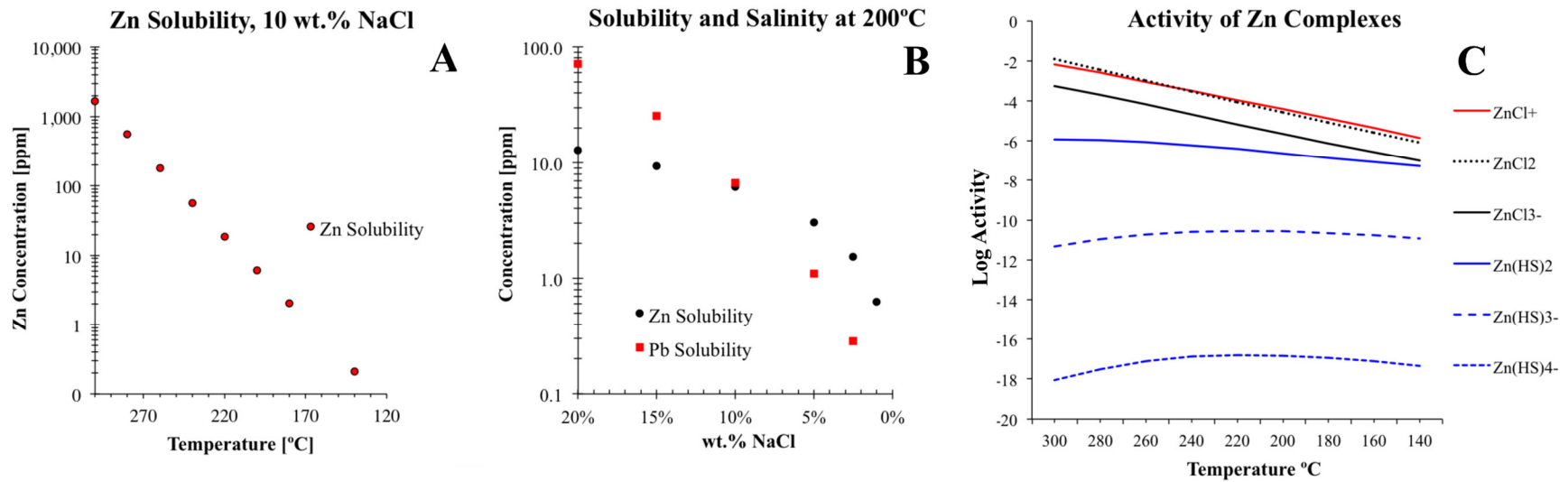


Figure 14. Zinc solubility calculated through TOUGHREACT, for all calculations pH set to 4.0 and aqueous sulfur concentration as HS⁻ set to 1•10⁻³ mol/kg. (A) Zinc solubility at constant 10 wt. % NaCl for temperatures between 300°C to 140 °C, solubility decreases with lower temperatures. (B) Base metal concentration as a function of fluid salinity at constant temperature, for a range of 20 to 2.5 wt% NaCl. (C) Activity of chloride and sulfide complexes of Zinc between 300°C to 140°C at constant 10 wt.% NaCl, Zn-chloride complexes are more active than Zn-bysulfide complexes, and more sensible to cooling.

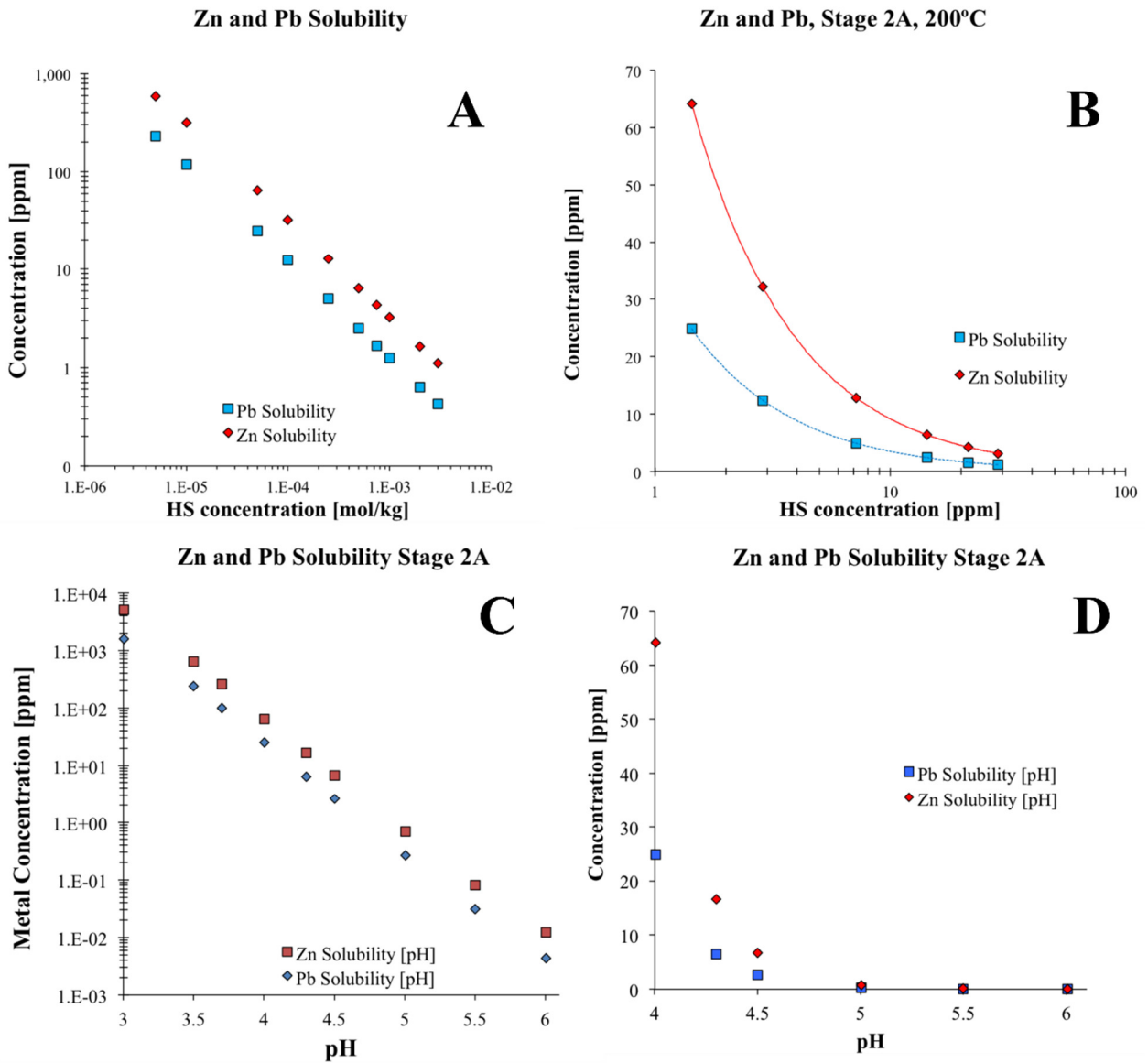


Figure 15. Zn and Pb solubility response to changes in pH and reduced sulfur (HS^-) in fluid. Solubility calculated for 200 °C and 5 % wt. NaCl. (A) and (B) base metal concentration (ppm) as a function of aqueous sulfur at constant pH= 4.0. Zn and Pb solubility decreases as aqueous sulfur concentration increases. (C) and (D) base metal concentration as a function of fluid acidity, at constant aqueous sulfur concentration ($1 \cdot 10^{-4}$ mol/kg of HS^- ; ~3 ppm). Acid pH favors a higher solubility of both Zn and Pb.

2.7.2 Formation of Base Metal Sulfides, mixing as ore forming mechanism

There are two modes of sulfide mineral precipitation (Reed and Palandri 2006):

In the first mode metal and sulfur are transported in the same fluid, precipitating sulphide minerals after a change in the chemical or physical conditions of the fluid, this mechanism requires fluid temperatures $> 300^{\circ}\text{C}$ (Reed and Palandri 2006). More recent research on Cu-Zn-Pb solubility had established that for temperatures $>400^{\circ}\text{C}$, base metals could be transported as bisulfide complexes, with precipitation being driven by fluid cooling (Zhong et al., 2015).

In the second mode, sulphide precipitation takes place after mixing of a metal-bearing fluid with another sulfur bearing fluid, this mode is compatible with temperatures $<250^{\circ}\text{C}$ (Reed and Palandri 2006) and involves chloride complexing, which is dominant in metal transport and temperatures $<400^{\circ}\text{C}$ (Zhong et al., 2015), ore precipitation is triggered when the ore fluid encounters reduced sulfur by fluid mixing or by sulfate reduction.

In the case of the Patricia deposit, the maximum fluid temperatures reported by fluid inclusions are $< 300^{\circ}\text{C}$, even considering for substage 2A temperature data from chlorite geothermometry which range from 152°C - 305°C (Chinchilla et al., 2016a) and for substage 2B temperatures ranging from $<170^{\circ}\text{C}$ - 230°C estimated from freibergite geothermometry (Chinchilla et al., 2016b), these temperatures are too low for the first mode of sulphide precipitation

Previously the precipitation of sulfides minerals through fluid mixing has been considered as a process with the potential to precipitate base metals in the epithermal environment (Hayba 1997, Huston 1998). It has been proposed that an initially H_2S poor, metal rich fluid, could deposit metal sulfides through mixing with H_2S -rich fluids providing reduced sulfur (Huston 1998, Paradis et al. 2007). For the Creed district, Colorado, isotopic evidence and geochemical modeling indicates that mixing was the depositional mechanism for sphalerite (Hayba 1997). In the case of this epithermal deposit, cooler groundwater mixing with the metal-bearing hydrothermal brine within the open fractures caused sphalerite deposition (Hayba 1997, Campbell and Barton 2005).

At first for the Patricia deposit we considered the first mode of sulfide formation, and we found that a single fluid with both base metals and sulfur in solution at temperatures $\leq 300^{\circ}\text{C}$ precipitated with high efficiency most of its metal charge (transported as chloride complexes) as sulfide minerals before the fluid reach a temperature of 200°C , becoming a fluid almost barren in base metals at 180°C . This single fluid saturated for sphalerite and galena at the ore stage temperatures will be able to form sulfide minerals through cooling by destabilizing chloride base metals complexes at higher temperatures (280°C - 240°C) that those reported by fluid inclusion data for substages 2A and 2B (Chinchilla et al. 2016a, Chinchilla 2016b). However, this mechanism did not bring positive results for lower temperatures, and was unable to form an extended vertical horizon of sulfide mineralization.

After this results we propose as a possible alternative that a fluid mixing process could account for the Patricia deposit ore formation at the lower temperatures reported for the main ore stage.

Mixing requires sustained interaction between fluids of different compositions and/or temperatures to produce ore precipitation (Hayba 1997, Paradis et al. 2007). Fluid mixing causes metal deposition by changing the sulfidation state of the metal bearing solution, lowering metal solubility and producing metal precipitation (Reed and Palandri 2006, Zhong et al. 2015). In the case of the

Patricia deposits we propose that fluid mixing could lower the metal solubility of the ore fluid and drive sphalerite and galena precipitation of the main ore stage.

In the conceptual model (Figure. 7), base metal sulfide precipitation occurs when the fluid transporting metals in chloride complexes coming from a magmatic source and carried by the up-flow stream, mixes with a fluid containing reduced sulfur, sourced by the lateral flow into the fractures, lowering the metal solubility and precipitating base metal sulfides along the fluid path.

2.7.3 Estimation of the Ore Stage duration

The ore stage in epithermal environment has been described as an episodic and transient process happening in a larger period of hydrothermal activity with fluids barren of metals (Simmons et al. 2005a, Simmons et al. 2016b). For the Patricia deposit model, a minimum estimate has been made for the ore stage duration as a function of the ore fluid metal content, the fluid flow rate and the efficiency of the precipitation mechanism. For a preliminary estimate we used a mass balance approach, considering a fluid flow rate of 100 kg/sec, and assuming at first 100% precipitation efficiency. Considering as a first approximation metal concentrations of 25 ppm of Zinc and Lead in the ore could have lasted < 2,500 years. We made adjustments to these preliminary estimates by testing the sensibility of the metal-bearing potential of the fluids of the ore stage.

Considering a total period of 10,000 years for the hydrothermal activity, we assumed for the pre-ore and post-ore stages a period of 3,000 years each. This period is consistent with previous numerical modelling (Hayba and Ingebritsen 1997, Kostova et al. 2004, Driesner and Geiger 2007) that constrain to 3,000 years the period over which a geothermal system with mean permeabilities $\leq 10^{-14}$ m² could maintain a certain fluid temperature before undergoing sustained cooling without a further magmatic intrusion into the igneous body supplying heat for the system.

2.7.4 Results of Reactive Transport Models of the Patricia deposit

Before achieving the present results almost 1,000 models were made to calibrate and analyse the sensibility of the parameters involved in the proposed conceptual model. The following results are the end-result build on those previous models and represent also the simplest model possible with the available data from the Patricia deposit.

We present the results of three reactive transport models, each model, after the first, building on the results of the previous model:

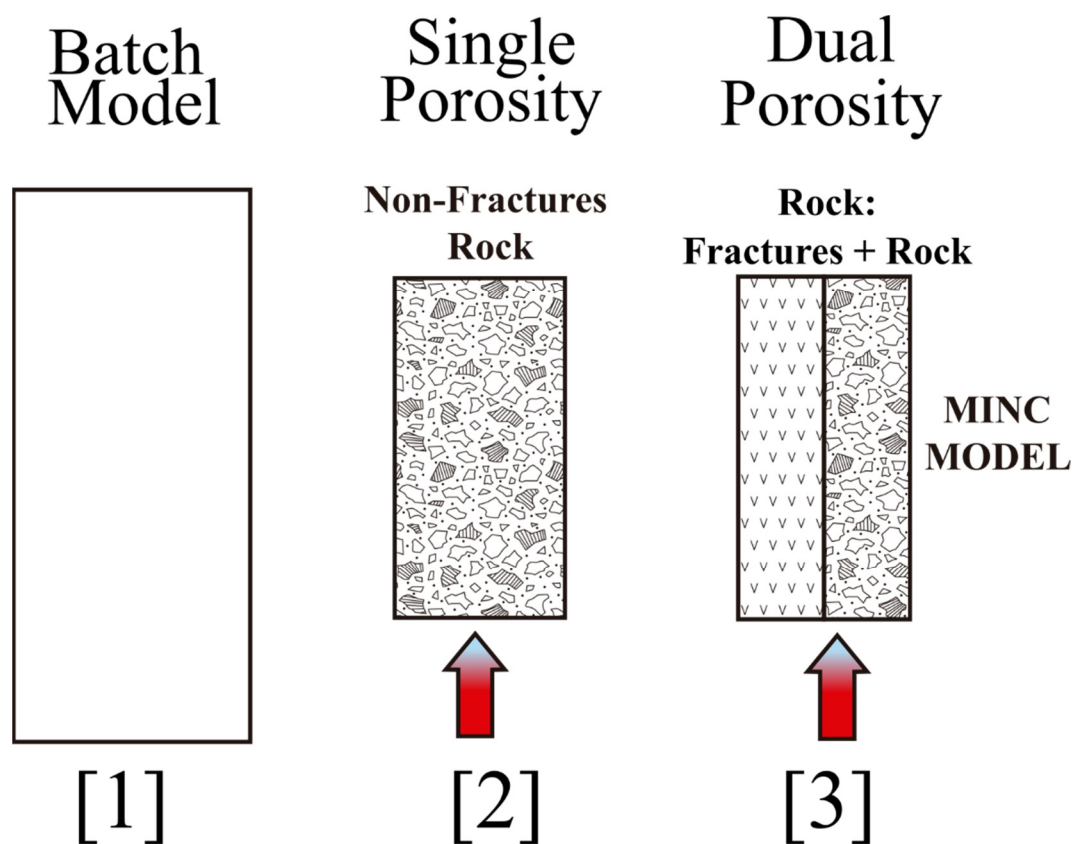


Figure 16. Model configurations implemented with TOUGHREACT: (1) Batch models were made to estimate fluid composition through fluid-mineral equilibrium (2) Reactive transport models with a single porous media model, with homogeneous rock properties to estimate the duration of the ore stage. (3) Reactive transport models with a dual porosity model, were made to study the differences of fluid-rock interaction between matrix and fractures, the fractured volume was assumed a 10% of the total modelled volume. All reactive transport models have dimensions of 700 m of vertical depth, and a square base of 300 m.

Distinctive features of each models are in Table 5.

Table 5. List of models, characteristic features of each one indicated according to minerals considered, porous media representation and simulated period.

Model	Mineralogy Considered	Representation of Porous Media	Period Modeled	Duration of Ore Stage	Total Duration
1	All minerals	Single homogeneous rock	System activity	5,000 y	10,000 y
2	All minerals	Fracture and Matrix	Ore Stage	5,000 y	5,000 y
3	Only vein assemblage	Fracture and Matrix	Ore Stage	5,000 y	5,000 y

1. Model 1, a comprehensive model of the Patricia hydrothermal system activity to estimate and calibrate the ore stage conditions and characterize the overall evolution of the system over 10,000 years of continuous geothermal activity. In this model we considered the host rock as a single homogeneous porous media (Figure 16, [2]). The estimated fluid conditions and the duration of the ore stage are used as feedback of Model 2.

2. Model 2, uses the estimated conditions from Model 1 for the Patricia deposit main ore stage, to study the interaction between the hydrothermal fluid, and both fractures and matrix in the host rock, using a dual continuum representation of the porous media, and the results of the fluid-rock interaction in the ore resources distribution in the system. This model only considers the ore stage for a total period of 5,000 years: 2000 years for the ore stage 2A and for stage 2B another 3,000 years for 2B (Figure 16, [3]). The results of the interaction of the ore fluid with both fractured rock and matrix rock indicated that the fracture mineralogy is relevant in the conditions of ore formation and in the lifetime permeability behavior of the geothermal system.

3. Model 3, considering the previous results of Model 2. In this model we explored the significance of the mineral assemblage of the fractures in both the evolution of the permeability and the distribution of the sulfide ore minerals in the system for an ore stage lasting 5,000 years (Figure 16 [3]).

2.7.4.1 Model 1 Results

In Model 1, the system activity is considered for 10,000 years through the start of the pre-ore stage to the end of the post-ore stage. We present the results of the fluid-rock interaction and the hydrological system, reporting the physical and mineralogical responses after each paragenetic stage of the Patricia deposit.

I. Porosity and Permeability

Figure 17 shows the changes of porosity and vertical permeability for Model 1, mineral dissolution is dominant along most of the system up to the upper levels where permeability and porosity have a marked decrease caused by mineral precipitation. With respect to the initial conditions, permeability and porosity increases along most of the vertical profile up to the upper 200 m, with porosity being reduced by more than 50% and permeability in more than one order of magnitude. After 10,000 years of hydrothermal activity permeability never decreases below 10^{-15} m^2 allowing constant advective fluid and heat flow.

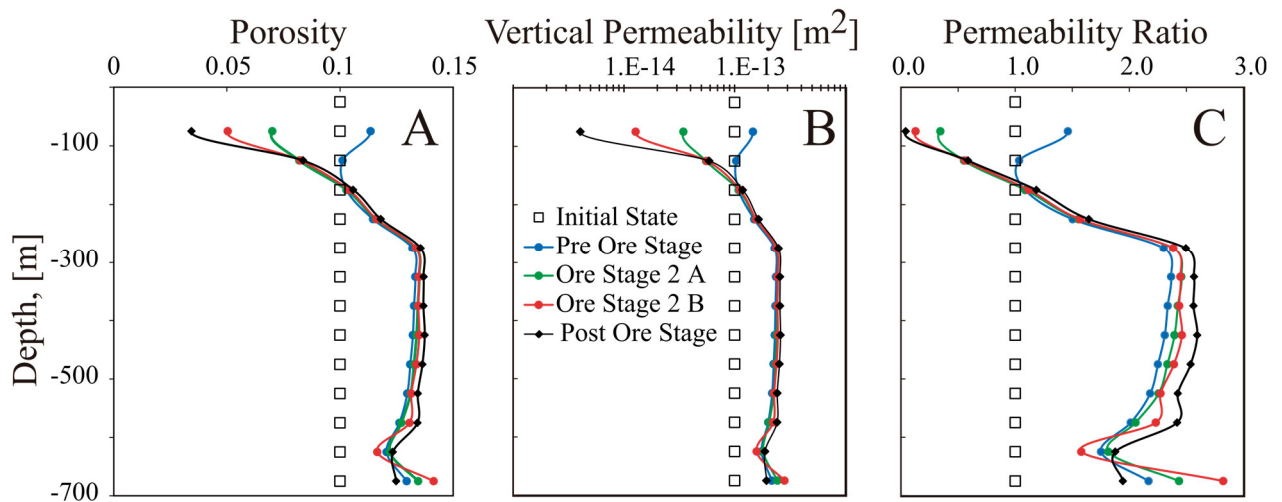


Figure 17. Changes of porosity and vertical permeability for Model 1. Each curve is traced at the end of a paragenetic stage. (A) Porosity increases by dissolution of the primary mineralogy below 300 m depth, but from 300 m upwards porosity decreases down to $< 5\%$. (B) Permeability follow a similar trend, decreasing from ~ 300 m depth upwards from $\sim 10^{-13}$ to $< 10^{-14} \text{ m}^2$. (C) Vertical permeability initial/final ratio along the vertical profile highlights the increase in permeability at depth followed by a significant decrease upwards.

II. Temperature and Pressure

The temperature and pressure profiles are shown in Figure 18. The temperature profile is almost isothermal up to 200 m depth, above 200 m depth the temperature follows closely the boiling curve, but the fluid never boils, the fluid is at all stages of the model a one phase liquid fluid.

At early stages of the system the modelled pressure profile is similar to the hydrostatic pressure profile, but at the end of post-ore stage pressure increases along the vertical profile. Pressure has a minor increase from the pre-ore stage to the end of the ore stage, and in the post-ore stage the

pressure increases above the hydrostatic pressure profile up to 80 bar at 700 m of depth and 40 bar at >100 m depth, respectively.

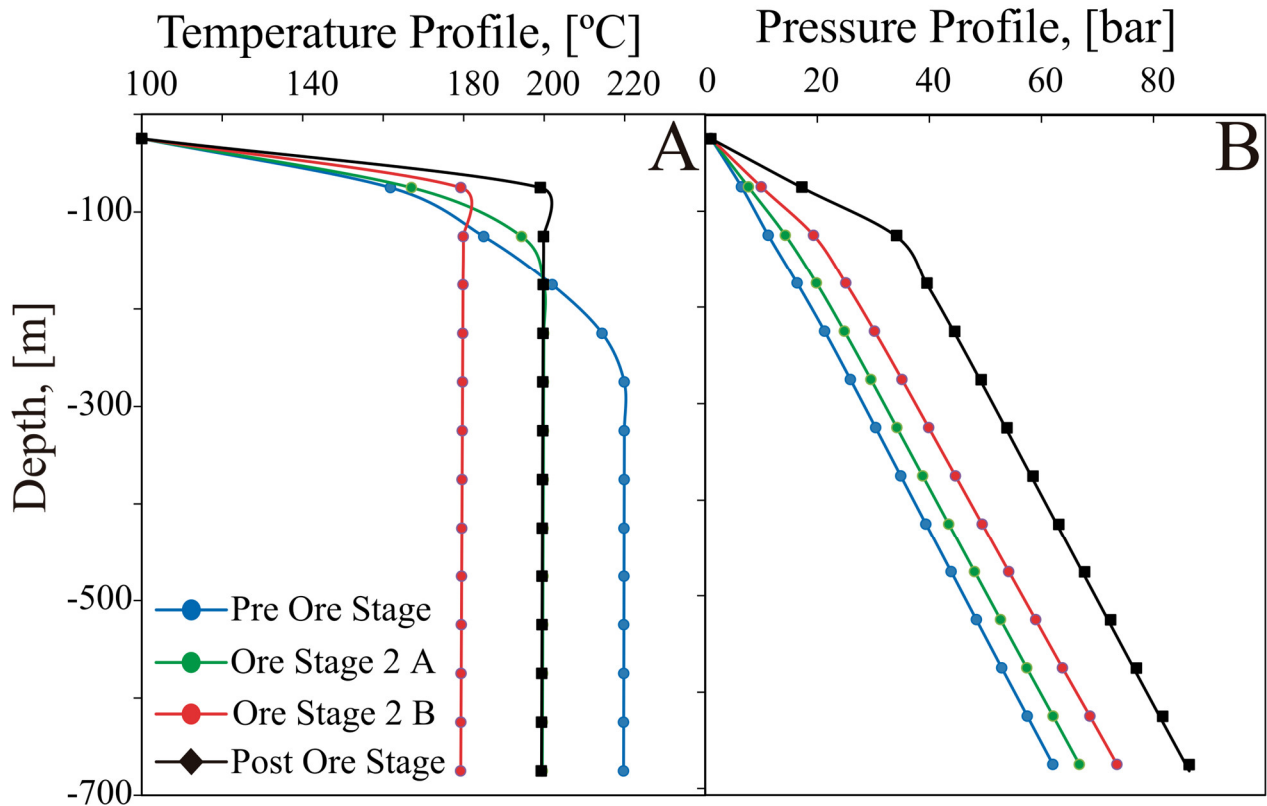


Figure 18. Temperature and pressure conditions of Model 1. (A) The temperature profile for pre-ore stage, ore stage A and, B, and post-ore stage looks isothermal up to ~250 m depth. (B) The pressure profile follows the hydrostatic pressure profile, over time pressure increases gradually all along the system.

III. Hydrothermal Alteration

The fluid-rock interaction causes the alteration of the initial andesite rock, with plagioclase + diopside as the primary rock minerals into an altered rock with a propylitic assemblage of quartz + chlorite ± epidote ± daphnite (Figure 19). The diopside is completely altered and disappears from the rock's mineral assemblage by the end of the pre-ore stage. Plagioclase suffer a significant decrease in abundance in the pre-ore stage but in later stages maintained constant volume abundance in the system up to the end of the modeled system's activity.

At the deepest portion, epidote is absent from the alteration assemblage being replaced by daphnite. The abundance of daphnite increases over time at the deeper boundary of the model and decrease along the vertical profile. By the end of the post-ore stage, minor amounts of illite are observed.

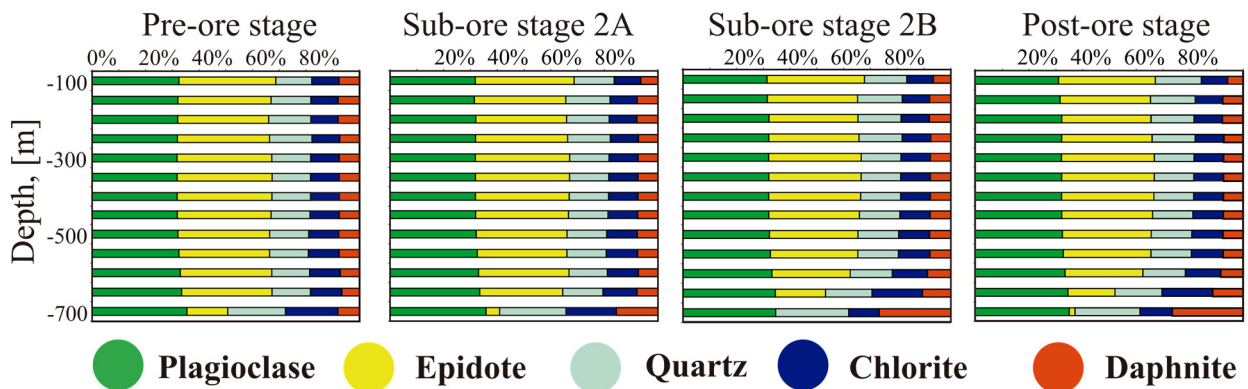


Figure 19. Changes over time in the alteration mineral assemblage for Model 1. The relative abundance of each alteration mineral is displayed along the vertical profile of the model at the end of each paragenetic stage. From the initial stage with andesite mineralogy, the silicate mineralogy develops into an assemblage of plagioclase + epidote + chlorite + daphnite + quartz, typical of the propylitic alteration.

IV. Fluid composition and Fluid-rock interaction

The Figure 20 shows the geochemical parameters relevant to base metal sulfide formation: acidity, reduced sulfur and base metal concentrations at different times, over lifetime of the system of Model 1.

From the pre-ore stage, during the ore and post-ore stages, acidity goes from pH 5.0 at the bottom of the system boundary and increases up to a pH 5.5.

Low reduced sulfur concentrations decrease from $\sim 10^{-4}$ mol/kg (~ 3 ppm of HS^-) and the beginning of the ore stage down to 10^{-6} mol/kg by the end of the ore stage. Reduced sulfur has higher concentrations during the pre-ore and post-ore stages and sulfur concentration is at a minimum during the ore stage, in the section of the vertical profile where base metal sulfide precipitates.

In the substage 2A, base metal concentration decreases gradually from the bottom up to 200 m depth. Reduced sulfur concentration increases from depth up to the top, when there are practically no metals in solution to be precipitated.

In substage 2B, base metal concentration decreases from the bottom boundary up to 200 m in depth. The reduced sulfur concentration increases after the amount of base metals carried in solution decreases. In the substage 2A, base metal concentration (aqueous Zn) decrease gradually from the bottom boundary up to 200 m depth. In substage 2B, the initial concentration of Zn and Pb decreases gradually from a maximum at the bottom boundary up to 200 m depth.

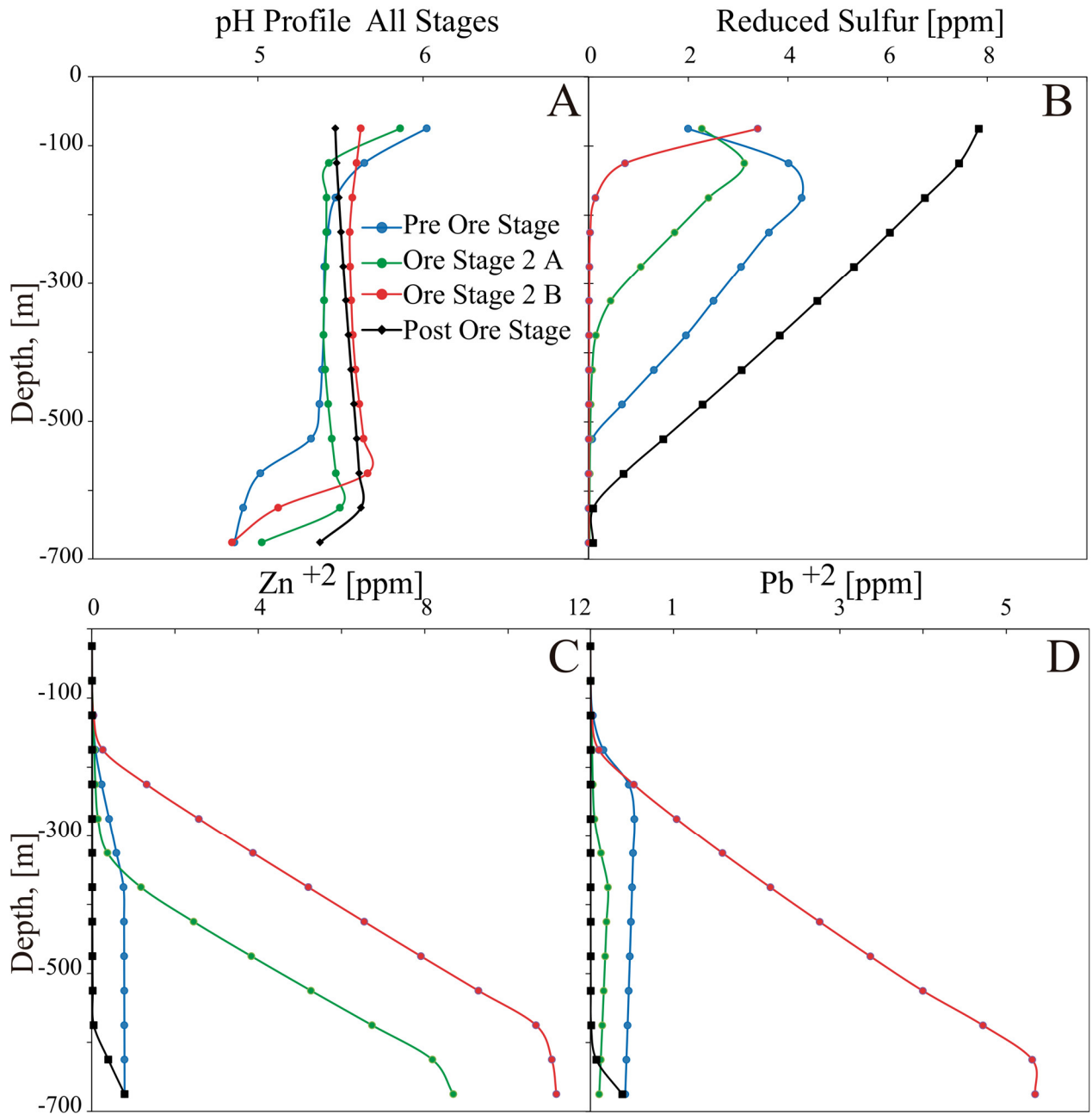


Figure 20. Changes in pH, reduced sulfur concentration [HS⁻], Zn²⁺ and Pb²⁺ for all the modeled lifetime of Model 1. (A) Vertical pH profile for all stages, (B) Reduced sulfur concentration, (C) Total Zn²⁺, (D) Total Pb²⁺. Fluid acidity is buffered by the rock mineral assemblage up to pH~5.5. Initial Zn²⁺ concentration during the ore stage is 10 ppm, and initial Pb²⁺ concentration during substage 2B is 6ppm.

V. Sulfides, Paragenesis, Base-Metals Resources

The sulfide paragenesis is replicated by changing the fluid compositions over time, the system lifetime is modelled as a sequential succession of consecutive stages of circulation of fluids, each with a different composition interacting with the host rock of the system. Using this approach, Model 1 paragenesis follows the same ore mineral sequence observed at Patricia deposit.

Figure 21 shows the development of a vertical horizon of base metal mineralization. Since Model 1 considers a single homogeneous porous media, the base metals sulfides precipitate homogeneously in the system's volume, corresponding to a disseminated mineralization style.

In this model, the resources are disseminated in the host rock, and during substage 2A, most of the Zn ~90% of total Zinc precipitated, precipitates below 300 m depth, whereas in substage 2B, the mineralization has a more wider vertical extension, being present from the bottom boundary at 700 m depth up to 200 m depth in the system. At the end of the post-ore stage, a total of 68,901 tons of lead and 192,477 tons of zinc have been precipitated from hydrothermal fluids.

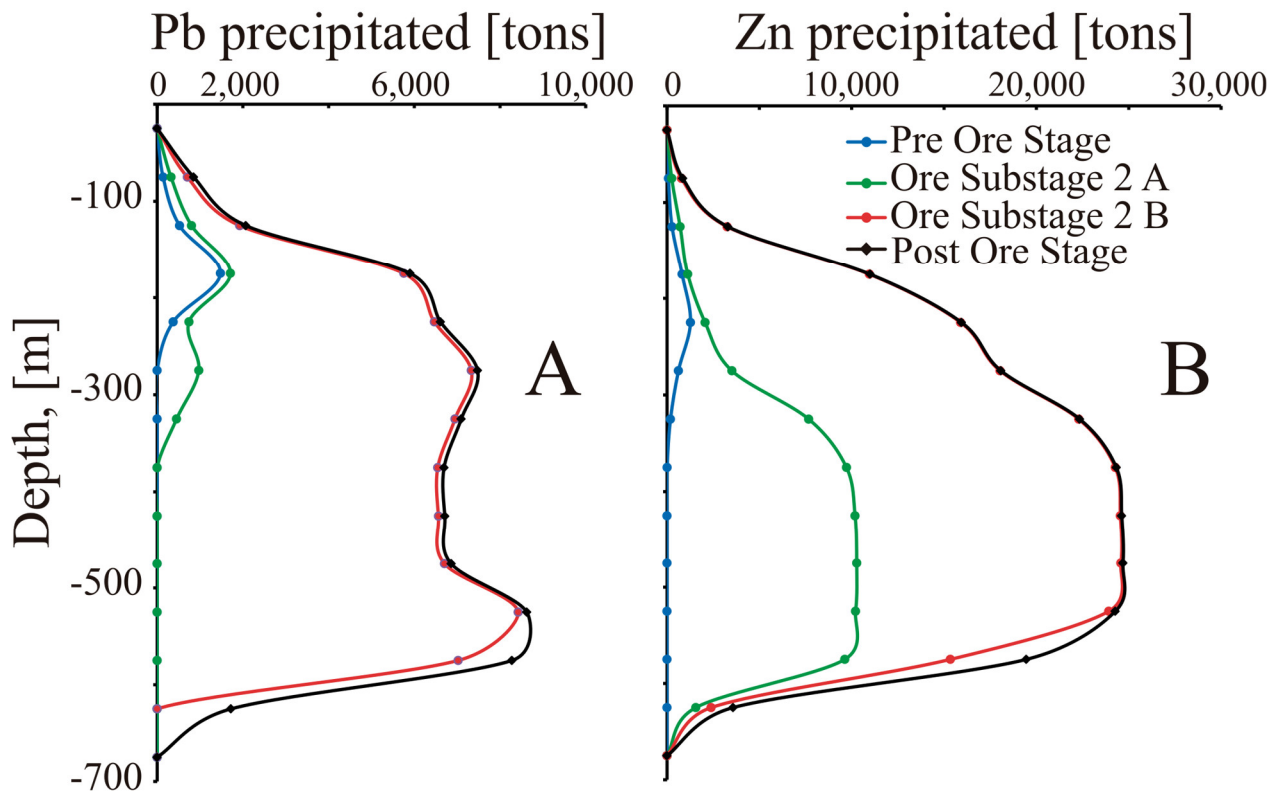


Figure 21. Vertical profile of base metals resources precipitated after each paragenetic stage for Model 1. Most of the base metals precipitated below 200 m depth, base metals are more abundant at depth and gradually decrease in abundance up to the surface. (A) Lead precipitated as galena (B) Zinc precipitated as sphalerite.

2.7.4.2 Model 2

In Model 2, the relevance of a zone with enhanced permeability in the distribution of the mineralization is explored using a representation of the host rock with two different medias. One representing a matrix with low permeability (10^{-15} m^2) and another of a fractured zone with higher permeability (10^{-13} m^2). This model reproduces the fluid rock interaction during the ore stage for 2A of 2,000 years and for ore stage 2B of 3,000 years for a total of 5,000 years. The initial distribution for the gangue mineral assemblage is taken from the mineral assemblage distribution at the end of the pre-ore stage in Model 1; ore fluid compositions for each substage are the same as for Model 1.

I. Porosity and Permeability

Figure 22 shows the permeability and porosity for the fractures (Figure 22 [A], [B], [C]) and for the matrix (Figure 22 [D], [E], [F]) of Model 2. The fractures and matrix of the model have a similar behavior for most of the vertical profile, with mineral dissolution dominating along most of the system up to the upper levels where the permeability and porosity decrease. However, at the bottom boundary, permeability decrease for the fractures up to 10^{-15} m^2 and increases for the matrix.

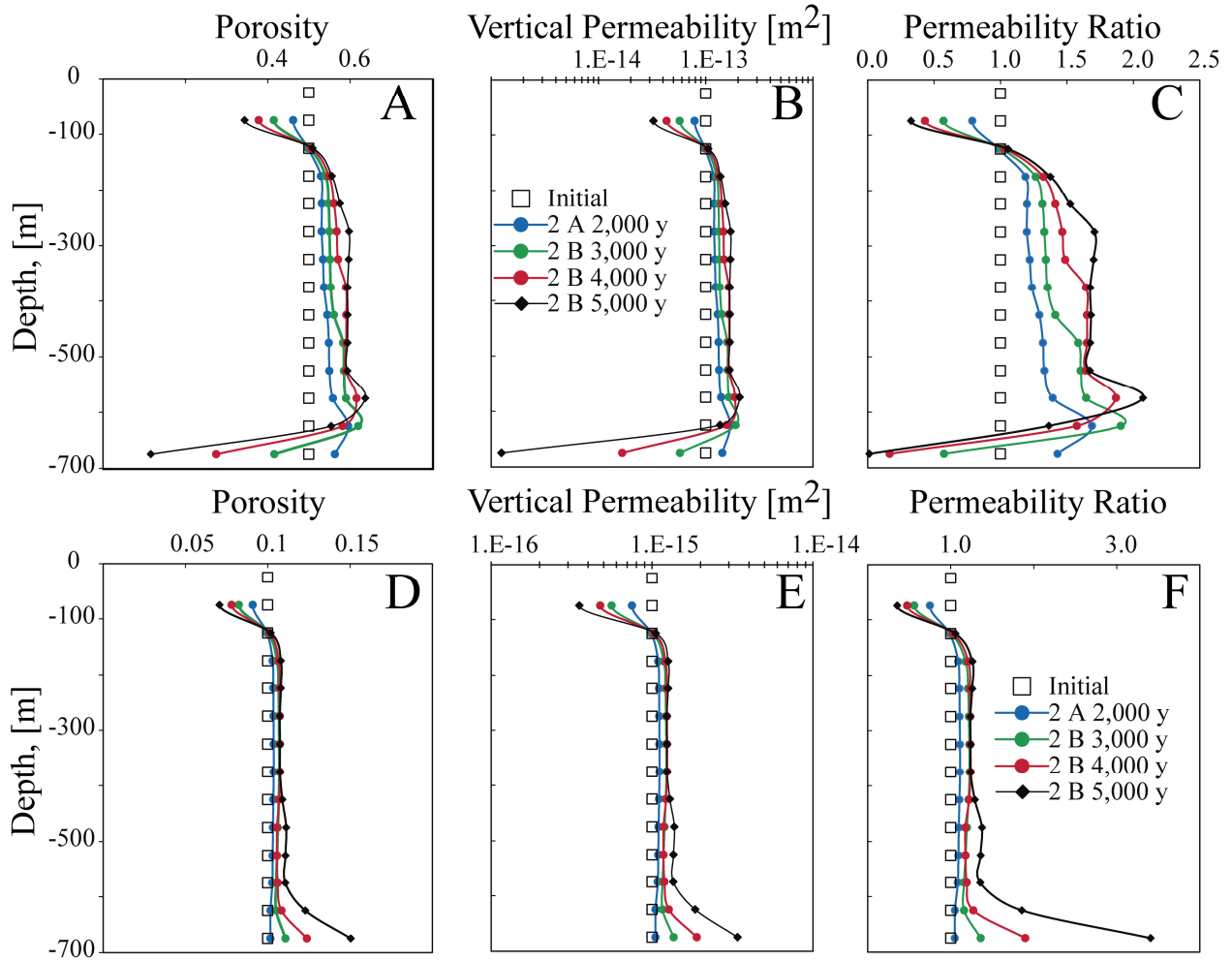


Figure 22. Changes of porosity and vertical permeability at different times for fractures and matrix media in Model 2. For fractures, porosity and permeability increased from 600 to 200 m depth, but decreased at the system's boundaries, especially at the system's bottom boundary: (A) Changes of porosity in the fractures. (B) Vertical permeability in m^2 in the fractures. (C) Vertical permeability initial/final ratio in the fractures. For the rock matrix, porosity and permeability showed significant increase below 600 m depth: (D) Changes of porosity in the rock matrix. (E) Vertical permeability in m^2 in the rock matrix. (F) Vertical permeability initial/final ratio in the rock matrix.

II. Temperature and Pressure

The modeled temperature profile in the fractures for this profile is almost isothermal up to 200 m depth (Figure 23 [A]). Above 200 m depth the profile follows closely the boiling curve, but the fluid never boils, as the fluid is at all stages of the model a one phase liquid fluid.

The modeled pressure profile (figure 23 [B]) is at first to the hydrostatic pressure profile but by the end of the ore-stage, in response to a significant decrease in the permeability of the fractures at the bottom boundary of the system, pressure also increases (> 100 bar at 700 m depth).

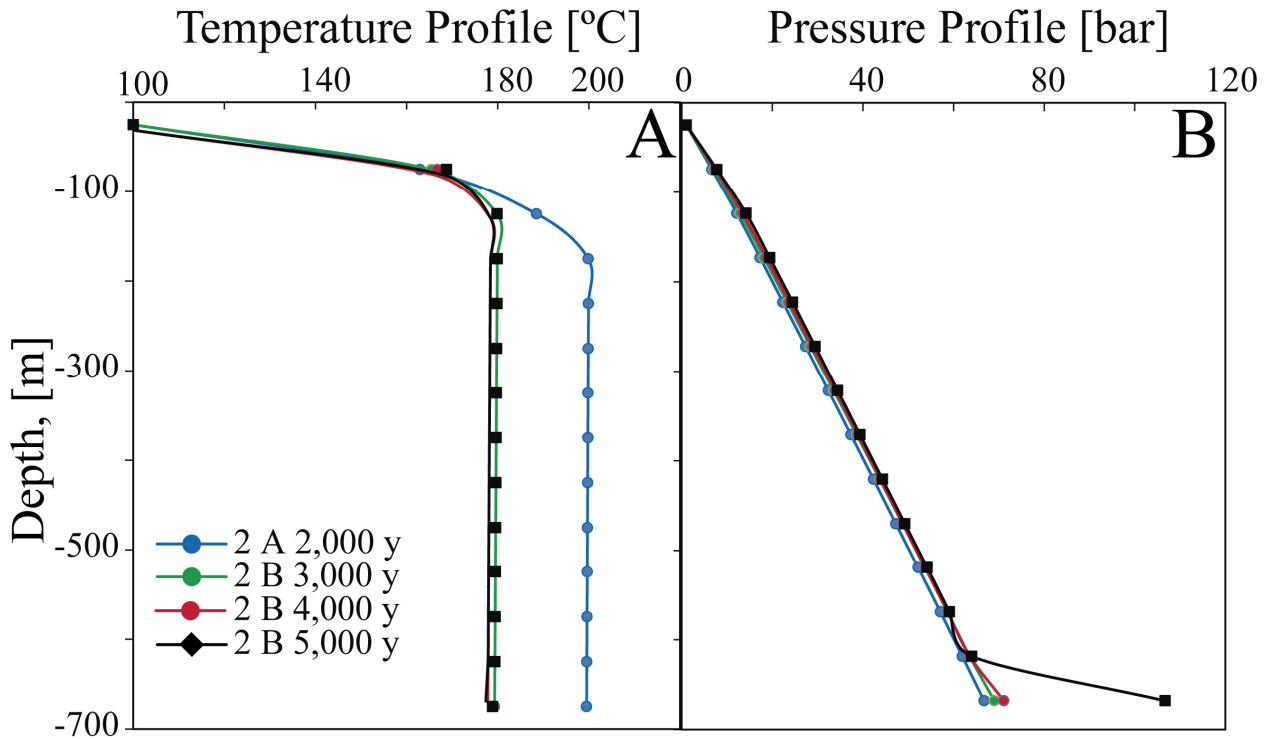


Figure 23. Temperature and pressure profile at different times for Model 2. (A) The temperature profile followed an isothermal trend up to 200 m depth, and then the boiling point curve upwards 200 m depth (B) The pressure profile followed the hydrostatic curve for most of the simulation, but by the end of the simulation increased below 600 m depth.

III. Hydrothermal Alteration

The alteration mineralogy distribution during the ore stage in both fractures and matrix of Model 2 is displayed along the vertical profile of the model in figure 20. The initial propylitic assemblage is a result of the pre-ore stage of the previous Model 1 consisting of plagioclase + epidote + chlorite + daphnite + quartz, in Model 2 this mineral assemblage developed in a similar fashion as the alteration during the ore stage of Model 1 (Figure 19).

For the fractures (Figure 24 [A]), epidote and chlorite are replaced by daphnite at depth, where the alteration assemblage becomes plagioclase + quartz ± chlorite + daphnite with minor amounts of illite. By the end of the ore stage, daphnite is the most abundant mineral at the bottom boundary of the model and epidote is not present below 300 m depth at 5,000 years.

In the matrix (Figure 24 [B]), epidote also decrease in abundance from the bottom of the model, but it did at a slower rate and was not completely replaced. In the matrix, the mineral alteration assemblage is plagioclase + epidote + chlorite + daphnite + quartz and is similar to the pre-ore stage assemblage at 5,000 years.

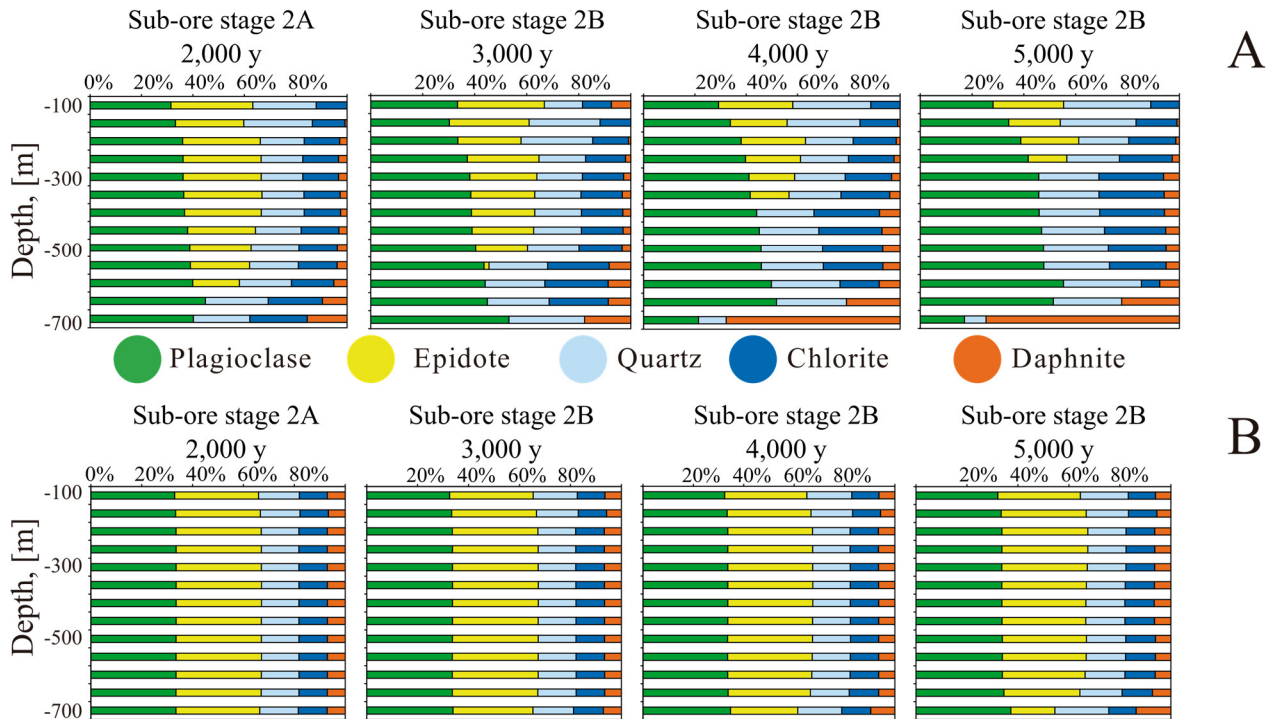


Figure 24. Changes in the alteration mineral assemblage of Model 2. Changes in relative abundance of each mineral, at different times for fractured and matrix media. (A) Alteration mineral assemblage of the fractures, in the fractures epidote is replaced by chlorite, Fe-chlorite (daphnite) is most abundant at the system’s bottom boundary. (B) In the matrix, the alteration minerals had only slight changes in relative abundance, remaining almost constant through time.

IV. Fluid composition and fluid-rock interaction

Model 2 simulate the conditions of the system during the ore stage. In the case of Model 2, the precipitation of sulfide minerals occurred only at the fractures of the system, and the most important changes in the fluid chemistry took place in the fractures. Figure 25 shows changes in pH, aqueous reduced sulfur and Zn^{+2} and Pb^{+2} concentrations at different times during the simulation.

First during substage 2A, at the system’s bottom boundary the fluid acidity is ~pH 4.8, and in the section above 600 m depth, the fluid gets buffered up to a pH 5.8-6.0. The concentration of aqueous reduced sulfur in the fluid increased as the concentration of aqueous Zinc decreased by precipitation of sphalerite in the fractures of the system. From 400 m depth upwards, the amount of Zn in the fluid is too low to precipitate base metal sulfides and the concentration of reduced sulfur becomes higher.

Later for substage 2B, the fluid acidity at the bottom of the system boundary is ~pH 4.4, becoming gradually buffered from 600-400 m depth to a fluid with pH~5.2, and from 400 to the surface boundary to a fluid with pH ~5.7-5.8. The concentration of aqueous Zinc and Lead decrease

gradually from bottom boundary up to 200 m depth. As base metals concentrations decreased from the bottom boundary to the top, reduced sulfur concentration (HS^-) increases and the pH is buffered from acid to neutral (Figure 21).

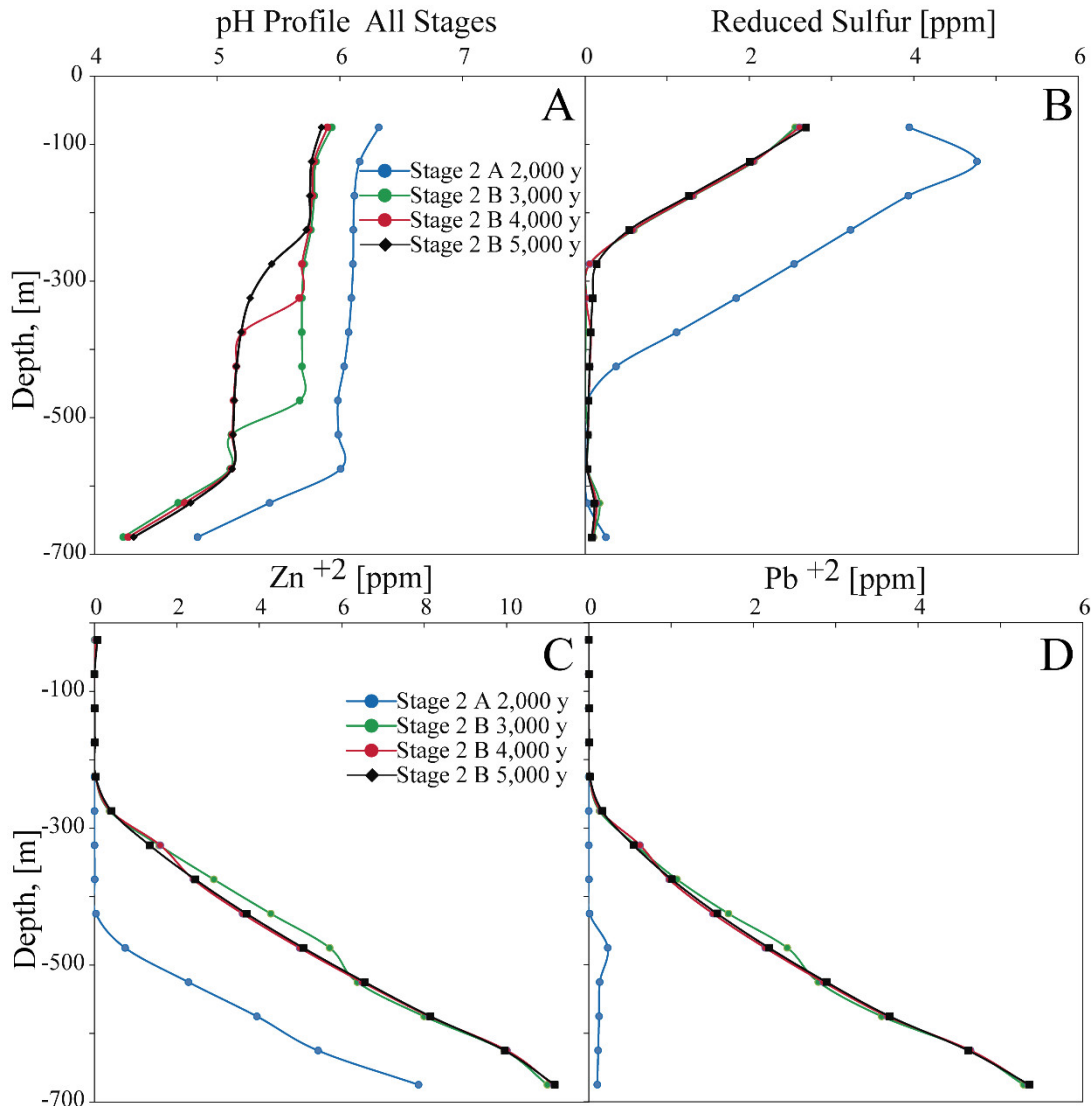


Figure 25. Changes of pH, reduced sulfur concentration [HS^-], Zn^{+2} and Pb^{+2} for Model 2. Model 2 simulated Patricia’s ore stage, the first 2,000 years simulated sub-stage 2A, the following 3,000 years simulated sub-stage 2B. (A) pH profile at different times, for the first 2,000 years the fluid’s acidity is buffered ~ pH 6.0 of 2,000 years, after 3,000 acidity increased below 300 m depth to ~pH 5.0 (B) Reduced sulfur concentration (C) Total Zn^{+2} (D) Total Pb^{+2} . Base metals concentrations are maximum at bottom and decrease up to 300 m. depth. Initial Zn^{+2} is 10 ppm at all times, from 3,000 years initial Pb^{+2} is 6 ppm.

V. Sulfides, Paragenesis, Base-Metals Resources

Using the same sequential approach as previous Model 1 and the same ore fluid compositions, Model 2 also replicates successfully the ore mineral sequence observed at the Patricia deposit. The base metal mineralization horizon (Figure 26) extends from ~ 600 m depth to 200 m depth; base

metals are more abundant at the deeper section of the system. In Model 2, sulfide ore minerals precipitated only in the fractured continuum, the mineralization concentrates in the fractures, being analogous to a vein mineralization style.

In substage 2A, minor amounts of lead precipitates as galena in the system, and ~95% of the zinc precipitates as sphalerite below 400 m depth (Figure 26 [B]). During substage 2B, galena precipitates in the bottom boundary, but sphalerite does not precipitate in the same region, and the sphalerite that precipitated in the previous 2A stage is not observed at the bottom boundary, being replaced most likely by galena. Base metal precipitation decreases gradually from the bottom boundary up to 200 m depth, with ~ 60% of the total base metal precipitated below 400 m depth. At the end of the ore stage in Model 2, after 5,000 years of fluid circulation, a total of 56,610 tons of lead and 156,030 tons of zinc had been precipitated as galena and sphalerite respectively by hydrothermal fluids.

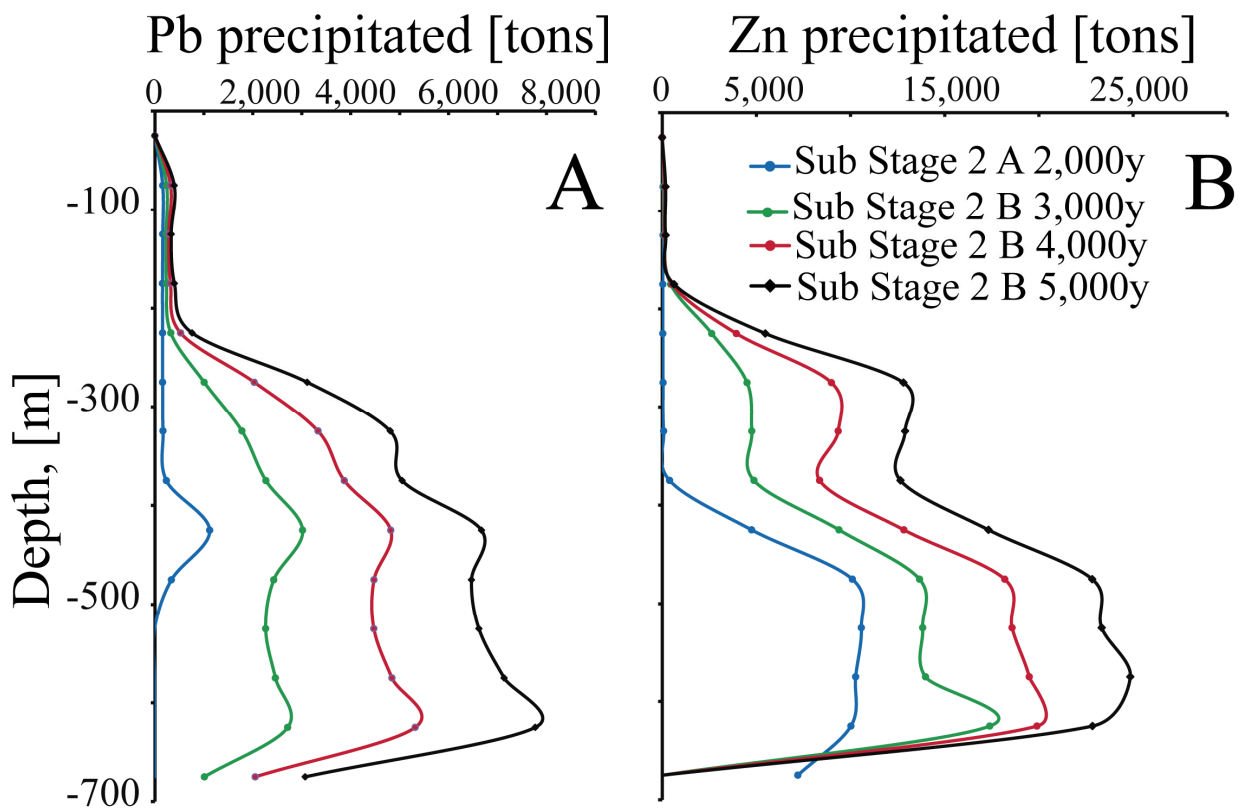


Figure 26. Vertical profile of base metals abundance at different times during ore substages 2A and 2B for Model 2. Most of the base-metal ore resources precipitated at fractures below 300 m depth, sulfide minerals did not precipitate in the matrix. (A) Lead precipitated as galena in fractures. (B) Zinc precipitated as sphalerite in fractures.

2.7.4.3 Model 3

Model 3 explored the role of the mineral alteration assemblage of the fractures in the formation of the base metal mineralization. For Model 3, the same representation of the host rock with two different medias of Model 2 was used, with a matrix with low permeability (10^{-15} m^2) and a fractured zone with higher permeability (10^{-13} m^2). This model reproduces the fluid rock interaction during the ore stage for a period of 5,000 years. The initial conditions for the gangue mineral

assemblage are the same as those from the assemblage obtained at the end of the pre-ore stage in Model 1. The ore fluid compositions are the same as Model 1 and Model 2. The main difference with Model 2, is that for substage 2B, mineral precipitation in the fractures is restrained to quartz, pyrite, galena and illite, and no other mineral phases are allowed to precipitate in the fractures. No further changes were made for the matrix mineralogy.

I. Porosity and Permeability

Figure 27 shows the permeability and porosity profile for both the fracture and matrix continuum of Model 3. In the fractures, permeability and porosity remained almost constant for most of the system with the exception of the upper 200 m, where permeability and porosity have a significant decrease.

The permeability and porosity of the rock's matrix have similar behavior as the fractures. Mineral dissolution dominates most of the system up to the upper levels where the permeability and porosity decrease. Along most of the vertical system's profile permeability and porosity have a minor increase compared with the previous models (less than 1.5 the initial permeability)

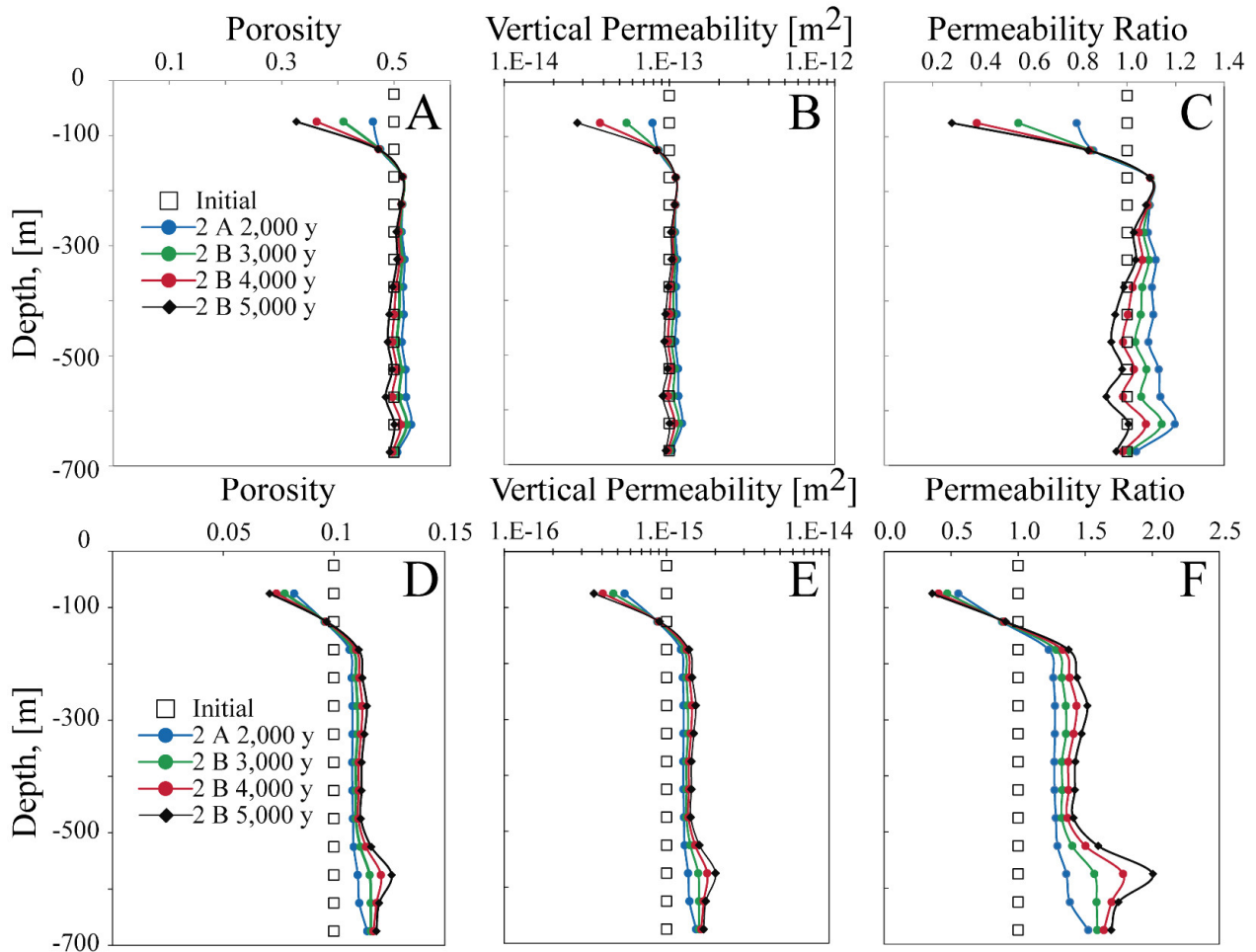


Figure 27. Changes in the porosity and vertical permeability distribution at different times for fractures and matrix media in Model 3. In Model 3, permeability and porosity changes at both fractures and matrix media were similar, with a decrease above 200 m. depth. (A) Changes of porosity in the fractures. (B) Vertical permeability in m^2 in the fractures. (C) Vertical permeability

initial/final ratio of the fractures. (D) Changes of porosity in the rock matrix. (E) Vertical permeability in m^2 in the rock. (F) Vertical permeability initial/final in the rock matrix.

II. Temperature and Pressure

The modeled temperature profile is shown in Figure 28 [A], this profile is almost isothermal up to 200 m depth. The profile closely follows the boiling curve, but the fluid never boils, at all stages of the model the fluid is a one phase liquid fluid.

The modeled pressure profile is shown in Figure 28 [B] and remained similar to the hydrostatic pressure profile through all the modeled period.

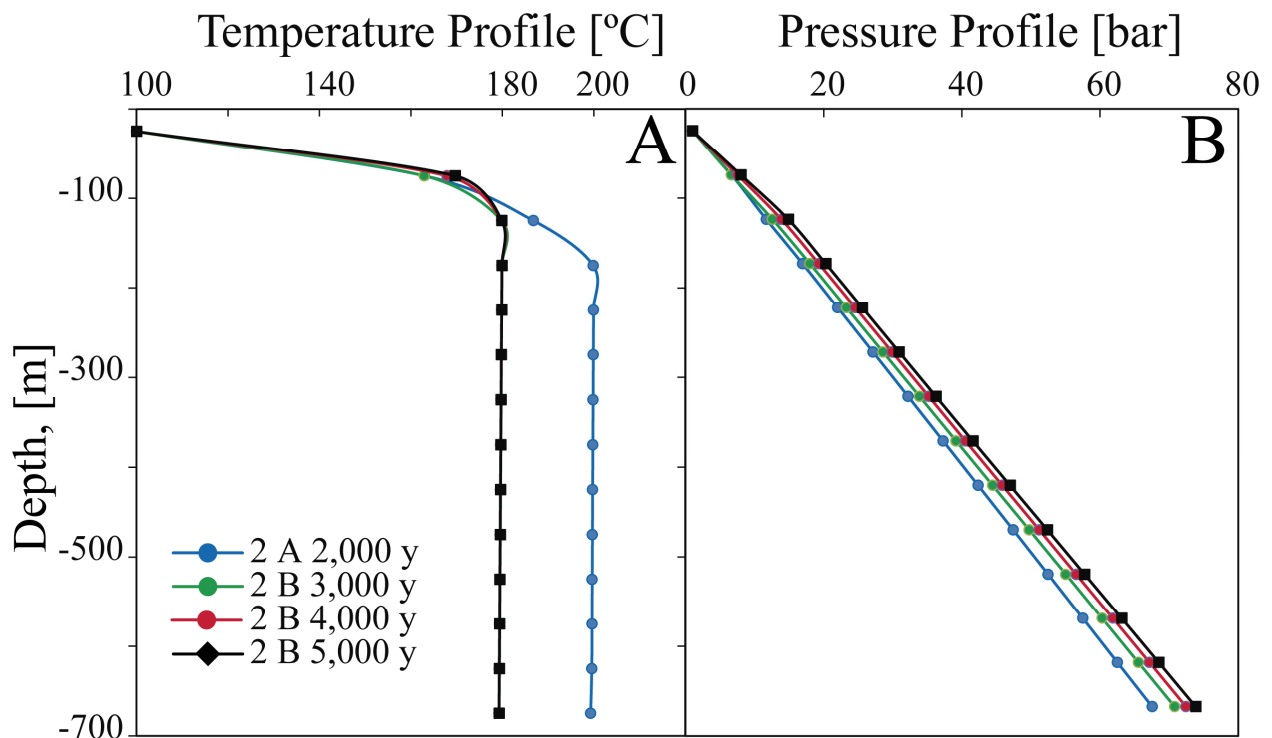


Figure 28. Temperature and pressure profile at different times for Model 3. (A) The temperature profile was isothermal below 200 m. depth, and followed the boiling point curve upwards. (B) Pressure profile, the pressure profile followed the hydrostatic curve during this simulation.

III. Hydrothermal Alteration

The veins at Patricia deposit have a mineral assemblage of quartz + sphalerite + galena \pm pyrite \pm daphnite. For this reason in Model 3 the mineralogy of the fractures was limited to quartz and base metal sulfides with a restriction on the precipitation of other mineral phases. Since most alteration minerals were not allowed to precipitate, the alteration assemblage of the fractures remained almost constant over time during the ore stage (Figure 29), with the only change being an increase in the abundance of quartz in the upper 200 m of the model.

For Model 3, the alteration assemblage of the matrix is the same as the resulting in previous Model 2 (as in Figure 24 [B]) with minor changes in the relative abundance of the mineral phases.

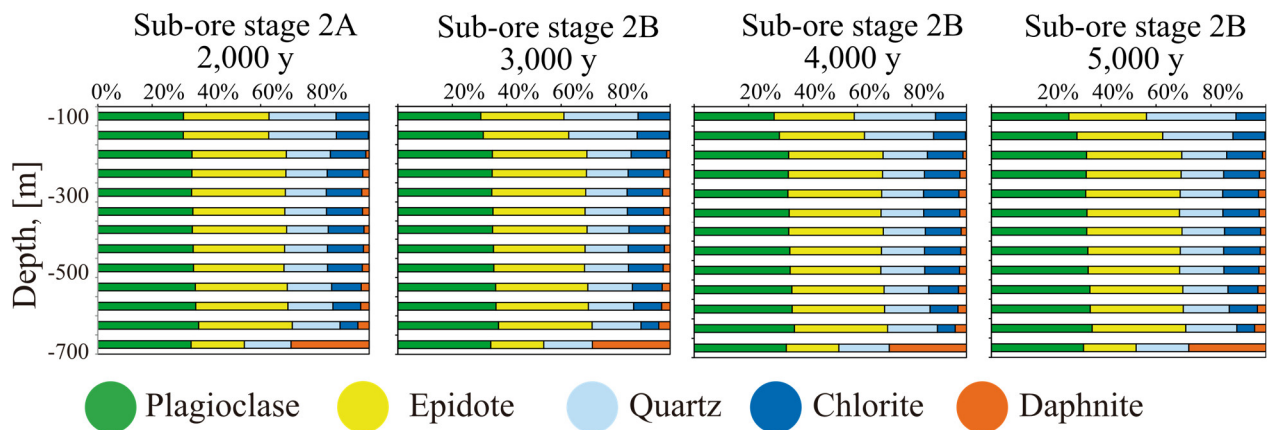


Figure 29. Changes at different times of the alteration mineral assemblage of the fractured media of Model 3. In this model, both fractures and matrix's responses to the fluid-rock interaction were similar, the alteration assemblage remained constant over time.

IV. Fluid composition and fluid-rock interaction

Figure 26 shows changes in pH, aqueous reduced sulfur, Zn^{+2} and Pb^{+2} concentrations at different times for the main ore stage period for the Patricia deposit simulated in Model 3.

During substage 2A, at the system's bottom boundary the fluid acidity is \sim pH 4.8, and in the section from 600 m depth, the fluid gets gradually buffered up to pH 5.5 -6.0. As the concentration of aqueous Zinc decreases by precipitation of sphalerite in the fractures of the system, the concentration of aqueous reduced sulfur in the fluid increases. From 400 m depth upwards, the amount of Zn in the fluid is too low to precipitate base metal sulfides and the concentration of reduced sulfur becomes higher.

For substage 2B, the fluid acidity at the system's bottom boundary is \sim pH 5.0, becoming gradually buffered up to 300 m depth to pH 5.3, and from 300 m to the surface boundary to a fluid has with pH \sim 5.7-5.8. Aqueous Zinc and Lead concentrations decrease gradually from the bottom boundary up to 300 m depth (Figure 30 [C], [D]).

As seen in the previous models' results, as the fluid ascends and base metals sulfides precipitated, base metals concentrations decreased, and reduced sulfur concentration increased while pH gets buffered from acid to neutral.

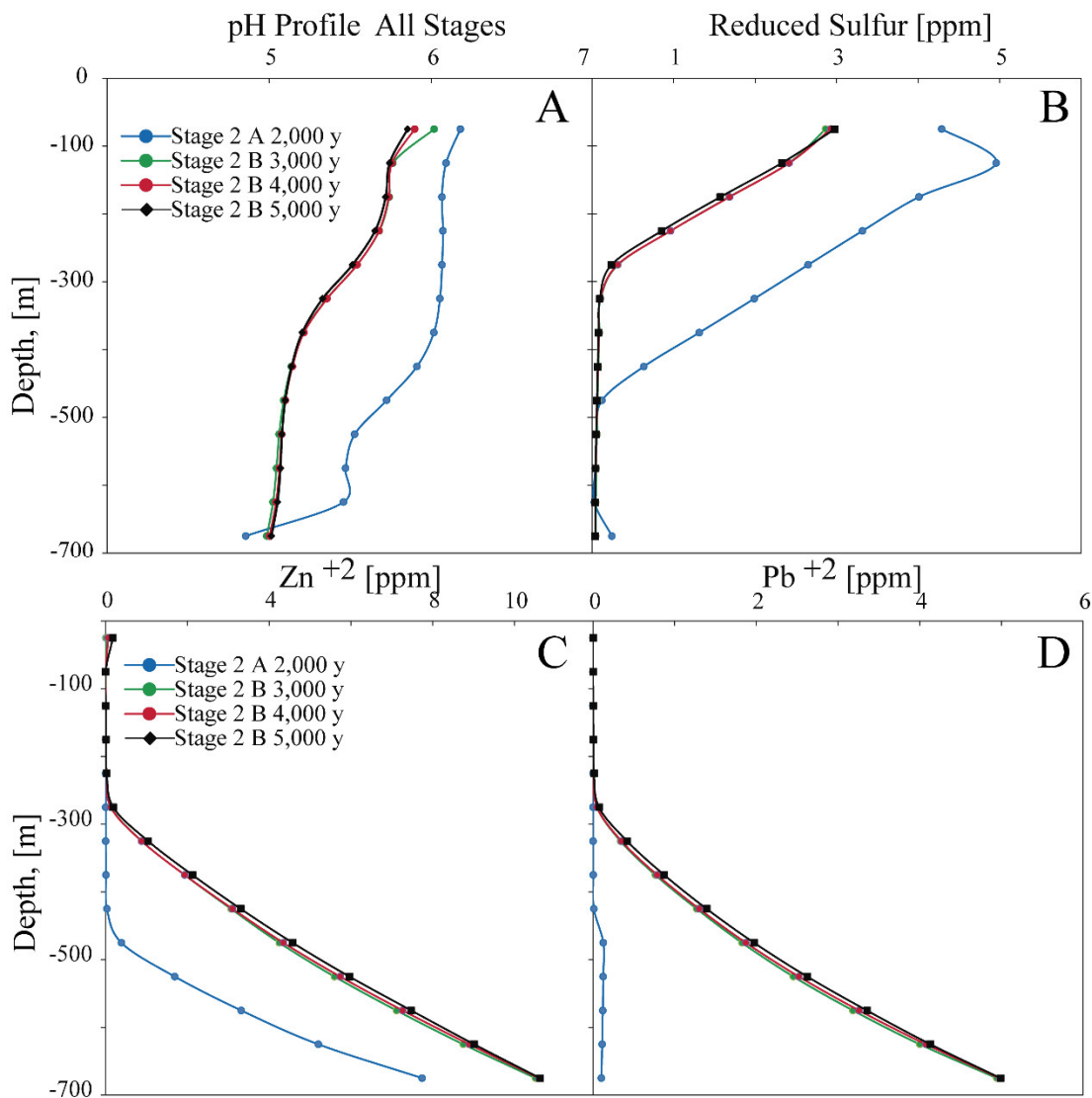


Figure 30. Changes of pH, reduced sulfur concentration [HS⁻], Zn⁺² and Pb⁺² for Model 3. Model 3 simulated Patricia’s ore stage, the first 2,000 years simulated sub-stage 2A, the following 3,000 years simulated sub-stage 2B. (A) pH profile at different times, fluid acidity changes from substage 2A to substage 2B, pH decreases over time. (B) Reduced sulfur concentration (C) Total Zn⁺² (D) Total Pb⁺². Base metals concentrations were maximum at bottom and decreased up to 300 m. depth. Initial Zn⁺² is 10 ppm at all times, from 3,000 years initial Pb⁺² is 6 ppm.

V. Sulfides, Paragenesis, Base Metals Resources

In Model 3, the base metal horizon extends from ~ 700 m depth to 200 m depth; base metals being more abundant at the deeper section of the system (Figure 31). Sulfide ore minerals precipitate only in the fractured continuum of the system, the mineralization concentrates in the fractures, being analogous to a vein mineralization style.

In substage 2A, scarce amounts of galena precipitate in the system, and ~95% of the zinc precipitates as sphalerite below 300 m depth (Figure 31 [B]). During substage 2B, lead and zinc precipitated as galena and sphalerite in the bottom boundary. Base metal precipitation decreased

gradually from the bottom boundary up to 200 m depth, with ~ 60% of the total base metals precipitated below 400 m depth. At the end of the ore stage, after 5,000 years of fluid circulation, a total of 52,602 tons of lead and 157,731 tons of zinc had been precipitated by hydrothermal fluids.

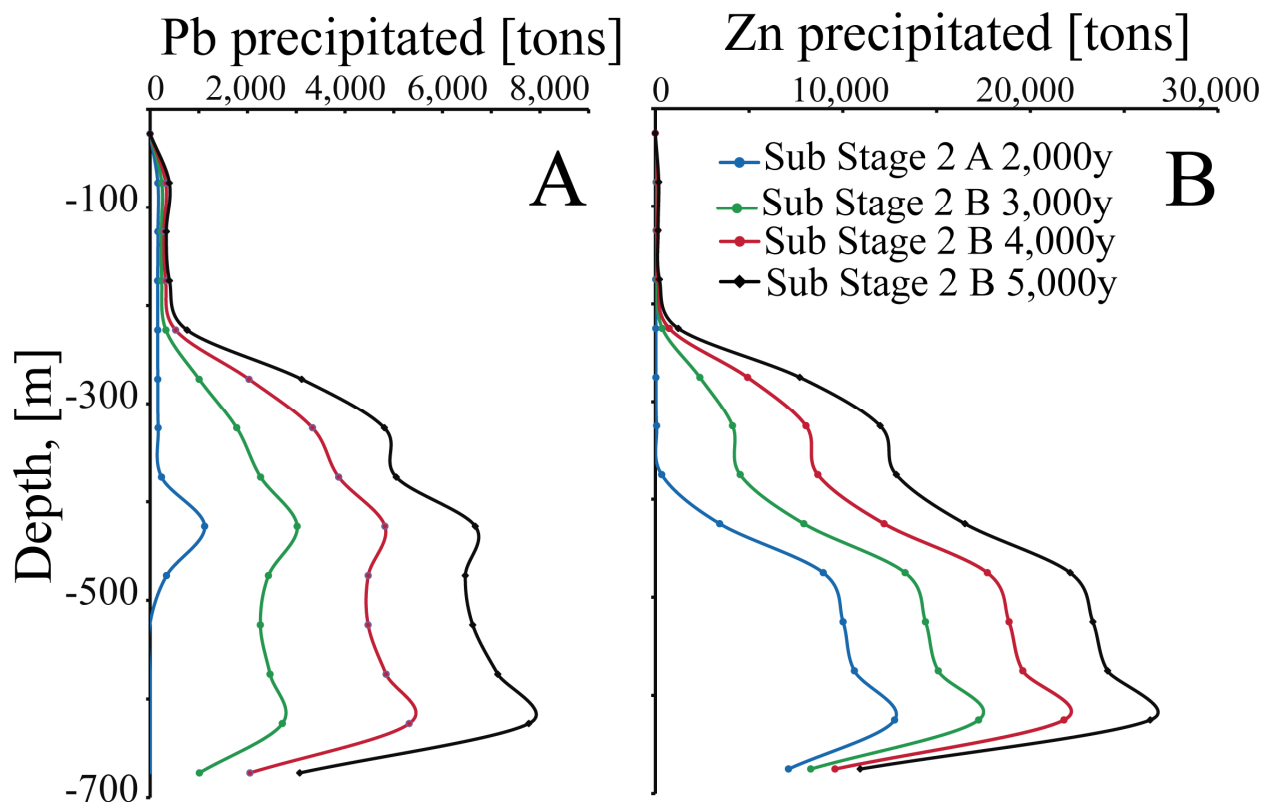


Figure 31. Vertical profile of base metals abundance at different times during ore stages 2A and 2B for Model 3. Most of the base-metal ore resources precipitated at fractures below 300 m depth, sulfide minerals did not precipitate in the matrix. (A) Lead precipitated as galena in the fractures. (B) Zinc precipitated as sphalerite in the fractures.

2.8 DISCUSSION

2.8.1 Conceptual Model

The model implemented with TOUGHREACT explains the formation of the Patricia deposit as the result of the interaction of the system's host rock mineralogy with hydrothermal fluids with variable compositions over time coupled with the occurrence of fluid mixing during the geothermal system active period.

TOUGHREACT made possible to model the system's geothermal activity, and emulates the fossil system's geologic features. The model is consistent with the Patricia deposit's features from field, mineralogy and fluid inclusion data.

Large periods of fluid circulation containing low metal budgets followed by shorter periods of circulation of fluids with ore forming metal budgets account for the formation of the Patricia ore deposit. This variability of the fluid composition over time explains the change of the system in response to the fluid-rock interaction resulting in the formation of sulfide mineralization and the related alteration assemblage. Given the thermodynamic and related metal solubility conditions of the ore stage fluids, the circulation and cooling of metal bearing fluids is not enough to produce an extended vertical horizon of base metal mineralization. In the absence of boiling, mixing of metal bearing fluids along the vertical fluid pathway with fluids carrying reduced sulfur is the mechanism, according to our model, able to precipitate sulfide minerals in the system.

Mixing of base metal chloride rich fluids poor in reduced sulfur with reduced sulfur bearing fluids has been proposed as an ore forming mechanism in sediment hosted Zn-Pb deposits SEDEX, Mississippi Valley-type and Irish types (Wilkinson et al. 2005, Paradis et al. 2007, Stoffell et al. 2008). For other epithermal deposits as the Creed base metal epithermal deposit, ore formation also has been interpreted as produced by fluid mixing (Hayba 1997).

The proposed period of 10,000 years for the total duration of the system's activity was considered taking in consideration previous numerical studies that constrain the activity of a geothermal system to periods ~ 10,000-20,000 years on the basis of the system's host rock initial permeability distribution. This estimation of the ore stage duration was based on the measured metal concentrations from fluid inclusion data and mass balance estimates accounting for moderate up-flow rates (100 kg/sec). The modeled ore stage duration was 5,000 years, this estimated period of time for the ore stage is consistent with the thermal stability of a geothermal system estimated from numerical models as a function of the initial permeability distribution. Similar periods are obtained also by estimates on the rate of metal diffusion on sulfides from the Creede ore deposit (Campbell and Barton 2005).

For Models 1, 2 and 3, the mass balance of the system is consistent with the estimated resources of the Patricia deposit and prove that fluid mixing could be an efficient mechanism to form base metal mineralization. The modeled alteration assemblage and mineral paragenesis resulting from these models is consistent with the geologic features of Patricia deposit.

2.8.2 Modelling approach: Single porous media and double porosity media models

Two different modeling approaches were made considering two different representations for the rock media involved in the hydrothermal interaction.

Model 1, considers one single porous media, to calibrate a first estimate of the duration of the ore stage and the fluid composition applying mass balance constrains on the ore formation process.

This approach describes the distribution of the ore minerals following a disseminated mineralization style. The principal results from Model 1 shows that the ore fluid was acidic, with low reduced sulfur concentrations, and base metal concentrations of ~10 ppm. Considering an up-flow rate of 100 kg/s for system, the ore stage would have lasted a total period of ~ 5,000 years. Under this conditions fluid mixing has the potential to form all the ore resources estimated for the Patricia deposit disseminated through the host rock.

For Model 1 porosity and permeability have a general increase along most of the system's vertical profile. Permeability increase more than 2 times the initial value for the host rock. Finally, the permeability and porosity had a notorious decrease at the upper system's boundary, where the thermal gradient is sharpest.

Since the single media approach does not describe the formation of base metal mineralization in a vein style, we used a porous media representation implemented with TOUGHREACT to monitor the fluid-rock interaction in both fractures and rock matrix. Matrix refers to an intact and non-fractured rock media of lower porosity and permeability than the fracture media, of higher permeability and porosity.

Since reactive transport is very taxing on computational resources, a simple multiple interacting continua representation was used, a dual porosity representation of fractures and rock media.

Models 2 and 3 consider only a period of 5,000 years for the ore stage of the Patricia deposit. The focus of these models are the differences between the fluid-rock interaction in fractures and matrix. In both model's results the sulfide minerals precipitate only in the fractures which corresponds to the 10% of the total system's volume, effectively concentrating the ore mineralization.

i. Permeability of models with a double porosity media description

Most models of geothermal activity do not consider the feedback over the initial permeability by the effects of both mineral precipitation and dissolution, in this model we also considered the feedback of mineral precipitation and dissolution on the permeability distribution of the system.

In Models 2 and 3, the same development is observed in the upper boundary of both models (Figures 18 and 23), in the fracture media and in the matrix media both porosity and permeability decrease in the upper 200 m of these models as the temperature decreases and pH increases, an increase in the precipitation rate of some minerals, especially quartz is observed, causing the decrease in permeability.

From the intermediate section of Models 2 and 3, between 200 m depth down to 600 m depth, both the rock matrix's permeability and porosity increase in both models. This increase it is more pronounced near the bottom boundary, around 700 m depth for the matrix of Model 2, and, although less pronounced, is also observed in Model 3.

A similar trend is observed for the fractures of Model 2 and 3, with a higher increase in permeability of the fractures of Model 2, by dissolution of the alteration minerals, specially epidote. In Model 3, where the alteration minerals are not considered in the fractures, permeability has a minor decrease caused by the precipitation of quartz and base metal sulfides.

At the bottom boundary of the fractures of Model 2 (figure 18 A, B, C), permeability decreases more than one order of magnitude. This is produced by the replacement of the alteration minerals in the fracture for daphnite, which became the most abundant mineral at the bottom boundary. This abrupt change in permeability is not observed in the fractures of Model 3 (figure 23 A, B, C) where daphnite is not allowed to precipitate.

The observed decreasing trend of the model's permeability at the upper and lower boundaries of the system highlights the necessity of a mechanism able to compete with the mineral changes that could decrease the permeability in a geothermal system, and enhancing the system's overall permeability. The majority of the studies on permeability control over the duration of geothermal activity considers a constant permeability distribution and assume a system's life activity controlled by the influence of a nearby magmatic body, providing the heat necessary to maintain fluid circulation. However, it has been found that a static permeability is not a realistic assumption, and the concept of "perturbed crust" is currently being considered to argue that permeability is not a static but a dynamic geological variable, depending among other factors on the tectonic control over geologic structures and the response of the rock media to the mineral precipitation/dissolution produced by fluid-rock interaction (Ingebritsen and Gleeson 2015).

Our models consider that apart from mineral feedback on permeability, there is no other mechanism controlling permeability, this is likely a major simplification. The Patricia deposit is located close to a structural system that represents a high permeability zone, along which hydrothermal fluids could have been circulating over a long period of time, and where a high permeability distribution could have been renewed in a periodic rate by the structural activity. The potential effects of this mechanism in the permeability of the system are not explored by our model.

ii. Temperature and pressure response to changes in permeability

Both temperature and pressure experience changes in direct response to the permeability change of the system. In Model 1, permeability decreases at the upper boundary causing changes in the temperature profile. The curve of the pre-ore stage is more similar to the boiling-point curve, meanwhile the temperature profile of the ore stage and the post-ore stage it is different for the boiling-point curve (figure 14 A). However, the fluid does not boil, because the pressure is also increased over the hydrostatic pressure profile (figure 14 B).

In Models 2 and 3, the temperature profile during the ore stage is similar to the boiling-point curve, and the pressure profile to the hydrostatic pressure profile. However, in Model 2, after a strong decrease of the permeability in the lower boundary of the model, pressure increases over the hydrostatic pressure curve.

2.8.3 Fluid-rock interaction along the vertical up flow pathway.

We discuss the interaction of the fluid-rock interaction considering together the changes in fluid composition and mineralogy. The fluid acidity is closely related to the alteration mineral assemblage, meanwhile whenever the fluid carries base metals in solution, metal concentrations are controlled by the fluid mixing mechanism that precipitates base metal sulfides. In all models pH increases from initial acid values into neutral range as a consequence of the buffering of the alteration minerals. In all models, along most of the vertical extension of the system, pH is controlled by the rock buffer. Low reduced sulfur concentrations ($< 10^{-4}$ mol/kg) are necessary to maintain the transport of base metals in the ore fluid along the fluid's path, the addition of small

amounts of reduced sulfur allow efficient precipitation of base metals into sulfides along the vertical fractures.

During the pre-ore stage, the injected fluid has a pH of 5.5 and the fluid maintains a pH > 5.5 through the system. The andesite primary mineralogy is altered into a propylitic assemblage. The diopside is completely replaced and disappears from the mineral assemblage, and there is partial replacement of plagioclase by epidote, chlorite and daphnite by the end of the ore stage.

Despite changes in the hydrothermal fluid acidity during the ore stage (pH 4.5) and during the post-ore stage (pH 6.0), pH remains near ~ 5.5 buffered by the mineral rock assemblage, pH is lower at the bottom boundary where epidote is replaced by daphnite, interestingly at the bottom boundary where pH < 5.0, base metal sulfides do not precipitate.

During the hydrothermal active period, there is dissolution of the silicate minerals along the fluid flow path, increasing the permeability of the host rock, this is a consequence of the composition of the injected hydrothermal fluid which is saturated in silica, but undersaturated in all the other silicate phases. Over time, daphnite replaces epidote as the most abundant mineral phase in the mineral assemblage. This replacement is most notorious at the bottom boundary of Model 1.

In Model 2 and Model 3, the results consider the fluid compositional changes in the fractures, the greater degree of fluid-rock interaction in these models takes place at the system's fractures. The fluid composition at the matrix continuum remains mostly unchanged.

Model 2 considers that all the alteration minerals are interacting with the fluid at the fractures. During substage 2A, the initially acid fluid gets buffered from 4.8 to pH 6. The increase in the fluid acidity is correlated to the decrease in epidote abundance at the deeper portion of the system, in the sections where epidote is present in the alteration assemblage, pH remains neutral.

During substage 2 B, epidote dissolves from the bottom up to the upper part of the system. If epidote and chlorite are completely replaced by daphnite pH decreases down to < 5.0, where epidote is absent but there is chlorite, pH is buffered up to ~ 5.1, and in the upper 300 m, where epidote and chlorite are present, the fluid pH is 5.7. Daphnite precipitates mainly at the bottom boundary of Model 2 and is far less abundant upwards.

The precipitation of Fe-chlorite (daphnite) could be a consequence of the reactive rate law and reactive surface area considered in the model allowing faster precipitation rates than in natural conditions. Perhaps, it could be caused by the fact that we did not consider another alteration mineral competing for the aqueous iron in the fluid.

In Model 2 base metals concentrations are also controlled by the fluid mixing and show an inverse correlation with the reduced sulfur content of the fluid.

Model 3, considers for the fracture the presence of only the minerals observed in the veins of the Patricia deposit. The minerals observed are quartz + base metal sulfides (pyrite + galena + sphalerite). The aim of this model was to describe the influence over the fluid geochemistry of the of the mineral assemblage present in the fractures.

During substage 2A, the initially acid fluid gets buffered from 4.8 to pH 5.4 and to pH 6.0 from 400 m upwards. This pH change is correlated with the upper limit of the precipitation of sphalerite. During substage 2 B, the profile of the fluid's acidity is much smoother starting at the bottom

boundary at pH 5.0, and gradually going up to pH 5.6-5.8 at depths < 300 m. The pH increase is correlated with the upper limit of the base metal mineralization horizon.

2.8.4 Sulfide distribution and fluid chemistry

All models showed a vertical horizon of base metal mineralization extending for hundreds of meters. This result indicate that fluid mixing is a viable ore forming mechanism for the conditions of the Patricia deposit. Both Model 2 and 3 results suggests that sphalerite precipitation is favoured by a fluid acidity ~ pH 5.0-5.3. Galena precipitation has the same trend. In Model 2, it appears that, during Stage 2 B, galena replaces the sphalerite precipitated in the bottom boundary during Stage 2 A. This suggest that galena could leach reduced sulfur from the sphalerite at pH < 5.0.

2.8.5 Pyrite Formation

The objective of the model is to replicate the formation of base metal sulfides in the epithermal environment however a major issue remained unaddressed in our models which is the formation of pyrite in the system. In our models pyrite only forms in the shallow upper boundary of the system where the temperature gradient is sharpest whereas it would have been expected a more conspicuous presence along the system. The reason for this could be a simplification of the behavior of aqueous iron in the hydrothermal fluid. In our geochemical framework either iron behaved as a non-reactive component of the fluid, or was consumed by daphnite formation in the deeper parts of the system. We did not consider the incorporation of iron into sphalerite, which could account for a different behavior of the solubility of aqueous iron in the hydrothermal solution. Another possible reason could be an unappropriated rate law for the precipitation of pyrite in this conditions. These inconsistencies suggests that the ore forming process of base metal mineralization is a lot more complex.

It is possible another mechanism able to form base metal sulfides without fluid mixing? In exploratory models, the initial pyrite formed in the pre-ore stage was dissolved and completely replaced in the ore stage, becoming a source of reduced sulfur for both galena and sphalerite. In that scenario, base metal sulfides could precipitate from a metal bearing fluid without mixing being a required condition. However, without fluid mixing, an extended pyrite vertical horizon could not be formed in our models and neither a vertical horizon of galena and sphalerite.

Similarly, sphalerite precipitated in the first ore substage could become a source of sulfur for the precipitation of galena if the fluid pH is <5.0. The following sequence of base metal sulfides dissolution and formation was observed: pyrite> sphalerite> galena, in which pre-existent sulfide minerals become precursor of another sulfides: pyrite is a precursor of sphalerite and sphalerite a precursor of galena, being potential sources of reduced sulfur for the formation of latter sulfides.

However, in the samples of sulfide minerals from the Patricia deposit, there is no evidence of this sulfide replacement sequence.

2.8.6 Limitations

The inherent complexity of the geochemistry of fluid-rock interactions in the epithermal environment made necessary simplifications and assumptions regarding the aqueous chemistry and the minerals considered. Chlorite and epidote are both minerals with solid solutions, thermodynamic and kinetic data for these minerals is available only for some solution end-members, and also in the case of epidote its kinetics also depends on whether the crystals are well

developed or amorphous. For the models here discussed the thermodynamic data for daphnite and crystalline epidote from the SOLTHERM database was considered, disregarding the diversity of these minerals.

Another important simplification is the assumption of a reducing environment. A reaction controlling the redox state of the system was not considered, given that the deposit mineral assemblage, suggests a single redox state accounting for all the mineralogy. Under this assumption all the thermodynamic data for the model was calculated for the Fe^{+2} iron species.

Reactive transport models of sulfide formation in epithermal deposit are scarce. To our knowledge there are no studies to compare the kinetic results of our model specially to compare the effect and relevance of the reaction rates used for the sulfide minerals. Usually, these rates are measured for dissolution under < 100 °C, although the same approach is used to model silicate minerals, whereas sulfide minerals kinetics are considered more complex and difficult to understand (Acero et al. 2007a, Acero et al. 2007b). Although the kinetic approach applied with TOUGHREACT has been used previously in other studies, it remains considerable uncertainty remains about the kinetic rate laws, the precipitation mechanism and the values of mineral reactive surface areas in natural conditions.

To account for this, we tested the sensibility of our model's behavior to the following parameters: flow rates, permeability, metal and sulfur aqueous concentration, the mineral assemblage, the mineral's reactive surface and the mineral's kinetic rates. Our current results are the end-product of this previous analysis. One interesting consideration from our initial exploratory models using reactive transport to describe the behavior of the fluid-rock interaction in a geothermal system is that although the life-time scale of the system is $\sim 1,000$ - $10,000$ years, the system could not be described by fluid-mineral reactions at equilibrium, even for periods of this magnitude and with the system being close to equilibrium, the kinetic approach became a necessity to describe the fluid-rock interaction and replicate the observed mineral distribution.

By calibrating reactive modeling with TOUGHREACT with solute geothermometry the results from Wanner et al. (2014), agree with the magnitude and range of reactive surface, fluid flow, and kinetic rates used in our model

Apart from the general agreement with the alteration assemblage, the sulfide distribution and the total resources precipitated, there is no more features available to us to validate or refine our model. The Patricia deposit is only studied up to an exploratory stage therefore more data from the deposit is also not available.

Overall our model supports the idea of sulfide mineralization formed by fluid mixing at temperatures < 300 °C and highlights the importance of pH buffers and high permeabilities in the formation of base metal mineralization. It could be of interest to use reactive transport models to understand and calibrate the degree in which mineral reactions control the permeability distribution in a well characterized active geothermal system.

2.9 CONCLUSIONS

A reactive transport model of the Patricia deposit was implemented with TOUGHREACT. Two different approaches to model the fluid-rock interaction were applied. First a model, with the host rock modeled as a homogeneous porous media to understand the process of sulfide mineralization formation in an epithermal environment with temperatures <300°C. And in second place, a model with the host rock modeled as two different medias: matrix and fractures, to explore the relevance of media with different permeabilities in the ore formation process.

The model with a single porous media considers the geothermal system's evolution for a period of 10,000 years and its results provide both insights into the ore forming process and estimates for the fluid geochemical conditions and the ore stage duration: For the inferred system's conditions for the Patricia deposit, and without the occurrence of boiling, the most efficient mechanism to form sulfide minerals in this system is fluid mixing between an acid fluid carrying base metals with little amounts of reduced sulfur 10^{-4} mol/kg; and another fluid providing reduced sulfur. These fluids are provided from the system's up-flow stream and from a lateral flow stream, respectively. Under fluid mixing conditions this model is able to precipitate a similar amount resources to the estimated of base metal resources for the Patricia deposit and also replicates the propylitic mineral assemblage of the deposit. The base metal mineralization distributes itself in an extended vertical horizon of hundreds of meters. Mass balance considerations provided an estimate for the ore stage duration of 5,000 years. In this single porous media model, sulfide minerals precipitate homogeneously in the system's volume in similar way to a disseminated mineralization style.

A dual porosity model representing the host rock as two different medias: matrix and fractures was made to explore the differences in the fluid interaction with the intact rock and the fractured rock media. This model results were also consistent with the deposit estimated resources, the sulfide minerals vertical distribution and the alteration mineral assemblage of the Patricia deposit.

In this second model, the permeability's control over the mineralization distribution was clearly observed, as sulfide minerals precipitated mainly in the system's fractures in a similar fashion to a vein-controlled mineralization style.

Permeability decreased at the upper model's boundary in the zone of sharpest temperature contrast but not up to the point to seal the system forming a rock cap.

The results of both models are validated by replicating the system evolution, reproducing the same mineral alteration assemblage, the expected base metal resource distribution and similar amounts of ore resources to those of the Patricia deposit.

From the reactive transport model, an interesting result was obtained on the control of the fluid's acidity in the formation of base metal sulfides. The fluid's acidity is controlled by the rock mineral assemblage, by buffering the fluid acidity. Galena and sphalerite precipitation is enhanced at 5.0-5.3 pH values, coinciding in the modeled mineral assemblage with the dissolution of epidote in the system's fractures and the formation of Fe-chlorite.

The models are limited by the simplifications considered and the absence of more specific data from the Patricia deposit, like a detailed characterization of the permeability and fracture distribution of the deposit, and a more detailed resource distribution. The model conforms to the general geologic features of the Patricia deposit and provides insight into the ore forming process

and the conditions favorable for the ore stage in a specific set of epithermal conditions but cannot be used to make more specific predictions.

Uncertainty also comes from the reactive modeling approach, a very simplified approach to the kinetic process of mineral dissolution and precipitation was considered. In this approach the degree of uncertainty over the magnitude of the mineral reactive surfaces is significant and is no less important the fact that the rate laws and kinetic mechanisms considered for the sulfide minerals are at best first order estimates for the conditions of the epithermal environment. The last limitation of the current model comes from numerical difficulties to achieve a more detailed and realistic representation of the system permeability's evolution as a response to mineral precipitation and dissolution. More kinetic studies on mineral precipitation and dissolution in the hydrothermal environment conditions are needed to understand the relevance of the alteration minerals in the evolution of the permeability of active geothermal systems.

Finally, our reactive transport model with TOUGHREACT supports fluid mixing as an efficient mechanism to form base metal mineralization in an extended vertical horizon in the epithermal environment without occurrence of boiling. This requires an acid fluid carrying the metals mixing with a different fluid carrying reduced sulfur. Permeability distribution exerts a major control on the distribution of the mineralization into the system: according to our results a porous media with contrasting permeabilities favors the concentration of the ore in the media with higher permeability. Fluid rock interaction provides a pH range favorable for the formation of sulfide minerals through dissolution of different minerals according to their buffer potential. Estimates from fluid inclusion data and mass balance were made of the potential duration of the ore stage giving a period of 5,000 years for a total geothermal activity of 10,000 years.

2.10 Acknowledgments

This study has been supported by the CONICYT-FONDAP project 15090013 and Conicyt (Fondecyt) Iniciacion 11170210. Numerical modeling was supported by computational resources provided by the National Laboratory for High Performance Computing Chile (NLHPC).

3 DISCUSIÓN

La evolución del sistema geotermal que formó el depósito de Zn-Pb-Ag Patricia fue replicada por medio de un modelo de transporte reactivo. El modelo reprodujo satisfactoriamente la paragenesis, la distribución de la mineralización y el tonelaje de recursos estimados para el depósito. A continuación, se discutirán los aportes del modelo planteado para el estudio de las condiciones de formación de Patricia. Además, se discutirá los supuestos considerados para acotar la permeabilidad, las duraciones del período de actividad geotermal y de la etapa de mineralización, y las tasas de flujo de fluidos y concentraciones de metales.

3.1 Revisión del Modelo de Formación del depósito de Zn-Pb-Ag Patricia

En las primeras etapas de este estudio, uno de los supuestos iniciales fue la validez del modelo de formación de mineralización de metales base propuesto previamente para Patricia (Chinchilla et al. 2015, Chinchilla 2017). Este modelo planteaba el enfriamiento gradual de los fluidos mineralizadores como el mecanismo principal de mineralización, un único fluido transportó juntamente metales y azufre en solución, siendo los metales base transportados como complejos acuosos bisulfurados; el mecanismo de desestabilización de esos complejos y de formación de sulfuros de metales base habría sido el enfriamiento de este fluido durante el estadio de mineralización. De esta manera el fluido habría precipitado gradualmente en su ascenso sulfuros de metales base al enfriarse, formándose así un perfil vertical de mineralización de sulfuros de metales base. En esta primera aproximación se descartaba el potencial rol de la mezcla de fluidos en la formación de la mineralización.

Los modelos de transporte reactivo, realizados teniendo en cuenta esta hipótesis, mostraron que, si bien es posible con un solo fluido replicar la paragénesis y el tonelaje de recursos estimados para el depósito, no es posible replicar el típico perfil vertical de distribución de mineralización de Zn-Pb en depósitos epitermales de metales base (Buchanan 1991, Albinson et al. 2001), observado también en terreno en el mismo depósito de Patricia (Chinchilla 2017, Golden Rim Resources 2017). La dificultad planteada por los resultados de estos modelos se mantuvo bajo distintas configuraciones y variaciones en las condiciones iniciales de los parámetros de transporte y la composición del fluido en las simulaciones. Un único fluido resultó incapaz de transportar metales y azufre, en complejos bisulfurados de manera simultánea. En todos los modelos evaluados, los metales bases precipitaron inmediatamente al entrar el fluido mineralizador en el sistema, acumulándose en el nivel más profundo, y el fluido restante reducido a una solución estéril e incapaz de transportar metales a niveles más someros continuó ascendiendo sin formarse el esperado perfil vertical de mineralización de sulfuros.

Esto hizo necesario la revisión del primer modelo conceptual de formación del depósito Patricia, planteado por Chinchilla (2017). En primer lugar, se hicieron estudios de solubilidad de metales, presentados en el Capítulo 2. Y de manera simultánea se revisaron referencias concernientes a la solubilidad de metales en el ambiente epitermal, la más relevante fue el estudio realizado por Zhong et al. (2015). En dicho estudio se plantean dos modos distintos de transporte de metales en función de la temperatura, en el ambiente Porfirico-Epitermal. El primer modo, dominado por complejos clorurados, para temperaturas $< 400^{\circ}\text{C}$, donde procesos de ebullición, cambios en las condiciones de oxidación-reducción del fluido, o mezcla de fluidos son los causantes de la mineralización. Y el segundo modo, dominado por complejos bisulfurados para temperaturas $> 400^{\circ}\text{C}$, donde el principal factor de mineralización es el enfriamiento.

De acuerdo a la evidencia disponible las condiciones de formación de Patricia, indican temperaturas $< 400^{\circ}\text{C}$ (Chinchilla et al. 2015a, Chinchilla et al. 2015b y Chinchilla 2017) para todas las asociaciones minerales observadas en el depósito. Es improbable entonces, dadas estas temperaturas que los metales hayan sido transportados como complejos bisulfurados, lo cual fue corroborado por las simulaciones realizadas considerando un transporte simultaneo de azufre y metales.

Al revisar los antecedentes geológicos disponibles y las consideraciones del mismo modelo previo (Chinchilla 2017), es interesante mencionar que para el estadio 1, previo a la mineralización y para el estadio 3, posterior a la mineralización, la mezcla de fluidos si fue considerada como un proceso relevante para la evolución de los fluidos del sistema. Estudios de isotopos de oxígeno por Chinchilla (2017) en cloritas del estadio 2A y cuarzo de los estadios 1 y 3, reportan evidencias de mezcla de fluidos magmáticos y meteóricos, aunque de menor relevancia, la gradual disminución de salinidad en las inclusiones desde el estadio 1 al estadio 3 sugiere un cierto grado de dilución, que podría haber sido causado también por mezcla de fluidos.

Con estos antecedentes, se modificó el modelo conceptual de formación usado en las simulaciones, y dada la incertidumbre respecto a la posible magnitud de la mezcla de fluidos, se escogió una razón de 10:1, en la cual los fluidos presentes en mayor proporción serían aquellos con una marcada componente magmática, con mayor salinidad y contenido metálico, y los presentes en menor proporción serían de origen meteórico con una cantidad moderada de azufre reducido en solución y bajas salinidades. Esta configuración mostrada esquemáticamente en la Figura 3, dio resultados satisfactorios, replicando la alteración, la paragénesis, mineral, la cantidad de recursos estimados en la exploración del depósito y la distribución vertical de metales base.

3.2 Mezcla de Fluidos en la formación de Depósitos Epitermales

La circulación de fluidos es un proceso intrínseco a la actividad de los sistemas geotermales, la circulación de fluidos causado por celdas de convección es un proceso de ocurrencia generalizada (White y Hedenquist 1990, Hedenquist y Lowenstern 1994, Arnórsson et al. 2007). Dada una distribución de permeabilidad que permita convección de fluidos, una anomalía termal generada por una intrusión hará circular las aguas subterráneas en su vecindad, formando un sistema que permite la interacción de fluidos de diferentes orígenes, en el cual la mezcla de fluidos es un proceso común (Arnórsson et al. 2007).

La geoquímica de los fluidos que circulan en sistemas geotermales proporciona evidencias de ocurrencia generalizada estos procesos de mezcla de fluidos, entre fluidos meteóricos y fluidos con signatura magmática (Giggenbach 1997b, Arnórsson et al. 2007). En general en los sistemas geotermales activos, los fluidos dominantes son de signatura meteórica, llegando a representar más del 90% de los fluidos circulantes (Hedenquist y Lowenstern 1994).

Los mismos procesos que se observan en sistemas geotermales activos, son esperables en sistemas geotermales fósiles, y la relevancia de algunos de estos procesos en la formación de mineralización en depósitos epitermales, se encuentra bien documentada. En particular ebullición, enfriamiento gradual, enfriamiento por conducción o por convección, interacción agua-roca y mezcla de fluidos son todos procesos descritos en sistemas geotermales activos que ocurrieron en sistemas geotermales fósiles, y que formaron mineralización en los depósitos epitermales (Simmons et al. 2005, Heinrich 2007).

Ahora en depósitos epitermales de metales preciosos, la ebullición de fluidos es uno de los procesos más importantes para la formación de la mineralización. ¿Pero tiene la mezcla de fluidos la misma relevancia en la formación de mineralización en depósitos epitermales? Como mecanismo alternativo en algunos depósitos epitermales de Au la respuesta es afirmativa, la mezcla de fluidos si tendría un rol significativo en la formación de mineralización de Au en sistemas epitermales de baja sulfidación (Leach y Corbett 2008, Corbett 2012).

En la misma línea, la caracterización de depósitos epitermales de baja sulfidación de metales preciosos y metales base en México, realizada por Albinson et al. (2001) con datos de análisis de gases y datos de isotopos de oxígeno e hidrogeno en inclusiones fluidas, proporciona evidencias de interacción de fluidos de distintos orígenes en estos depósitos, con composiciones que no pueden ser explicadas exclusivamente por ebullición de fluidos e interacción fluido-roca, en estos depósitos la mezcla de fluidos también habría tenido un rol significativo en la formación de la mineralización

En el caso particular del depósito polimetálico epitermal, Cerro de Pasco en Perú, donde la mineralización habría sido formada por mezcla de fluidos de salinidades bajas y moderadas, este proceso de mezcla fue estudiado en cristales de cuarzo con inclusiones fluidas, análisis de elementos traza con LA-ICP-MS y análisis in situ de isotopos de oxígeno SIMS, mostrando que, durante la formación de un cristal, las condiciones de mezcla de fluidos no fueron continuas, sino que experimentaron variaciones abruptas, con la ocurrencia episódica de múltiples pulsos de fluidos de origen magmático interactuando con fluidos meteóricos durante la formación del mismo cristal, revelándose así un proceso complejo y dinámico (Rottier et al. 2021).

La mezcla de fluidos sería un proceso favorecido por el control estructural del depósito, al haber proveído permeabilidades favorables y canales de mezcla para los fluidos hidrotermales (Corbett 2012). La mezcla de fluidos es también un proceso complejo y dinámico (Lester et al. 2012), no necesariamente constante en el tiempo, sino más bien de carácter episódico, entre fluidos de composiciones también variables.

3.3 El modelo de Mezcla de Fluidos implementado para el depósito Patricia

En el caso de estudio, la presencia de tres estadios paragéneticos diferentes, ha sido interpretada como el resultado de la interacción entre la roca y fluidos circulantes a diferentes temperaturas y distintas composiciones químicas. Cada estadio es el resultado de la circulación e interacción sostenida de un fluido distinto a través de la roca de caja del sistema.

El modelo planteado asume que estos estadios fueron estables por períodos extensos con respecto a la duración total de la actividad geotermal, durante estos estadios las condiciones de mezcla de fluidos se asumieron constantes. Sin embargo, si se considera la evidencia de inclusiones fluidas y la presencia de ciertas características mineralógicas como bandeados composicionales en cristales de esfalerita, es evidente que los fluidos experimentan variaciones durante los estadios paragéneticos de Patricia y no tuvieron ni composiciones ni temperaturas de circulación constantes, las transiciones entre un estadio y otro pudieron haber sido causadas por cambios graduales en los fluidos y las condiciones de los procesos de mezcla, pudieron haber sido mucho más complejas de lo considerado.

En el modelo aquí presentado, a pesar de simplificar totalmente esas variaciones se replica una condición similar al estado final del sistema. Pero estas observaciones plantean preguntas: ¿Cuál es la relevancia de estos cambios dentro de una misma etapa paragenética? ¿Qué explica los

cambios entre un estadio estéril y el estadio de mineralización principal? ¿En qué momento y por cuál causa ingresaron fluidos ricos en metales al sistema geotermal? Estas preguntas van más allá del alcance de este estudio.

3.4 El rol de la Permeabilidad

3.4.1 Distribución de la Permeabilidad del Sistema

El parámetro de mayor relevancia para las condiciones de transporte del sistema es la distribución de permeabilidad asignada al sistema geotermal fósil modelado. Asumiendo la existencia de una intrusión magmática que introduzca un gradiente termal, es el parámetro más crítico para el desarrollo de un sistema geotermal es una distribución de permeabilidad apropiada en las formaciones rocosas en la vecindad de la intrusión (Cathles 1977, Hayba e Ingebritsen 1997). En los sistemas geotermales, la permeabilidad está acotada al rango de 10^{-16} - 10^{-12} m² (Figure 4). En el contexto de los sistemas geotermales, sistemas con permeabilidades intrínsecas $<10^{-15}$ m² son considerados de baja permeabilidad, sistemas de permeabilidad intermedia tienen permeabilidades $\sim 10^{-15}$ m² y sistemas de alta permeabilidad tienen permeabilidades $> 10^{-15}$ m². (Scott et al. 2016).

El valor mínimo de permeabilidad para la viabilidad comercial de un reservorio geotermal es $\sim 10^{-15}$ m² (Ingebritsen y Appold 2012), este es el valor óptimo de permeabilidad para mantener por períodos extensos altas temperaturas y condiciones de ebullición en un sistema geotermal (Hayba e Ingebritsen 1997), permeabilidades $>10^{-15}$ m² enfriarán más rápidamente el sistema y permeabilidades $< 10^{-15}$ m² atenuarán la circulación de fluidos en el sistema, enfriándolo más lentamente (Hayba e Ingebritsen 1997).

En el caso de Patricia, la distribución inicial de permeabilidad durante la actividad geotermal es desconocida, por lo cual se consideró inicialmente una permeabilidad de 10^{-15} m² para la roca de caja del sistema, mismo valor considerado para simular la actividad del sistema geotermal Tolhuaca (Sanchez-Alfaro et al. 2016). El marcado control estructural observado en el depósito incrementa esta permeabilidad por la presencia de estructuras, se asignó pues a las rocas fracturadas una permeabilidad de 10^{-13} m², este valor es apropiado para rocas fracturadas a profundidades < 2 km (Ingebritsen y Manning 2010, Achtziger-Zupančič et al. 2017).

3.4.2 Permeabilidad y Duración de la Actividad del Sistema

La distribución de permeabilidad asignada al sistema limita también la duración de la actividad de un sistema geotermal al controlar la tasa de enfriamiento del sistema, con altas permeabilidades un sistema se enfriará más rápido y tendrá un menor período de actividad que un sistema con bajas permeabilidades (Hayba e Ingebritsen 1997, Weis 2015, Scott et al. 2016).

Para una permeabilidad media de $\sim 10^{-15}$ m², el tiempo de vida estimado de un sistema geotermal mantenido por un solo evento magmático puede ser superior a 20,000 años (Hayba e Ingebritsen 1997, Weis 2015). Si la distribución de permeabilidad de un sistema geotermal se encuentra entre 10^{-14} - 10^{-13} m², el sistema sustentaría actividad geotermal por períodos $< 10,000$ años, durante gran parte de ese período los fluidos se encontrarían en una sola fase, y el desarrollo de condiciones de ebullición sería muy limitado comparado a lo estimado para un sistema de permeabilidad intermedia (Hayba e Ingebritsen 1997, Scott et al. 2016). Condiciones similares a las observadas en Patricia, donde la ausencia de evidencias de ebullición, hace razonable suponer que las permeabilidades del sistema durante su etapa activa fueron más bien altas, lo cual implicaría un período relativamente breve de actividad geotermal.

Al tener también limitaciones computacionales para modelar períodos extensos (>10,000 años), se limitó la duración de la actividad a 10,000 años, un período mínimo para modelar la actividad del sistema geotermal pero que se considera suficiente para estudiar las condiciones de la etapa de mineralización, de mayor interés para los objetivos de este estudio que la etapa estéril del sistema.

3.4.3 Permeabilidad y Duración de la Etapa de Mineralización

La solubilidad de metales transportados como complejos clorurados es particularmente sensible a la temperatura (Figure 14), luego el tiempo que el sistema pueda mantener los rangos de temperaturas estimados para el estadio de mineralización es una limitante para la duración de la etapa de mineralización.

Es relevante entonces considerar también el control de la distribución de permeabilidad en la estabilidad termal del sistema, esto es, el tiempo durante el cual el sistema puede mantener fluidos circulando a una temperatura determinada. Para permeabilidades intermedias ($\sim 10^{-15} \text{ m}^2$) un sistema geotermal puede mantener temperaturas elevadas y condiciones de ebullición por 7,000 a 10,000 años. Si las permeabilidades son más altas ($10^{-14} - 10^{-13} \text{ m}^2$) la ocurrencia de ebullición será limitada, y el sistema tiene la capacidad de mantener temperaturas $>200^\circ\text{C}$ solamente por períodos de 2,500-5,000 años antes de comenzar a enfriarse (Hayba e Ingebritsen 1997, Scott et al. 2016).

3.5 Consideraciones de Balance de Masas y Duración de la Etapa de Mineralización

Es posible obtener otra estimación para la duración del período de mineralización por medio de un balance de masas, entre el tonelaje estimado del depósito, y el tiempo necesario para acumular dicho tonelaje en función de la tasa de flujo de fluidos y de la concentración de metales en solución en dichos fluidos.

Se aplicó un planteamiento similar al usado por Moncada et al. (2019) para estimar la cantidad de fluidos necesaria para depositar cierta cantidad de recursos minerales en un tiempo determinado.

Primero se calculó la cantidad de recursos depositados en un año para una tasa de flujo y una concentración de metales dadas usando la siguiente ecuación:

$$\text{Recursos por año} = 3.15 \times 10^7 [\text{seg}] \quad \text{Tasa de flujo} \left[\frac{\text{kg}}{\text{seg}} \right] \quad \text{Concentración} \left[\frac{\mu\text{g}}{\text{kg}} \right]$$

Donde el coeficiente 3.15×10^7 segundos corresponde a 1 año convertido a segundos.

Luego se dividió el tonelaje de recursos estimados de Zinc y Plomo para Patricia por la cantidad de recursos transportados en un año (convertidos a toneladas), para distintas combinaciones de tasas de flujo y concentraciones de Zinc y Plomo en solución. Algunos de los resultados obtenidos se presentan en las Figuras 32 y 33.

Time necessary to transport Estimated Resources of Zinc
at given flow rates and metal concentrations

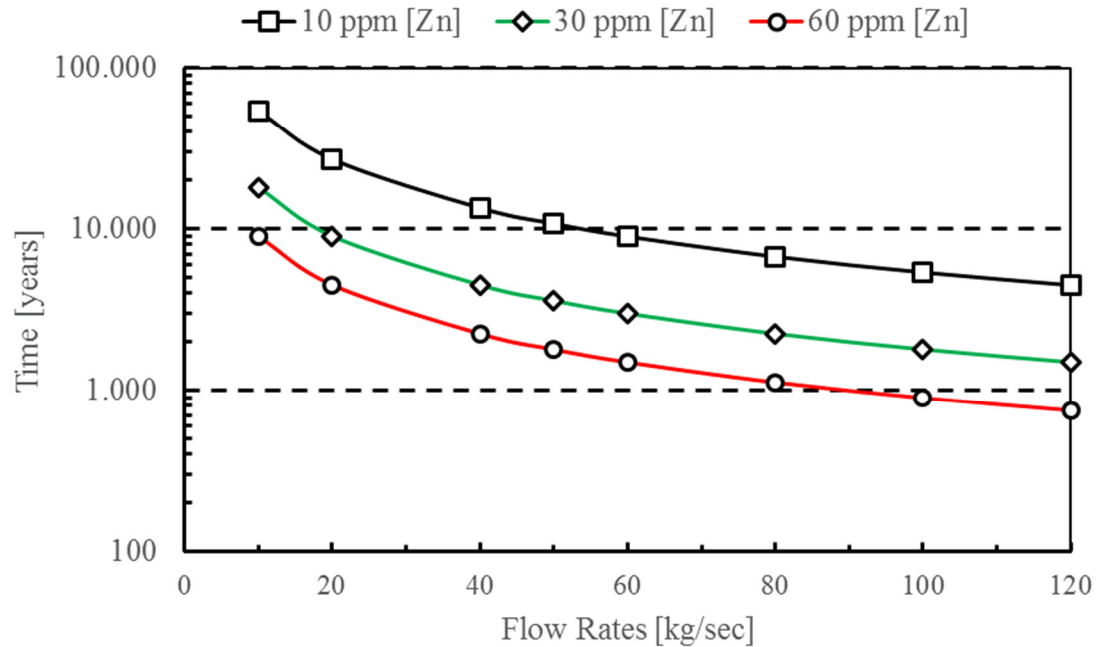


Figure 32. Tiempo necesario para depositar los recursos estimados de Zinc para Patricia, con diferentes tasas de fluidos, para distintas concentraciones de Zinc (~10, 30 y 60 ppm). El eje vertical representa el tiempo transcurrido y se encuentra en escala logarítmica. Para una tasa constante de 100 kg/segundo y 10 ppm de Zn en solución, son necesarios ~5,300 años para depositar el total de las reservas estimadas de Zinc. Sin embargo, para una tasa de 60 kg/segundo, con 30 ppm este período disminuye a ~3,000 años, y a la mitad de esto (~1,500 años) para una concentración de 60 ppm de Zn en solución.

Time necessary to transport Estimated Resources of Lead at given flow rates and metal concentrations

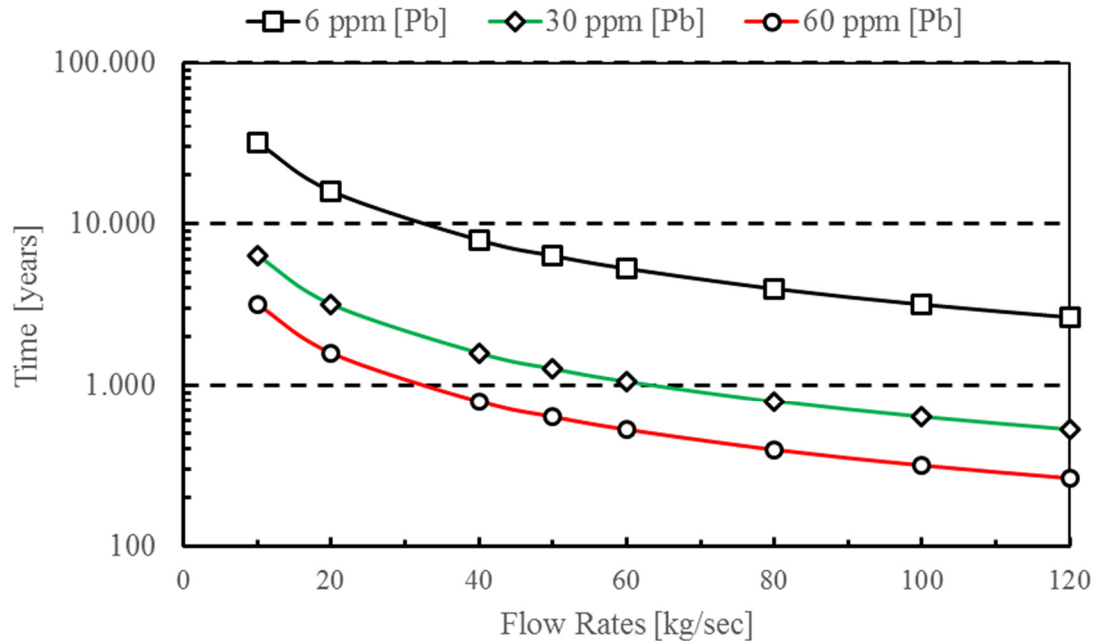


Figure 33. Tiempo necesario para depositar los recursos estimados de Plomo para Patricia, con diferentes tasas de fluidos, para distintas concentraciones de Pb en solución (~6, 30 y 60 ppm). El eje vertical se encuentra en escala logarítmica. Para una tasa constante de 100 kg/segundo y ~6 ppm de Pb en solución, son necesarios ~3,100 años para depositar el total de las reservas estimadas de Plomo. Sin embargo, para una tasa de 60 kg/segundo, con 30 ppm este período disminuye a ~1,000 años, y a la mitad de esto (~500 años) para una concentración de 60 ppm de Pb en solución.

De estas figuras se observa que la concentración de metales en solución tiene mayor incidencia en el tiempo necesario para acumular una cantidad determinada de recursos que las tasas de flujo. Los resultados presentados en el Capítulo 2, consideraron una tasa constante de 100 kg/segundo y concentraciones de 10 ppm de Zn y 6 ppm de Pb. A continuación, se discute la elección de estos valores.

3.5.1 Tasas de Flujo

Durante la revisión preliminar de referencias concernientes a la estimación de la duración de la etapa de mineralización en depósitos epitermales, se halló la reiterada mención del valor de 100 kg/segundo, como valor promedio para tasas de flujo en sistemas hidrotermales (Wilkinson et al. 2013, Simmons et al. 2016a), este valor corresponde al promedio de la tasa de flujo estimada para un sistema geotermal en Nueva Zelanda. Por esta razón ese valor fue considerado en todas las simulaciones realizadas, sin embargo, es necesario indicar que las tasas de flujo pudieron haber sido al menos un orden de magnitud menores de acuerdo a la compilación de tasas de flujo en sistemas geotermales activos y fuentes termales realizada por Moncada et al. (2019). Es factible entonces, que la tasa de flujo de 100 kg/segundo, usada en las simulaciones esté sobreestimada.

3.5.2 Concentraciones de Metales en Solución

Por otro lado, la concentración de metales base en solución usada en las simulaciones (~10 ppm de Zn y ~6 ppm de Pb) corresponden a una estimación mínima, obtenida al calcular las concentraciones de metales en solución para condiciones de equilibrio con la asociación mineralógica del estadio de mineralización usando “batch models”. Comparadas con las concentraciones de metales medidas en inclusiones fluidas de los estadios 1 y 3 de Patricia, las concentraciones estimadas para el estadio de mineralización son ~ 5 veces mayores.

Es posible obtener otra estimación para las concentraciones de los fluidos mineralizadores de Patricia, en función de la temperatura y salinidad, usando las estimaciones empíricas propuestas a partir de la compilación de concentraciones de metales en fluidos corticales por Yardley (2005). En el caso de Patricia, para salinidades similares a las del sub-estadio 2A (~5% NaCl), las concentraciones estimadas para una solución a 200°C varían entre 0.4 -46 ppm de Zn en solución y entre 0.6-68 ppm de Pb en solución. Si se mantiene constante la salinidad, pero se recalculan los posibles rangos de solubilidad para una solución a 260°C, se obtienen concentraciones de 3.4-300 ppm de Zn y de 4-400 ppm de Pb. En relación a estas estimaciones, las concentraciones usadas en las simulaciones, son menores, y sugieren que se puede estar subestimando la carga metálica de los fluidos mineralizadores.

Wilkinson et al. (2009) plantea que, durante la etapa de mineralización, las soluciones mineralizadoras serían soluciones super-saturadas en metales, si esto fuera una ocurrencia generalizada, entonces en las simulaciones realizadas, las concentraciones de metales asumidas para el estadio 2 de mineralización estarían subestimadas. Y dejarían planteada la posibilidad de que el período de mineralización en el depósito de Patricia, fue más breve de lo estimado en las simulaciones, incluso con menores tasas de flujo.

3.6 ¿Si la mezcla de fluidos es un proceso tan extendido, porque no hay más recursos minerales en sistemas geotermales activos?

Las condiciones de transporte favorables para la formación de un depósito epitermal son comunes en los sistemas geotermales activos, y también lo son procesos tales como ebullición, enfriamiento, interacción agua-roca y mezcla de fluidos, sin embargo, no todos los sistemas geotermales representan acumulaciones económicas de recursos minerales (Simmons et al. 2016a y 2016b). En el caso de Patricia, las condiciones de permeabilidad y presencia de estructuras, fueron favorables para la formación de un sistema geotermal, y para canalizar fluidos hidrotermales a una zona de mezcla, pero estas condiciones no hubieran sido suficientes para formar un depósito epitermal, sin el ingreso de un fluido enriquecido en metales al sistema, este fluido fue el factor crítico para formar el depósito.

Ahora es interesante mencionar que, desde un principio, la idea de que el proceso de mineralización es por naturaleza de carácter episódico fue parte integral del modelo conceptual de este estudio, luego esta idea inevitablemente sesgó la toma de decisiones al decidir las condiciones de borde de las simulaciones. Dado el grado de incertidumbre en factores como la permeabilidad y la tasa de flujo, es muy tentador construir un modelo que no plantee ningún cuestionamiento a la hipótesis inicial, en el caso de este estudio, la metodología de transporte reactivo, fue lo suficientemente robusta para desafiar y refutar el modelo de formación previo de Patricia, y añadir revisiones significativas a dicho modelo. En la cuestión acerca del carácter de la mineralización depósitos formados en el ambiente epitermal, entre un modo episódico o continuo de mineralización, y entre

un proceso excepcional y muy breve relativo a la escala temporal de procesos geológicos o un proceso de carácter continuo y que requiere principalmente condiciones estables de transporte, este estudio se inclina a favor de procesos de carácter episódico y excepcional, pero el sesgo conceptual mencionado es una influencia que no debe ser ignorada al evaluar críticamente los resultados presentados.

4 CONCLUSIONES

Se realizó un modelo de transporte reactivo del depósito Patricia usando el código TOUGHREACT. A partir de las condiciones dadas por la mineralogía, los datos de inclusiones fluidas y la ausencia de evidencias de ebullición en el depósito Patricia, se propone como un mecanismo eficiente para formar sulfuros en este sistema la mezcla de fluidos, entre un fluido ácido con metales en solución como complejos clorurados, y bajas concentraciones de azufre reducido $<10^{-4}$ mol/kg; y otro fluido más rico en azufre reducido. Estos fluidos habrían sido aportados por flujos ascendentes y laterales durante la actividad geotermal del sistema. De acuerdo a los resultados obtenidos la distribución de la permeabilidad en el sistema habría ejercido un control de primer orden la distribución de la mineralización en el depósito. Un medio poroso con contrastes de permeabilidad, favorece la acumulación de mineralización preferencial en espacios de mayor permeabilidad donde tiene lugar un mayor desarrollo de la interacción fluido-roca, esta interacción mantiene un rango de pH favorable para la formación de sulfuros en las fracturas del sistema. A partir de datos de las inclusiones fluidas, estimaciones conservadoras de solubilidad de metales base en los fluidos mineralizadores y balance de masas, asumiendo 10,000 años de actividad geotermal, el evento mineralizador habría tenido una duración de 5,000 años.

Para describir la interacción fluido-roca en el sistema se utilizaron dos aproximaciones diferentes: Primero, con un solo medio poroso para estudiar las condiciones de formación de mineralización de sulfuros de metales base en este ambiente epitermal. Luego se implementó un modelo con dos medios de distinta permeabilidad para explorar el efecto de fracturas de mayor permeabilidad en la distribución de la mineralización.

Considerando un solo medio poroso se simuló un período total de actividad geotermal de 10,000 años, los resultados de este modelo permitieron dilucidar el proceso de formación del depósito, acotar las condiciones geoquímicas de los fluidos mineralizadores y estimar el período de mineralización. Este modelo replicó la asociación mineral propilítica y precipitó una cantidad similar de metales base a los recursos estimados para el depósito Patricia, estos metales se acumularon en un horizonte vertical siguiendo la distribución típica de los depósitos epitermales de metales base. Consideraciones de balance de masas permiten estimar en 5,000 años la duración del período de mineralización. En esta aproximación, los fluidos hidrotermales interactúan con un único medio poroso homogéneo, y los sulfuros precipitan de manera similar a un estilo de mineralización diseminada en todo el volumen del sistema. Este modelo no proporciona una perspectiva más amplia en el rol de medios con distintas permeabilidades en la mineralización, como son una matriz rocosa y los espacios abiertos en rocas fracturadas.

Para explorar este aspecto, se realizó un modelo de doble porosidad que examinó las diferencias en el desarrollo de la interacción fluido-roca en un medio análogo a una roca intacta y en otro medio similar a una roca fracturada. Los resultados de este modelo también replicaron la alteración mineral, la distribución vertical de sulfuros y los recursos estimados del depósito Patricia. En los resultados del modelo de doble porosidad, el control de la permeabilidad en la distribución de la mineralización es observado claramente, los sulfuros precipitan mayoritariamente en las fracturas del sistema, de manera similar a un estilo de mineralización en vetas. La mineralización se concentra en las zonas de mayor permeabilidad del sistema.

Una observación común a ambos modelos, es la disminución de la permeabilidad en la cercanía del límite superior del volumen modelado, asociada a un marcado contraste de temperatura, esta disminución no llega a sellar el sistema.

Para la descripción de las condiciones de transporte y duración de la actividad del sistema, la mayor limitación del modelo está dada por la ausencia de un mayor nivel de detalle en la caracterización disponible de la distribución de permeabilidad, y las fracturas del sistema. En tanto para la estimación de la duración del evento de mineralización, dado que esta depende de la carga metálica y de las tasas de flujo de los fluidos hidrotermales; y como los antecedentes disponibles a partir del mismo depósito para acotar estos parámetros tienen un alto grado de incertidumbre, es posible que varias combinaciones de tasas de flujo y de carga metálica pudieran haber formado este depósito, e incluso que hayan fluctuado simultáneamente durante el mismo estadio mineralizador. Una posible dirección de interés en el estudio de los depósitos de origen hidrotermal, sería la exploración de la relación existente entre la geología del depósito y la paleo-hidrología del sistema fósil buscando acotar estas condiciones de transporte en el sistema.

Pese a las simplificaciones empleadas, fue posible con la información disponible reproducir los rasgos geológicos generales del depósito Patricia con un modelo de transporte reactivo y obtener una perspectiva más amplia del proceso y de las condiciones favorables para la formación de mineralización de metales base en el ambiente epitermal. Estos resultados fueron validados al replicarse por un lado la evolución paragenética y la asociación mineral del depósito, y por otro la distribución y tonelaje estimado de recursos minerales del depósito Patricia.

Finalmente, los factores que permitieron la formación del depósito de Zn-Pb-Ag Patricia, fueron primero una distribución de permeabilidad favorable para la formación de un sistema geotermal, luego la presencia de estructuras, capaces de canalizar los fluidos hidrotermales ascendentes y formar una zona de mezcla eficiente de fluidos, pero estas condiciones no hubieran sido suficientes para formar el depósito, sin el ingreso de un fluido enriquecido en metales al sistema, este fluido fue el factor crítico para formar el depósito de Patricia.

5 BIBLIOGRAFIA

- Acero, P., J. Cama and C. Ayora (2007a). Rate law for galena dissolution in acidic environment. Chemical Geology **245** (3): 219-229.
- Acero, P., J. Cama and C. Ayora (2007b). Sphalerite dissolution kinetics in acidic environment. Applied Geochemistry **22** (9): 1872-1883.
- Albinson, T., D. I. Norman, D. Cole and B. Chomiak (2001). Controls on formation of low-sulfidation epithermal deposits in Mexico; constraints from fluid inclusion and stable isotope data. Special Publication (Society of Economic Geologists (U. S.)) **8**: 1-32.
- Albinson, T. and M. A. Rubio (2001). Mineralogic and thermal structure of the Zuloaga vein, San Martin de Bolanos district, Jalisco, Mexico. Special Publication (Society of Economic Geologists (U. S.)) **8**: 115-132.
- Achtziger-Zupančič, P., Loew, S., & Mariethoz, G. (2017). A new global database to improve predictions of permeability distribution in crystalline rocks at site scale. Journal of Geophysical Research: Solid Earth, 122(5), 3513-3539.
- Arnórsson, S., Stefánsson, A., & Bjarnason, J. O. (2007). Fluid-fluid interactions in geothermal systems. Reviews in Mineralogy and Geochemistry, 65(1), 259-312.
- Bodnar, R. J., P. Lecumberri-Sanchez, D. Moncada and M. Steele-MacInnis (2014). 13.5 - Fluid Inclusions in Hydrothermal Ore Deposits. Treatise on Geochemistry (Second Edition). H. D. Holland and K. K. Turekian. Oxford, Elsevier: 119-142.
- Bodnar, R. J., T. J. Reynolds and C. A. Kuehn (1985). Fluid-inclusion systematics in epithermal systems. Reviews in Economic Geology **2**: 73-97.
- Buchanan, L. J. (1981). Precious metal deposits associated with volcanic environments in the Southwest. Arizona Geological Society Digest **14**: 237-262.
- Campbell, W. R. and P. B. Barton (2005). Environment of ore deposition in the Creede mining district, San Juan Mountains, Colorado: Part VI. Maximum duration for mineralization of the OH vein. Economic Geology **100**(7): 1313-1324.
- Casadevall, T. and H. Ohmoto (1977). Sunnyside Mine, Eureka mining district, San Juan County, Colorado; geochemistry of gold and base metal ore deposition in a volcanic environment. Economic Geology **72**(7): 1285-1320.
- Cathles, L. M. (1977). An analysis of the cooling of intrusives by ground-water convection which includes boiling. Economic Geology **72**(5): 804-826.

- Cathles, L. M., A. H. J. Erendi and T. Barrie (1997). How long can a hydrothermal system be sustained by a single intrusive event? Economic Geology **92**(7-8): 766-771.
- Chinchilla, D., X. Arroyo, R. Merinero, R. Piña, F. Nieto, L. Ortega and R. Lunar (2016a). Chlorite geothermometry applied to massive and oscillatory-zoned radiated Mn-rich chlorites in the Patricia Zn-Pb-Ag epithermal deposit (NE, Chile). Applied Clay Science **134**: 210-220.
- Chinchilla, D., L. Ortega, R. Piña, R. Merinero, D. Moncada, R. J. Bodnar, C. Quesada, A. Valverde and R. Lunar (2016b). The Patricia Zn-Pb-Ag epithermal ore deposit: An uncommon type of mineralization in northeastern Chile. Ore Geology Reviews **73**, Part **1**: 104-126.
- Chinchilla, D. (2017). Caracterización y modelización metalogénica del yacimiento de Zn-Pb-Ag de Patricia (Proyecto Paguanta, NE Chile); Memoria para optar al grado de Doctor; Universidad Complutense de Madrid.
- Corbett, G. J. (2012). Structural controls to, and exploration for, epithermal Au-Ag deposits. Australian Institute of Geoscientists Bulletin, 56, 43-47.
- Dobson, P. F., S. Salah, N. Spycher and E. L. Sonnenthal (2004). Simulation of water-rock interaction in the Yellowstone geothermal system using TOUGHREACT. Geothermics **33**(4): 493-502.
- Driesner, T. and S. Geiger (2007). Numerical simulation of multiphase fluid flow in hydrothermal systems. Reviews in Mineralogy and Geochemistry. **65**: 187-212.
- Giggenbach, W. F. (1992a). Isotopic shifts in waters from geothermal and volcanic systems along convergent plate boundaries and their origin. Earth and Planetary Science Letters **113**(4): 495-510.
- Giggenbach, W. F. (1992b). Tectonic regime and major processes governing the chemistry of water and gas discharges from the Rotorua geothermal field, New Zealand. Geothermics **21**(1-2): 121-140.
- Giggenbach, W. F. (1995). Variations in the chemical and isotopic composition of fluids discharged from the Taupo Volcanic Zone, New Zealand. Journal of Volcanology and Geothermal Research **68**(1-3): 89-116.
- Giggenbach, W. F. (1997a). Relative importance of thermodynamic and kinetic processes in governing the chemical and isotopic composition of carbon gases in high-heatflow sedimentary basins. Geochimica et Cosmochimica Acta **61**(17): 3763-3785.

- Giggenbach, W. F. (1997b). The origin and evolution of fluids in magmatic-hydrothermal systems, in Barnes, H. L., ed., *Geochemistry of hydrothermal ore deposits*, Third Edition: New York, John Wiley & Sons, p. 737-796
- Golden Rim Resources Ltd. (2017). New Resource Estimation for Paguanta. ASX/Media Announcement, 30 may 2017, 22 p.
- Haas, J. L. (1971). The effect of salinity on the maximum thermal gradient of a hydrothermal system at hydrostatic pressure. *Economic Geology* **66**(6): 940-946.
- Hardardóttir, V., K. L. Brown, T. Fridriksson, J. W. Hedenquist, M. D. Hannington and S. Thorhallsson (2009). Metals in deep liquid of the Reykjanes geothermal system, southwest Iceland: Implications for the composition of seafloor black smoker fluids. *Geology* **37**(12): 1103-1106.
- Hayba, D. O. (1997). Environment of ore deposition in the Creede mining district, San Juan Mountains, Colorado; Part V, Epithermal mineralization from fluid mixing in the OH Vein. *Economic Geology* **92**(1): 29-44.
- Hayba, D. O. and S. E. Ingebritsen (1997). Multiphase groundwater flow near cooling plutons. *Journal of Geophysical Research B: Solid Earth* **102**(6): 12235-12252.
- Heald-Wetlaufer, P., D. O. Hayba, N. K. Foley and J. A. Goss (1983). Comparative anatomy of epithermal precious- and base-metal districts hosted by volcanic rocks. *Open-File Report - U. S. Geological Survey*: 83-0710:0720 pp.
- Hedenquist, J. W., A. Arribas R and E. Gonzalez-Urien (2000). Exploration for epithermal gold deposits. *Reviews in Economic Geology* **13**: 245-277.
- Hedenquist, J. W. and J. B. Lowenstern (1994). The role of magmas in the formation of hydrothermal ore deposits. *Nature* **370**(6490): 519-527.
- Heinrich, C. A. (2007). Fluid-Fluid Interactions in Magmatic-Hydrothermal Ore Formation. *Reviews in Mineralogy and Geochemistry* **65**(1): 363-387.
- Helgeson, H. C. and R. M. Garrels (1968). Hydrothermal transport and deposition of gold. *Economic Geology* **63**(6): 622-635.
- Henley, R. W. (1985). The geothermal framework of epithermal deposits. *Reviews in Economic Geology* **2**: 1-24.
- Henley, R. W. and A. J. Ellis (1983). Geothermal systems ancient and modern: a geochemical review. *Earth-Science Reviews* **19**(1): 1-50.

- Hu, X., X. Li, F. Yuan, A. Ord, S. M. Jowitt, Y. Li, W. Dai and T. Zhou (2020). Numerical modeling of ore-forming processes within the Chating Cu-Au porphyry-type deposit, China: Implications for the longevity of hydrothermal systems and potential uses in mineral exploration. Ore Geology Reviews **116**: 103230.
- Huston, D. L. (1998). The hydrothermal environment. AGSO Journal of Australian Geology & Geophysics, **17**(4).
- Ingebritsen, S. E. and M. S. Appold (2012). The physical hydrogeology of ore deposits. Economic Geology **107**(4): 559-584.
- Ingebritsen, S. E., S. Geiger, S. Hurwitz and T. Driesner (2010). Numerical simulation of magmatic hydrothermal systems. Reviews of Geophysics **48**(1): RG1002.
- Ingebritsen, S. E. and T. Gleeson (2015). Crustal permeability: Introduction to the special issue. Geofluids **15**(1-2): 1-10.
- Ingebritsen, S. E. and C. E. Manning (2010). Permeability of the continental crust: Dynamic variations inferred from seismicity and metamorphism. Geofluids **10**(1-2): 193-205.
- Kamilli, R. J. and H. Ohmoto (1977). Paragenesis, zoning, fluid inclusion, and isotopic studies of the Finlandia Vein, Colqui District, central Peru. Economic Geology **72**(6): 950-982.
- Kostova, B., T. Pettke, T. Driesner, P. Petrov and C. A. Heinrich (2004). LA ICP-MS study of fluid inclusions in quartz from the Yuzhna Petrovitsa deposit, Madan ore field, Bulgaria. Schweizerische Mineralogische und Petrographische Mitteilungen **84**(1-2): 25-36.
- Landtwing, M. R., T. Pettke, W. E. Halter, C. A. Heinrich, P. B. Redmond, M. T. Einaudi and K. Kunze (2005). Copper deposition during quartz dissolution by cooling magmatic-hydrothermal fluids: The Bingham porphyry. Earth and Planetary Science Letters **235**(1-2): 229-243.
- Lasaga, A. C. (1984). Chemical kinetics of water-rock interactions. Journal of geophysical research: solid earth, **89**(B6), 4009-4025.
- Lasaga, A. C., J. M. Soler, J. Ganor, T. E. Burch and K. L. Nagy (1994). Chemical weathering rate laws and global geochemical cycles. Geochimica et Cosmochimica Acta **58**(10): 2361-2386.
- Leach, T., & Corbett, G. (2008, October). Fluid mixing as a mechanism for bonanza grade epithermal gold formation. In Terry Leach Symposium.
- Lester, D. R., Ord, A., & Hobbs, B. E. (2012). The mechanics of hydrothermal systems: II. Fluid mixing and chemical reactions. Ore geology reviews, **49**, 45-71.

- Loucks, R. R., J. Lemish and P. E. Damon (1988). Polymetallic epithermal fissure vein mineralization, Topia, Durango, Mexico; Part I, District geology, geochronology, hydrothermal alteration, and vein mineralogy. Economic Geology **83**(8): 1499-1527.
- Moncada, D., S. Mutchler, A. Nieto, T. J. Reynolds, J. D. Rimstidt and R. J. Bodnar (2012). Mineral textures and fluid inclusion petrography of the epithermal Ag–Au deposits at Guanajuato, Mexico: Application to exploration. Journal of Geochemical Exploration **114**(0): 20-35.
- Moncada, D., J. D. Rimstidt and R. J. Bodnar (2019). How to form a giant epithermal precious metal deposit: Relationships between fluid flow rate, metal concentration of ore-forming fluids, duration of the ore-forming process, and ore grade and tonnage. Ore Geology Reviews **113**: 103066.
- Norton, D. and J. Knight (1977). Transport phenomena in hydrothermal systems; the nature of porosity. American Journal of Science **277**(8): 913-936.
- Palandri, J. L. and Y. K. Kharaka (2004). A compilation of rate parameters of water-mineral interaction kinetics for application to geochemical modeling [electronic resource] / by James L. Palandri and Yousif K. Kharaka ; prepared in cooperation with the National Energy Technology Laboratory, United States Department of Energy, Menlo Park, Calif. : U.S. Dept. of the Interior, U.S. Geological Survey, 2004.
- Paradis, S., Hannigan, P., Dewing, K. (2007). Mississippi valley-type lead-zinc deposits. In: W.D. Goodfellow ed., mineral deposits of Canada: A synthesis of major deposit types, district metallogeny, the evolution of geological provinces, and exploration methods: Geological Association of Canada. Mineral Deposits Division, Special Publication No. 5 pp. 185–203.
- Pruess, K. (1999). A mechanistic model for water seepage through thick unsaturated zones in fractured rocks of low matrix permeability. Water Resources Research **35**(4): 1039-1051.
- Reed, M. H. and J. Palandri (2006). Sulfide mineral precipitation from hydrothermal fluids. Reviews in Mineralogy and Geochemistry. **61**: 609-631.
- Rissmann, C., M. Leybourne, C. Benn and B. Christenson (2015). The origin of solutes within the groundwaters of a high Andean aquifer. Chemical Geology **396**: 164-181.
- Romberger, S.B. (1991). Transport and deposition of precious metals in epithermal deposits. In Geology and ore deposits of the Great Basin. Symposium Proc. Geological Society of Nevada, Reno, Nevada, 219-232.
- Rottier, B., Kouzmanov, K., Casanova, V., Bouvier, A. S., Baumgartner, L. P., Wälle, M., & Fontboté, L. (2021). Tracking fluid mixing in epithermal deposits—Insights from in-situ $\delta^{18}\text{O}$ and trace element composition of hydrothermal quartz from the giant Cerro de Pasco polymetallic deposit, Peru. Chemical Geology, 576, 120277.

- Sanchez-Alfaro, P., Reich, M., Arancibia, G., Pérez-Flores, P., Cembrano, J., Driesner, T., ... & Campos, E. (2016). Physical, chemical and mineralogical evolution of the Tolhuaca geothermal system, southern Andes, Chile: insights into the interplay between hydrothermal alteration and brittle deformation. *Journal of Volcanology and Geothermal Research*, 324, 88-104.
- Scott, S., Driesner, T., & Weis, P. (2016). The thermal structure and temporal evolution of high-enthalpy geothermal systems. *Geothermics*, 62, 33-47.
- Seward, T. M. (1989). The hydrothermal chemistry of gold and its implications for ore formation; boiling and conductive cooling as examples. *Economic Geology Monograph* 6: 398-404.
- Sillitoe, R. H. and J. W. Hedenquist (2003). Linkages between volcanotectonic settings, ore-fluid compositions, and epithermal precious metal deposits. *Special Publication (Society of Economic Geologists (U. S.))* 10: 315-343.
- Simmons, S. F. and K. L. Brown (2006). Gold in magmatic hydrothermal solutions and the rapid formation of a giant ore deposit. *Science* 314(5797): 288-291.
- Simmons, S. F. and K. L. Brown (2007). The flux of gold and related metals through a volcanic arc, Taupo Volcanic Zone, New Zealand. *Geology* 35(12): 1099-1102.
- Simmons, S. F., K. L. Brown, P. R. L. Browne and J. V. Rowland (2016a). Gold and silver resources in Taupo Volcanic Zone geothermal systems. *GEO THERMICS* 59(Part B): 205-214.
- Simmons, S. F., K. L. Brown and B. M. Tutolo (2016b). Hydrothermal transport of Ag, Au, Cu, Pb, Te, Zn, and other metals and metalloids in New Zealand geothermal systems: Spatial Patterns, Fluid-mineral equilibria, and implications for epithermal mineralization. *Economic Geology* 111(3): 589-618.
- Simmons, S. F., N. C. White and D. A. John (2005a). Geological characteristics of epithermal precious and base metal deposits. Littleton, CO, Society of Economic Geologists.
- Simmons, S. F., N. C. White and D. A. John (2005b). Geological Characteristics of Epithermal Precious and Base Metal Deposits. Economic Geology 100th Anniversary Volume Economic Geology; One Hundredth Anniversary Volume, 1905-2005: 485-522.
- Sonnenthal, E., A. Ito, N. Spycher, M. Yui, J. Apps, Y. Sugita, M. Conrad and S. Kawakami (2005). Approaches to modeling coupled thermal, hydrological, and chemical processes in the drift scale heater test at Yucca Mountain. International Journal of Rock Mechanics and Mining Sciences 42(5): 698-719.

- Steeffel, C. I. and A. C. Lasaga (1994). A coupled model for transport of multiple chemical species and kinetic precipitation/dissolution reactions with application to reactive flow in single phase hydrothermal systems. American Journal of Science(5): 529.
- Steeffel, C. I., DePaolo, D. J., & Lichtner, P. C. (2005). Reactive transport modeling: An essential tool and a new research approach for the Earth sciences. Earth and Planetary Science Letters, 240(3-4), 539-558.
- Stoffell, B., M. S. Appold, J. J. Wilkinson, N. A. McClean and T. E. Jeffries (2008). Geochemistry and evolution of mississippi valley-type mineralizing brines from the Tri-State and Northern Arkansas districts determined by LA-ICP-MS microanalysis of fluid inclusions. Economic Geology **103**(7): 1411-1435.
- Todaka, N., C. Akasaka, T. Xu and K. Pruess (2004). Reactive geothermal transport simulations to study the formation mechanism of an impermeable barrier between acidic and neutral fluid zones in the Onikobe Geothermal Field, Japan. Journal of Geophysical Research: Solid Earth **109**(B5).
- Valenzuela, J. I., S. Herrera, L. Pinto and I. Del Real (2014). Carta Camiña, regiones de Arica-Parinacota y Tarapacá. C. G. d. C. Servicio Nacional de Geología y Minería, Serie Geología Básica 170.
- Wanner, C., L. Peiffer, E. Sonnenthal, N. Spycher, J. Iovenitti and B. M. Kennedy (2014). Reactive transport modeling of the Dixie Valley geothermal area: Insights on flow and geothermometry. Geothermics **51**: 130-141.
- Weis, P. (2015). The dynamic interplay between saline fluid flow and rock permeability in magmatic-hydrothermal systems. Geofluids **15**(1-2): 350-371.
- White, E. D. (1955). Thermal springs and epithermal ore deposits. Economic Geology 50th Anniversary Volume: 99-154.
- Wilkinson, J. J., S. L. Eyre and A. J. Boyce (2005). Ore-forming processes in Irish-type carbonate-hosted Zn-Pb deposits: Evidence from mineralogy, chemistry, and isotopic composition of sulfides at the Lisheen Mine. Economic Geology **100**(1): 63-86.
- Wilkinson, J. J., Stoffell, B., Wilkinson, C. C., Jeffries, T. E., & Appold, M. S. (2009). Anomalously metal-rich fluids form hydrothermal ore deposits. Science, 323(5915), 764-767.
- Wilkinson, J. J., S. F. Simmons and B. Stoffell (2013). How metalliferous brines line Mexican epithermal veins with silver. Scientific Reports **3**.

- Xu, T. and K. Pruess (2001). On fluid flow and mineral alteration in fractured caprock of magmatic hydrothermal systems. Journal of Geophysical Research: Solid Earth **106**(B2): 2121-2138.
- Xu, T., E. Sonnenthal, N. Spycher and K. Pruess (2006). TOUGHREACT - A simulation program for non-isothermal multiphase reactive geochemical transport in variably saturated geologic media: Applications to geothermal injectivity and CO₂ geological sequestration. Computers and Geosciences **32**(2): 145-165.
- Xu, T., N. Spycher, E. Sonnenthal, G. Zhang, L. Zheng and K. Pruess (2011a). TOUGHREACT Version 2.0: A Simulator for Subsurface Reactive Transport Under Non Isothermal Multiphase Flow Conditions. Computers & Geosciences **37**: 763–774.
- Xu, T., N. Spycher, E. Sonnenthal, G. Zhang, L. Zheng and K. Pruess (2011b). TOUGHREACT version 2.0: A simulator for subsurface reactive transport under non-isothermal multiphase flow conditions. Computers and Geosciences **37**(6): 763-774.
- Zerai, B., B. Z. Saylor and G. Matisoff (2006). Computer simulation of CO₂ trapped through mineral precipitation in the Rose Run Sandstone, Ohio. Applied Geochemistry **21**(2): 223-240.
- Zhang, W., T. Xu and Y. Li (2011). Modeling of fate and transport of coinjection of H₂S with CO₂ in deep saline formations. Journal of Geophysical Research: Solid Earth **116**(2).
- Zhong, R., Brugger, J., Chen, Y., Li, W. (2015). Contrasting regimes of Cu, Zn and Pb transport in ore-forming hydrothermal fluids. Chemical Geology, 395,154-164.
- Zou, Y., Y. Liu, T. Dai, X. Mao, Y. Lei, J. Lai and H. Tian (2017). Finite difference modeling of metallogenic processes in the Hutouya Pb-Zn deposit, Qinghai, China: Implications for hydrothermal mineralization. Ore Geology Reviews **91**: 463-476.